

Intramolecular Phosphine-oxide stabilized Germanium(IV) Di-cation with Enhanced Lewis Acidity and Catalytic Applications

Akanksha Kumari^a, Balakrishna Peddi^a, Cem B. Yildiz^{*,b} and Moumita Majumdar^{*,a}

^aDepartment of Chemistry, Indian Institute of Science Education and Research, Pune, Dr. Homi Bhabha Road, Pashan, Pune-411008, Maharashtra, India. Email: moumitam@iiserpune.ac.in

^b Department of Basic Sciences, Faculty of Engineering, Architecture and Design, Bartın University, 74100 Bartın, Türkiye;
Email: cbyildiz@bartin.edu.tr

Table of Contents

Experimental and Computational Detail	S2
1^{iPr}PO	S4
1^{iPr}PO.Et₃PO (Gutmann-Beckett Method)	S13
1^{iPr}PO.DMAP	S16
1^{iPr}PO-F	S20
1^{iPr}PO-H	S30
Catalytic Hydrodefluorination	S36
Catalytic Hydrosilylation	S45
Cartesian coordinates of optimized geometries	S55

General Experimental Procedures and Computational Methods

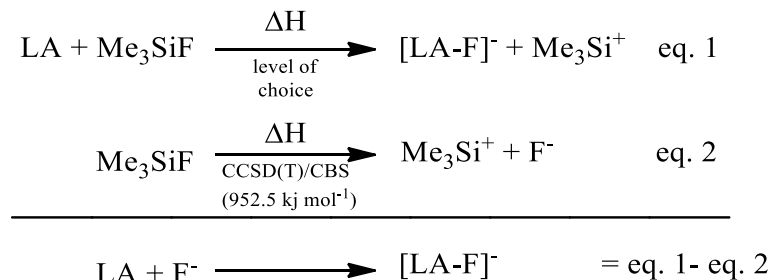
General Experimental Procedures:

All manipulations were carried out under a protective atmosphere of argon applying standard Schlenk techniques or in a dry box. Acetonitrile and dichloromethane (DCM) were stirred and refluxed over calcium hydride and kept over 3 Å molecular sieves. Tetrahydrofuran (THF) was refluxed over sodium/benzophenone. All solvents were distilled and stored under Argon and degassed prior to use. CD₃CN ampoules were purchased from Sigma Aldrich and used as it is. **1*i*P_rP** was synthesized following the literature method.^[S1] All other chemicals were used as purchased. ¹H and ¹³C{¹H} NMR spectra were referenced to external SiMe₄ using the residual signals of the deuterated solvent (¹H) or the solvent itself (¹³C). ¹⁹F was referenced to external C₆H₅CF₃ (TFT). NMR spectra were recorded on Bruker AVANCE III HD ASCEND 9.4 Tesla/400 MHz, Jeol 9.4 Tesla/400 MHz and Bruker AVANCE III HD ASCEND 14.1 Tesla/600 MHz NMR spectrometers. Melting points were determined under Argon in closed NMR tubes and are uncorrected. Single crystal data were collected on both Bruker SMART APEX Duo and Bruker APEX-II CCD diffractometers using Mo radiation (0.71073 Å). The structures were solved by methods of SHELXT from SHELXL-2018/136, and refined by full matrix least-squares methods against F2 with the SHELXL program.^[S2] Olex2^[S3] were used as graphical interface for the refinements. Mass analysis was performed in MALDI-TOF Applied Biosystems - 4800 Plus MALDI TOF/TOF Analyzer.

Computational Methods:

The TPSS-D3(BJ)/def2-TZVPP level of theory was applied for the gas-phase optimizations of the initial geometries from the initial geometries of the X-ray files using ORCA 5.0.0 package program.^[S4] The RIJCOSX (RI approximation for the Coulomb integrals) with combinations of corresponding auxiliary basis set was performed in all cases.^[S5] Then the NBO (natural bond orbital) properties of the title compounds were calculated with the optimized geometries using Gaussian 16 Rev.B.01 at the B3LYP-D3(BJ)/def2-TZVPP level of theory.^[S6] The selected NBO orbitals, donor-acceptor interactions, and Wiberg bond indexes were distilled out from the output files.^{[S7],[S8]} Additionally, Electrostatic Potential map of **1^{iPr}PO** was rendered from the optimized structure to provide that of positively and negatively charged sides in the range of 0.05 (red) – 0.4 (blue). All the figures were prepared by Gaussview 5.0 package program.^[S9]

The fluoride ion affinities (FIA) and hydride ion affinities (HIA) of **1^{iPr}PO**, **SbF₅**, and **B(PhF₅)₃** with respect to the scheme proposed by Krossing (TMS system).^[S10] Additionally, the solvation correction was performed with CPCM (Acetonitrile, DCM, and THF) to get solvated models of FIA and HIA as implemented in ORCA.



Experimental Detail

Synthesis of $\mathbf{1}^{\text{Pr}}\mathbf{PO}$: To a 20 mL dichloromethane solution of $\mathbf{1}^{\text{Pr}}\mathbf{P}^{[\text{S1}]}$ (0.80 g, 0.87 mmol), was added two equivalents of iodosobenzene (0.406 g, 1.74 mmol) and stirred for 24 hours at room temperature. The solution was then completely evaporated to dryness. Small amount of tetrahydrofuran was added to the solid, which led to a white precipitation. The supernatant solution was decanted and the white solid residue was redissolved in dichloromethane. The dichloromethane solution was layered with pentane and kept at room temperature conditions to obtain colourless single crystals of $\mathbf{1}^{\text{Pr}}\mathbf{PO}$ (0.682 g, 75% yield). Melting point > 200°C.

^1H NMR (400 MHz, CD_3CN , 298 K) 8.13-8.08 (dd, $J = 15$ Hz, 7.5 Hz, 2H, Acn- CH), 7.99 (d, $J = 7.1$ Hz, 2H, Acn- CH), 7.84 (dd, $J = 7.4$, 2.3 Hz, 2H, Acn- CH), 7.73 (d, $J = 7.1$ Hz, 2H, Acn- H), 3.62 (s, 8H, Acn- CH_2), 3.13-3.06 (m, 4H, $^{\text{Pr}}$ - CH), 1.37-1.21 (m, 24H, $^{\text{Pr}}\text{-CH}_3$).

$^{13}\text{C}\{^1\text{H}\}$ NMR (101 MHz, CD_3CN , 298 K) 158.81 (d, $J = 3.2$ Hz, Acn-C), 157.86 (s, Acn-C), 140.73 (s, Acn-C), 140.04 (d, $J = 9.2$ Hz, Acn-C), 137.32 (d, $J = 4.6$ Hz, Acn-CH), 136.85 (d, $J = 15$ Hz, Acn-C), 123.31 (s, Acn-C), 122.37 (d, $J = 14.7$ Hz, Acn-C), 122.09 (q, $J = 321.1$ Hz, OTf), 114.11 (d, $J = 3.6$ Hz, Acn-CH), 107.23 (s, Acn-CH), 106.67 (s, Acn-CH), 31.59 (d, $J = 7.8$ Hz, $^{\text{Pr}}\text{-CH}$), 27.71 (s, Acn- CH_2), 27.35 (d, $J = 6.6$ Hz, $^{\text{Pr}}\text{-CH}$), 26.98 (s, Acn- CH_2), 15.30-15.26 (m, $^{\text{Pr}}\text{-CH}_3$), 14.48-14.35 (m, $^{\text{Pr}}\text{-CH}_3$).

$^{31}\text{P}\{^1\text{H}\}$ NMR (162 MHz, CD_3CN , 298 K) = + 97.17 ppm

$^{19}\text{F}\{^1\text{H}\}$ NMR (377 MHz, CD_3CN , 298 K) = - 79.34 ppm

MALDI-TOF (CD Matrix): Observed m/z = 645.40 (calculated m/z= 645.21) $[(\text{C}_{36}\text{H}_{44}\text{GeO}_2\text{P}_2)(\text{H}^\cdot)]^+$

Elemental Analysis: Calcd. for $\text{C}_{38}\text{H}_{44}\text{O}_8\text{S}_2\text{P}_2\text{GeF}_6$. CH_2Cl_2 : C, 45.64; H, 4.52; S, 6.04. Found: C, 46.03; H, 4.54, S, 6.48.

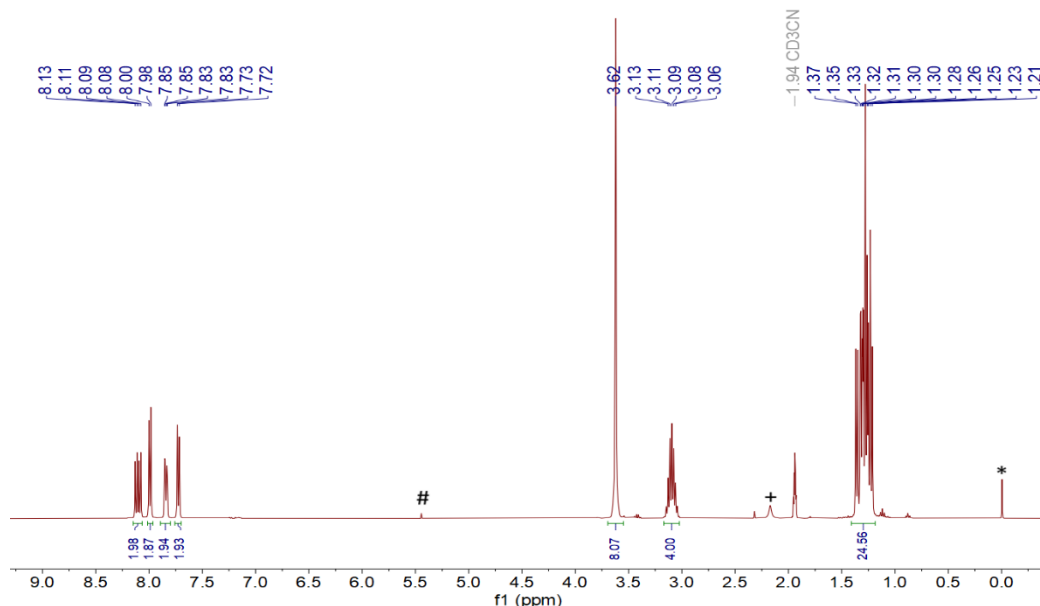


Figure S1. ^1H NMR spectrum (400 MHz, CD_3CN , 298 K) of $\mathbf{1}^{\text{Pr}}\mathbf{PO}$ (# = DCM, + = H_2O , * = TMS)

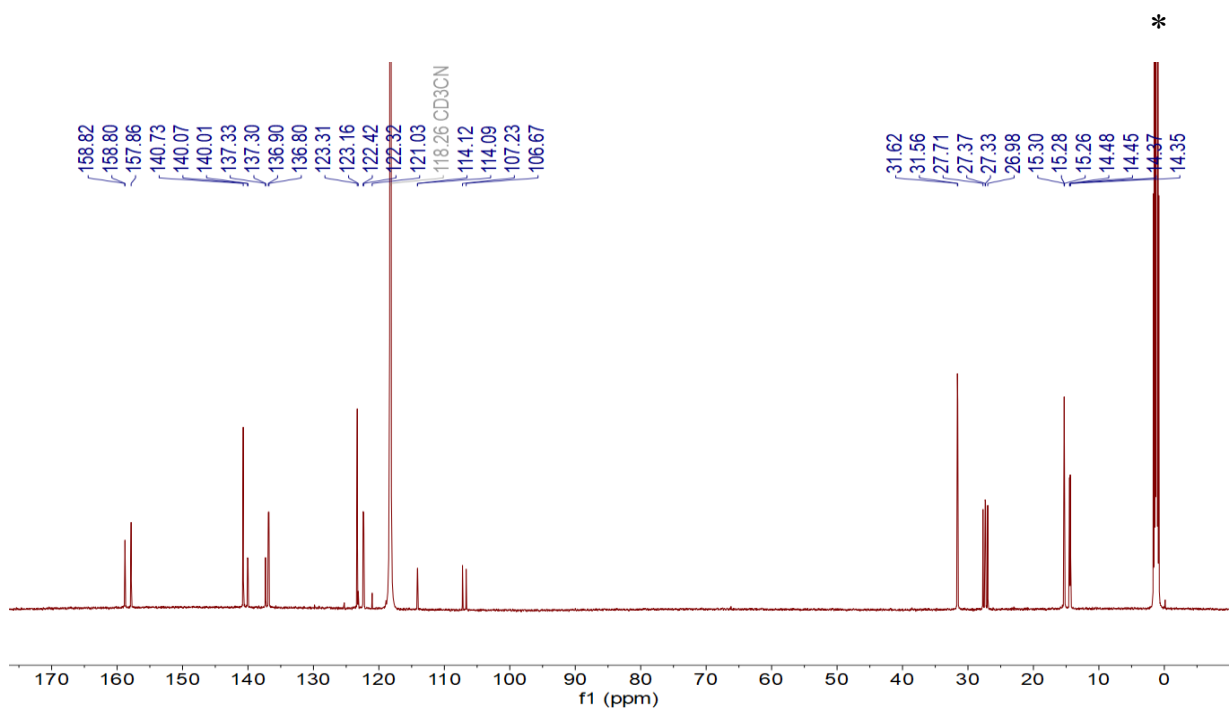


Figure S2. $^{13}\text{C}\{^1\text{H}\}$ NMR spectrum (101 MHz, CD_3CN , 298 K) of $\mathbf{1}^{\text{iPr}}\text{PO}$ ($*$ = CD_3CN)

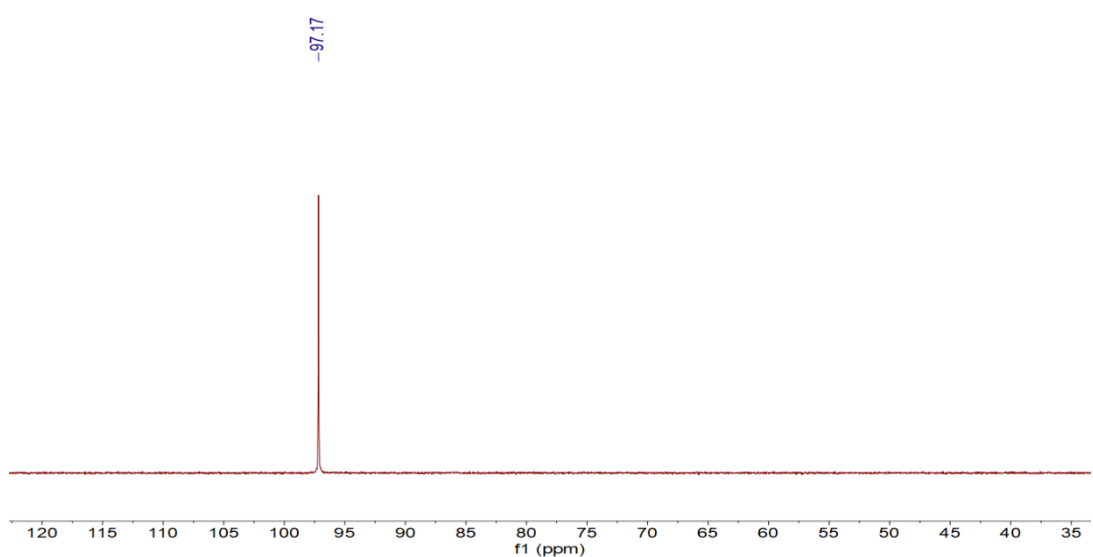


Figure S3. $^{31}\text{P}\{^1\text{H}\}$ NMR spectrum (162 MHz, CD_3CN , 298 K) of $\mathbf{1}^{\text{iPr}}\text{PO}$

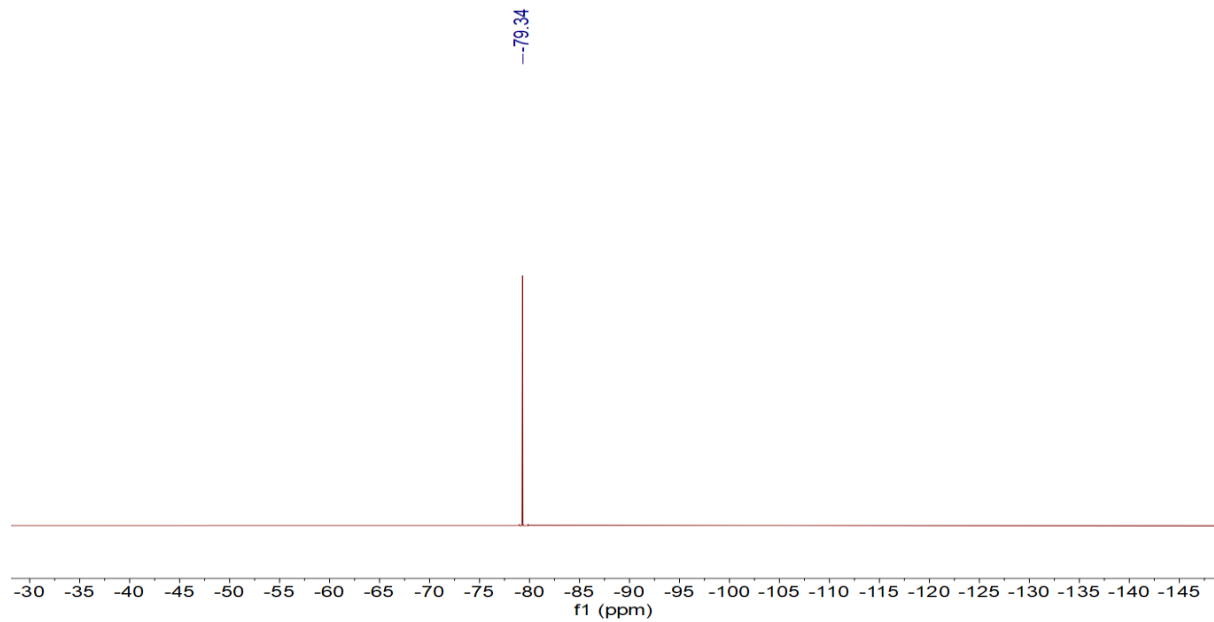


Figure S4. ${}^{19}\text{F}\{{}^1\text{H}\}$ NMR spectrum (377 MHz, CD_3CN , 298 K) of $\mathbf{1}^{\text{Pr}}\text{PO}$

Figure S5. Selected NBO orbitals and Molecular Electrostatic Potential Map (Range: 0.05-0.4) for $\mathbf{1}^{\text{Pr}}\text{PO}$ at the B3LYPD3(BJ)/def2-TZVPP//TPSS-B3(DJ)/def2-TZVPP level of theory (Isovalue: 0.03). H atoms are omitted for clarity

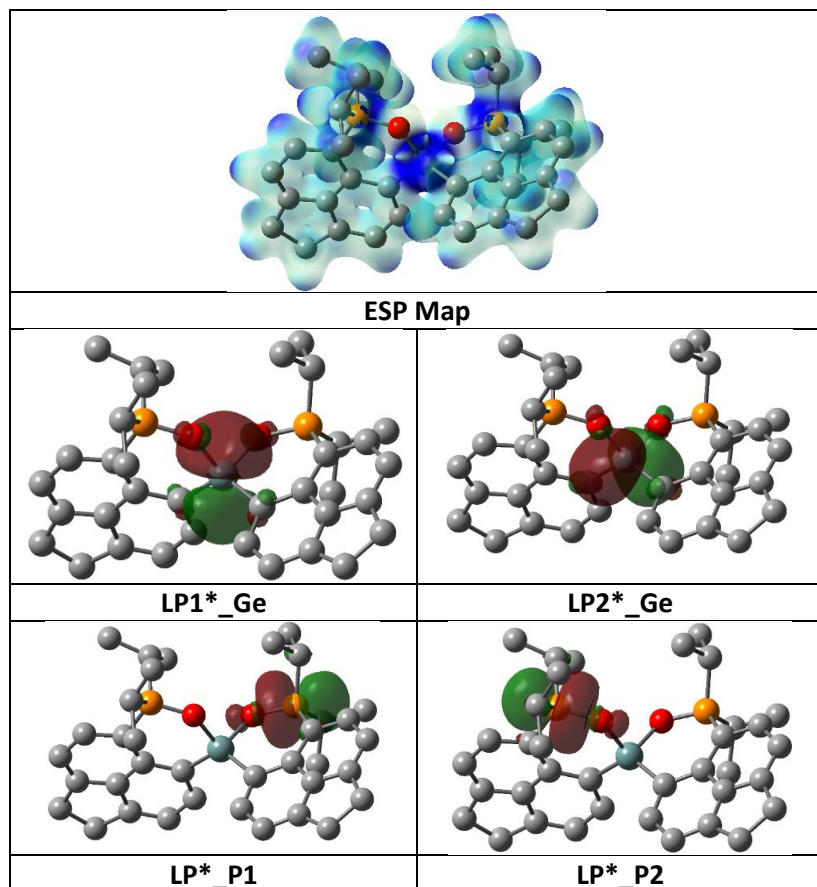
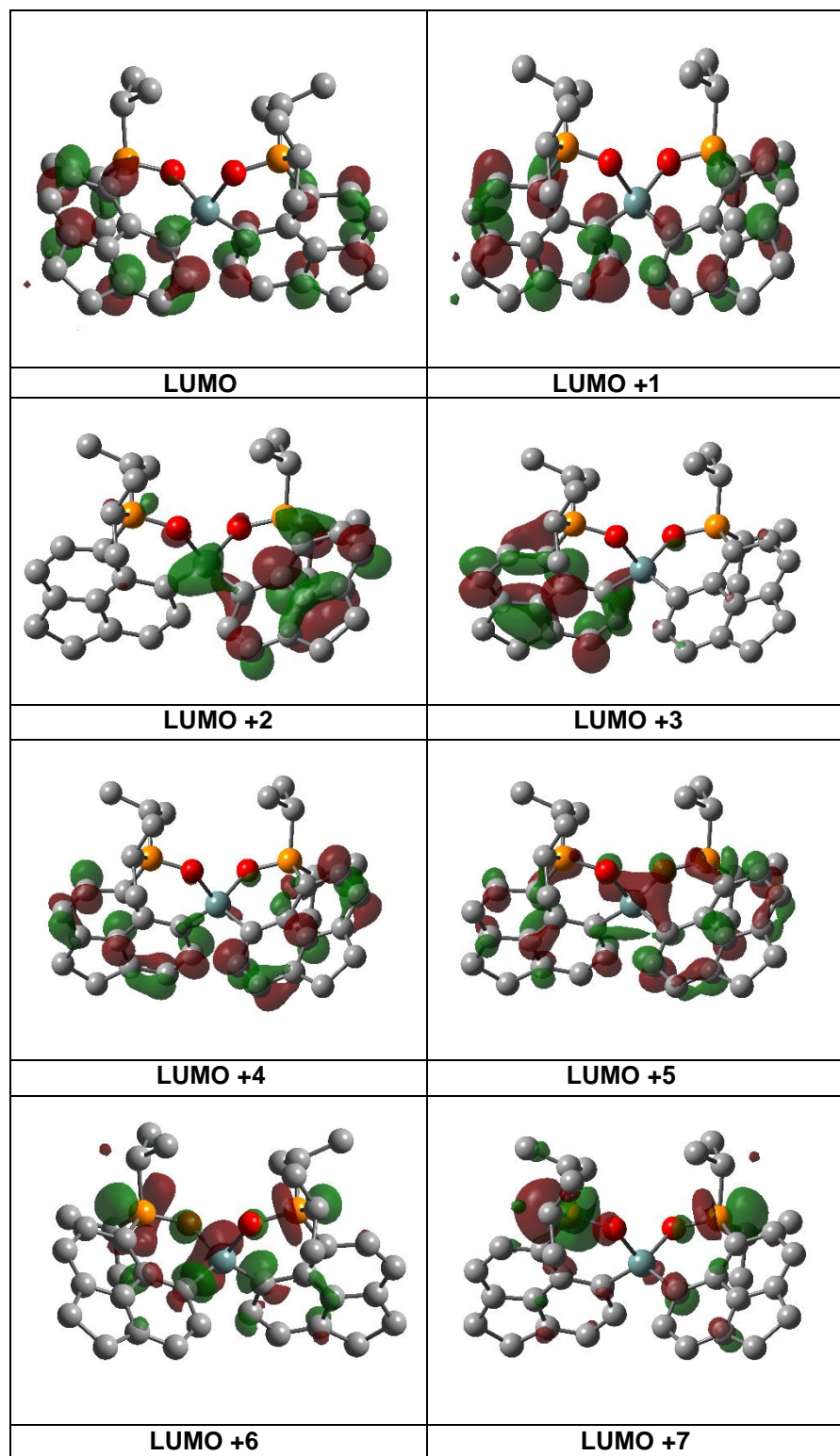


Figure S6. Selected Molecular orbitals for 1^{Pr}PO .



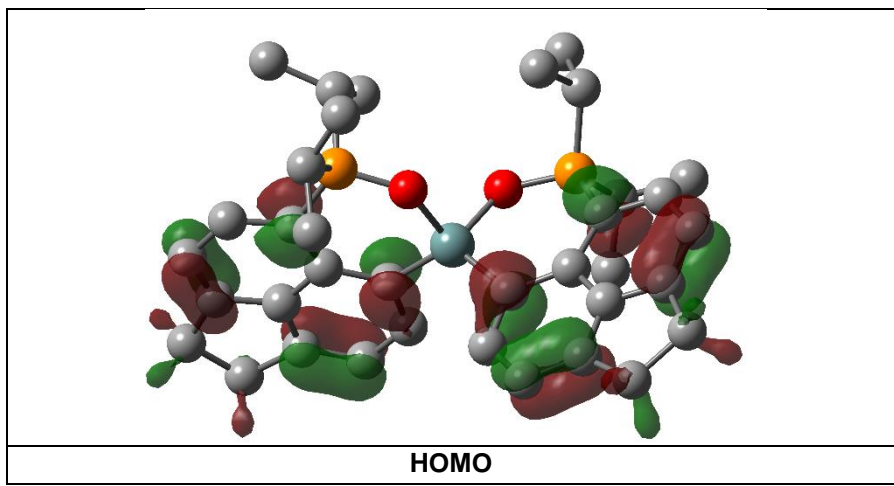


Table S1. Selected bonding orbitals, hybridizations, Donor-Acceptor Interactions, and WBO values for 1^{Pr}PO .

1^{Pr}PO	
BD_{Ge-C1}	(30.17%) Ge s(44.13%)p1.26(55.72%) (69.83%) C1 s(26.92%)p2.71(72.94%)
BD_{Ge-C2}	(29.93%) Ge s(43.70%)p1.28(56.15%) (70.07%) C s(27.06%)p2.69(72.80%)
LP1*_{Ge}	s(12.26%)p 7.13(87.37%)
LP2*_{Ge}	s(0.00%)p1.00(99.70%)
LP*_{P1}	s(11.90%)p7.31(86.96%)
LP*_{P2}	s(11.98%)p7.25(86.88%)
WBO_{Ge-C1}	0.797
WBO_{Ge-C1}	0.791
WBO_{Ge-O1}	0.456
WBO_{Ge-O2}	0.456
WBO_{P-O1}	0.811
WBO_{P-O2}	0.813
Donor-Acceptor Interactions in 1^{Pr}PO	
LP3O1→LP1* _{Ge}	88.79 kcal/mol
LP3O1→LP2* _{Ge}	60.02 kcal/mol
LP3O2→LP1* _{Ge}	90.38 kcal/mol
LP3O2→LP2* _{Ge}	59.47 kcal/mol

Table S2. FIA and HIA calculations at the Ge site for $^{1\text{P}}\text{rPO}$, SbF_5 , and $\text{B}(\text{PhF}_5)_3$ at the TPSS-D3(BJ)/def2-TZVPP level of theory.

	electr. energy sp LA [kJ mol-1]	total thermal correction LA [kJ mol-1]	electr. energy sp TMSF [kJ mol-1]	total thermal correction TMSF [kJ mol-1]	→	electr. energy sp LAF [kJ mol-1]	total thermal correction LAF [kJ mol-1]	electr. energy sp TMS [kJ mol-1]	total thermal correction TMS [kJ mol-1]	deltaH	FIA(gas)
FIA											
$^{1\text{P}}\text{rPO}_\text{FIA}$	-11312024,017447	113,2	-1336970,229967	22,18	→	-11575126,872274	116,260000	-1073775,135490	14,4	88	865
SbF_5	-1942108,495774	19,5	-1336970,229967	22,2	→	-2204843,000589	22,3	-1073775,135490	14,4	442	497
HIA											
$^{1\text{P}}\text{rPO}_\text{HIA}$	-10916518,548726	108,5	-1076072,823952	19,9	→	-11314283,161598	114,170000	-1073775,135490	14,4	34	925
$\text{B}(\text{PhF}_5)_3$	-5800599,954353	77,1	-1076072,823952	19,9	→	-5802448,926715	76,1	-1073775,135490	14,4	442	517

Table S3. Solvated models of FIA (MeCN and DCM) and HIA (MeCN and THF) at the Ge site for **1*i*PrPO**, **SbF₅**, and **B(PhF₅)₃** at the TPSS-D3(BJ)/def2-TZVPP level of theory.

Gas	LA	F/H·	→	LAF/ LAH	deltaH
1<i>i</i>PrPO_FIA	-10916518,548726	-262213,286341	→	-11179631,270812	-899
1<i>i</i>PrPO_HIA	-11312024,017447	-1322,132272	→	-11314283,161598	-937
SbF₅	-1942108,495774	-262213,286341	→	-2204843,000589	-521
B(PhF₅)₃	-5800599,954353	-1322,132272	→	-5802448,926715	-526

Solv	LA	F·	→	LAF	deltaH	FIA _{solv}
1<i>i</i>PrPO_FIA_MeCN	-11312527,465407	-262590,084293	→	-11575284,434842	-167	142
SbF₅_MeCN	-1942123,593950	-262590,084293	→	-2205053,028423	-339	315
Solv	LA	H·	→	LAH	deltaH	HIA _{solv}
1<i>i</i>PrPO_HIA_MeCN	-11312527,465407	-1713,426268	→	-11314438,133402	-197	185
B(PhF₅)₃_ MeCN	-5800619,826029	-1713,426268	→	-5802587,080667	-254	244

Table S4. Crystal data and structure refinement for **1ⁱPrPO** (CCDC No.: 2416600)

Empirical formula	C39H46Cl2F6GeO8P2S2
Color	Colorless
Formula weight	1026.31 g/mol
Temperature	150(2) K
Wavelength	0.71073 Å
Crystal system	triclinic
Space group	P $\bar{1}$
Unit cell dimensions	$a = 11.237(4)$ Å $\alpha = 86.231(8)^\circ$ $b = 13.727(5)$ Å $\beta = 72.039(8)^\circ$ $c = 15.396(5)$ Å $\gamma = 80.057(8)^\circ$
Volume	2225.0(13) Å ³
Z	2
Density (calculated)	1.532 g/cm ³
Absorption coefficient	1.049 mm ⁻¹
F(000)	1052
Size	0.050 x 0.070 x 0.100 mm ³
Theta range for data collection	2.01 to 25.20°
Index ranges	-13≤h≤10, -16≤k≤16, -18≤l≤18
Reflections collected	17291
Independent reflections	7824 [R(int) = 0.0455]
Completeness to theta = 25.20°	97.3%
Absorption correction	multi-scan
Refinement method	Full-matrix least-squares on F2
Data / restraints / parameters	7824 / 712 / 724
Goodness-of-fit on F2	1.077
Final R indices 6078 data; [I>2σ(I)]	R1 = 0.0484, wR2 = 0.1206
R Indices (all data)	R1 = 0.0672, wR2 = 0.131
Extinction coefficient	n/a
Largest diff. peak and hole	0.938 and -1.063 eÅ ⁻³

Reaction of $1^{Pr}PO$ with Et_3PO (Effective Lewis acidity determination by Guttmann Beckett method): To a solution of $1^{Pr}PO$ (0.021 g, 0.02 mmol, 1 equiv.) in CD_3CN , triethylphosphine oxide ($OPEt_3$) was successively added (0.2 equiv. to 2 equiv.) and the reaction was monitored by $^{31}P\{^1H\}$ NMR spectroscopy.

$^{31}P\{^1H\}$ NMR (162 MHz, CD_3CN , 243 K) for $1^{Pr}PO.Et_3PO$ δ +75.57 ($^{Pr_2}P=O$), +75.08 (bound $Et_3P=O$)

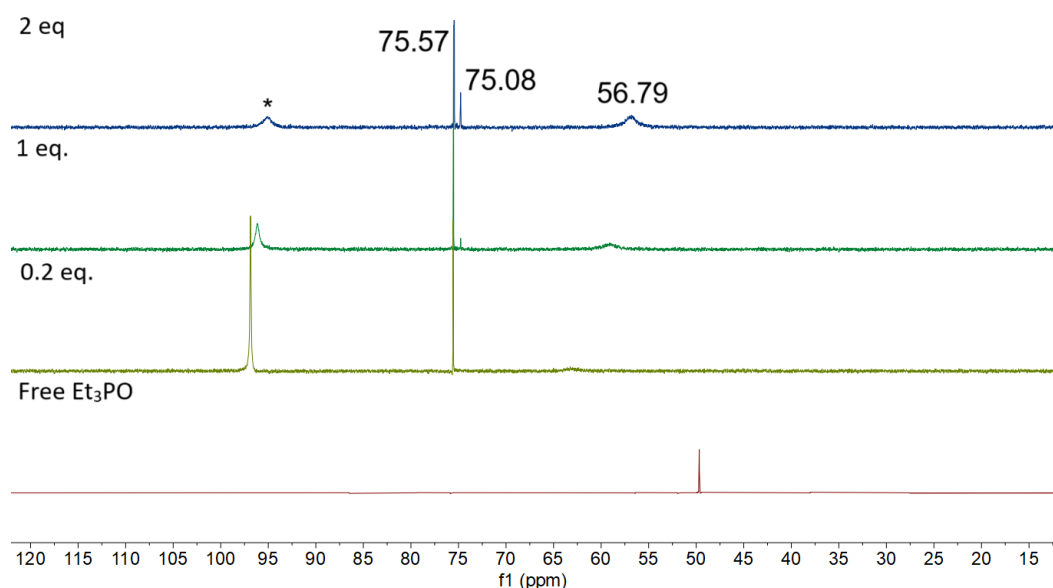


Figure S7. $^{31}P\{^1H\}$ NMR spectra (162 MHz, CD_3CN , 298 K) from the addition of varying equivalents of Et_3PO to $1^{Pr}PO$ (* = peak for $1^{Pr}PO$)

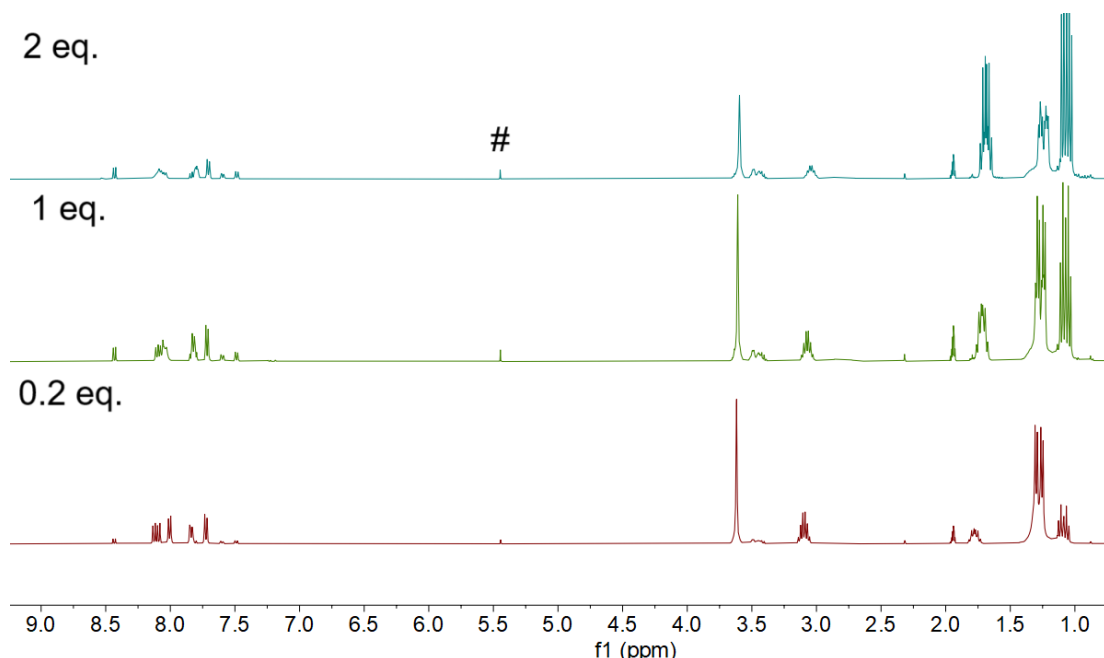


Figure S8. 1H NMR spectra (400 MHz, CD_3CN , 298 K) from the addition of varying equivalents of Et_3PO to $1^{Pr}PO$ (# = DCM) showing the formation of the mono-adduct $1^{Pr}PO.Et_3PO$

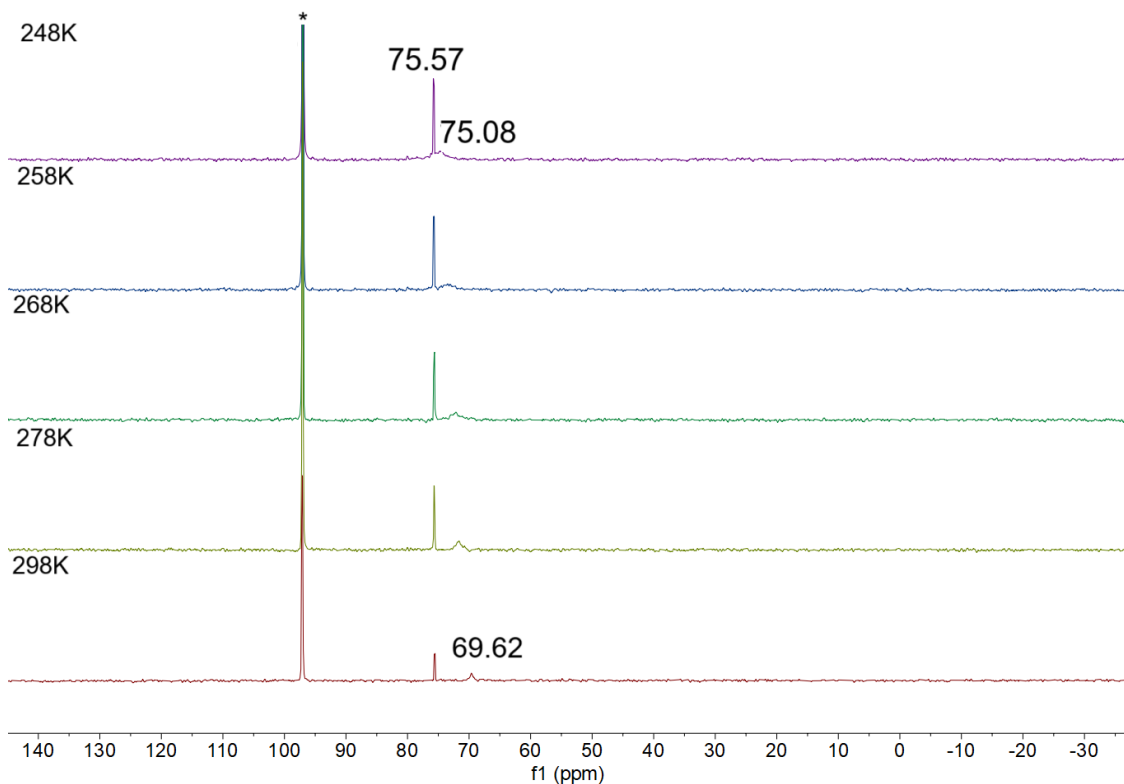


Figure S9. Variable temperature $^{31}\text{P}\{\text{H}\}$ NMR spectrum (162 MHz, CD_3CN) from the addition of 0.2 equivalent of Et_3PO (* = peak for $\mathbf{1}^{\text{Pr}}\text{PO}$)

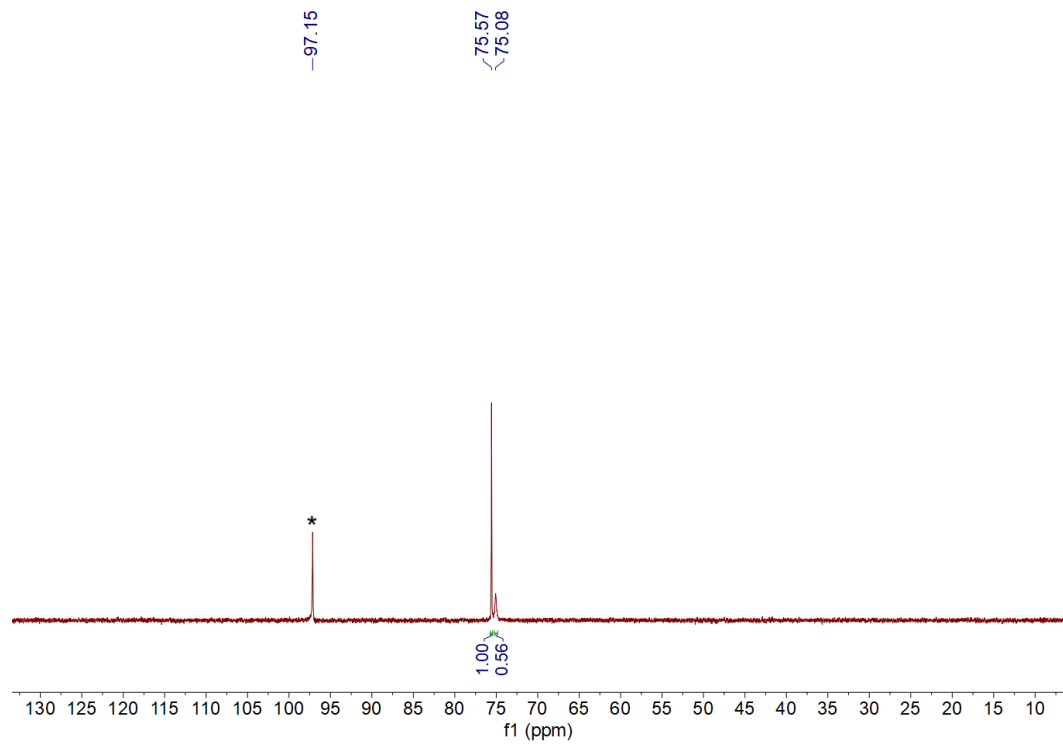


Figure S10. $^{31}\text{P}\{\text{H}\}$ NMR spectrum (162 MHz, CD_3CN) from the addition of 1 equivalent of Et_3PO to $\mathbf{1}^{\text{Pr}}\text{PO}$ (* = peak for $\mathbf{1}^{\text{Pr}}\text{PO}$)

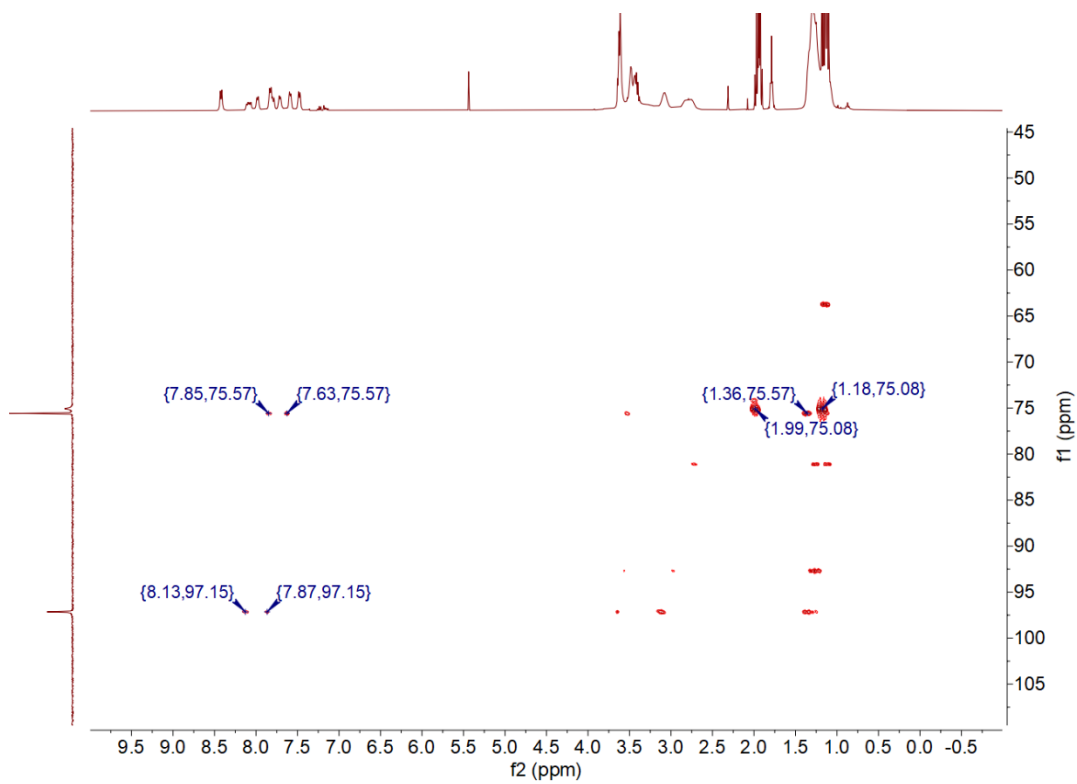


Figure S11. 2D ^1H - ^{31}P Heteronuclear Multiple Bond Correlation (HMBC) (400MHz/162MHz, CD_3CN , 298K) for the addition of 1 equivalent of Et_3PO to 1^{Pr}PO .

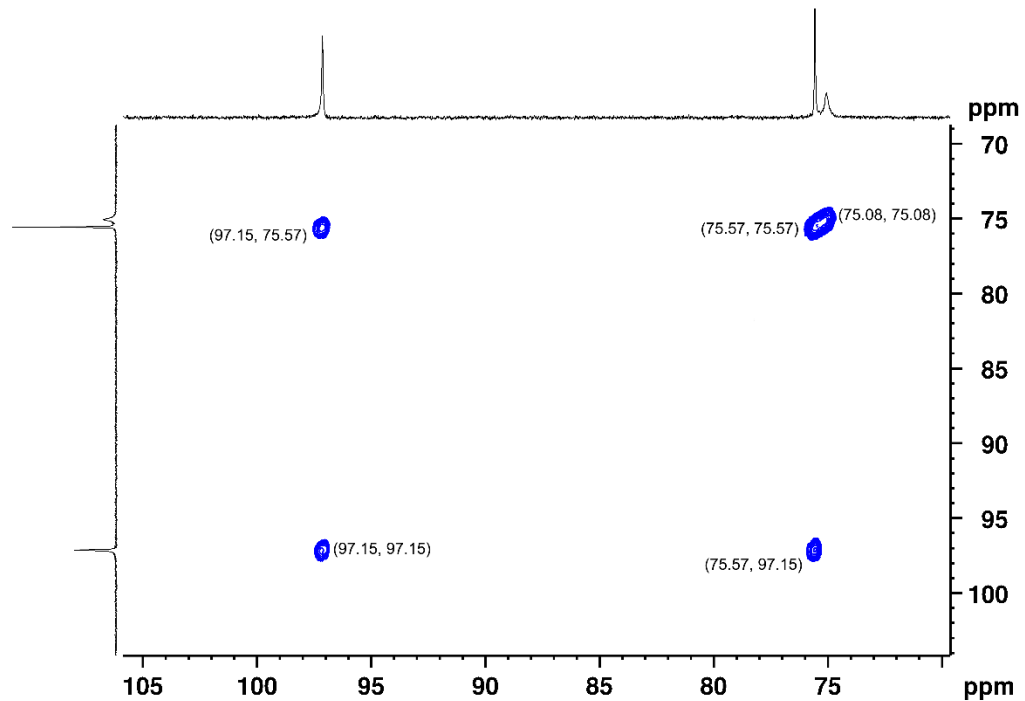


Figure S12 2D ^{31}P - ^{31}P Exchange Spectroscopy (EXSY) NMR spectrum (162 MHz, CD_3CN , 298K) for the addition of 1 equivalent of Et_3PO to 1^{Pr}PO .

Synthesis of $\mathbf{1}^{\text{Pr}}\text{PO.DMAP}$: To a 15 mL dichloromethane solution of $\mathbf{1}^{\text{Pr}}\text{PO}$ (0.06 g, 0.06 mmol), was added one equivalent of 4-*N*, *N'* - dimethylamino pyridine (DMAP) (0.077 g, 0.06 mmol) and stirred overnight at room temperature. The solution was then concentrated and layered with pentane. Colourless needle-shaped single crystals of $\mathbf{1}^{\text{Pr}}\text{PO.DMAP}$ (0.037 g, 77% yield) were obtained from this layering at room temperature. Melting point = 180-182 °C. Anion exchange reaction was carried out in dichloromethane, which led to the exchange of two triflate counter anions in $\mathbf{1}^{\text{Pr}}\text{PO.DMAP}$ with hexafluoroantimonate anions at room temperature. Better quality single crystals were obtained for structure elucidation.

^1H NMR (400 MHz, CD₃CN, 298 K) 8.43 (d, J = 7.3 Hz, 2H, Py-H), 7.99 (d, J = 7.8 Hz, 2H, Acn-CH), 7.85-7.80 (dd, J = 7.3 Hz, 14 Hz, 2H, Acn-CH), 7.60-7.58 (dd, J = 7.2 Hz, 1.8 Hz, 2H, Acn-CH), 7.48 (d, J = 7.3 Hz, 2H, Acn-CH), 6.81 (d, J = 7.8 Hz, 2H, Py-H), 3.49-3.42 (m, 8H, Acn-CH₂), 3.16 (s, 6H, py-CH₃), 2.83-2.77 (m, 4H, $\text{iPr}-\text{CH}$), 1.35-1.10 (m, 24H, $\text{iPr}-\text{CH}_3$)

$^{13}\text{C}\{^1\text{H}\}$ NMR (101 MHz, CD₃CN, 298 K) 158.33 (s, Py-C), 155.86 (d, J = 3.2 Hz, Acn-C), 152.22 (d, J = 1.7 Hz, Acn-C), 141.02 (s, Acn-C), 140.19 (s, Py-CH), 140.14-140.12 (m, Acn-CH), 138.57 (d, J = 5.5 Hz, Acn-CH), 134.27 (d, J = 13 Hz, Acn-C), 121.52 (s, Acn-C), 121.90 (q, J = 320.15 Hz, OTf) 120.14 (d, J = 14.2 Hz, Acn-C), 114.02 (s, Acn-CH), 113.44 (s, Acn-CH), 107.80 (s, Py-CH), 40.41 (s, Py-CH₃), 31.24 (s, Acn-CH₂), 30.49 (s, Acn-CH₂), 27.93-27.24 (m, $\text{iPr}-\text{CH}$), 16.73-15.29 (m, $\text{iPr}-\text{CH}_3$).

$^{31}\text{P}\{^1\text{H}\}$ NMR (162 MHz, CD₃CN, 298 K) = + 75.58 ppm

$^{19}\text{F}\{^1\text{H}\}$ NMR (377 MHz, CD₃CN, 298 K) = - 78.30 (s, OTf) ppm

MALDI-TOF (DHB Matrix): Observed m/z = 791.52 (calculated m/z= 791.29) [(C₄₃H₅₄GeN₂O₂P₂)(H⁻₂Na⁺)]⁺

Elemental Analysis: Calcd. for C₄₅H₅₄O₈S₂P₂GeF₆N₂(CH₂Cl₂)₂ C, 45.77; H, 4.74; S, 5.20; N, 2.27. Found: C, 46.17; H, 3.77, S, 5.57; N, 2.30.

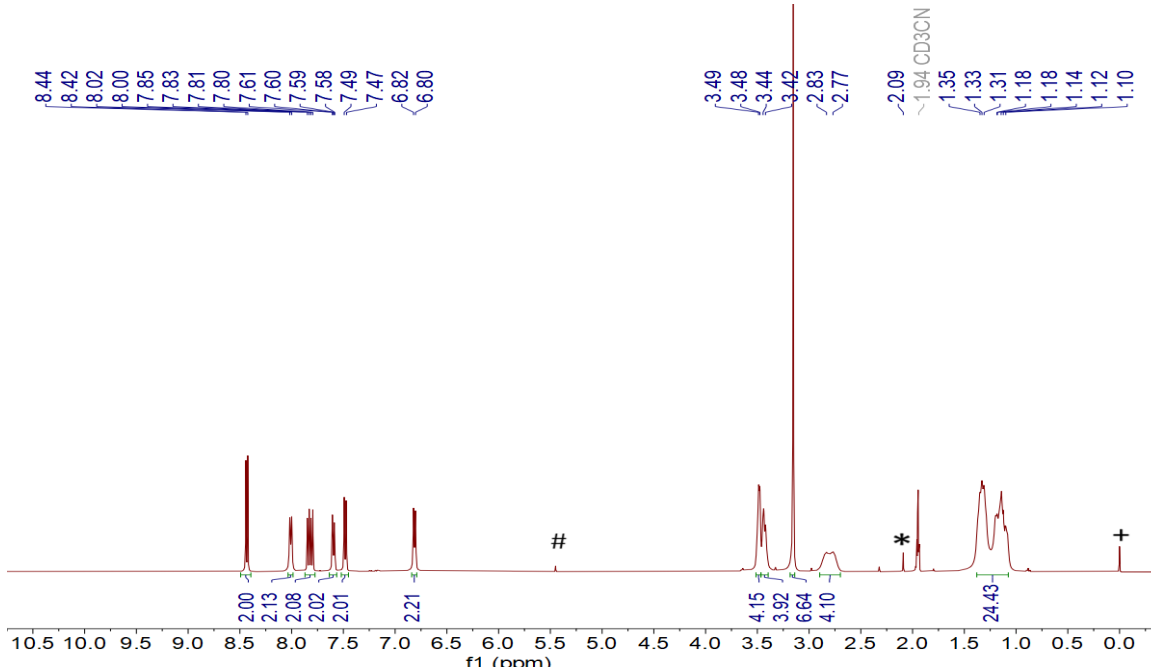


Figure S13. ^1H NMR spectrum (400 MHz, CD₃CN, 298 K) of $\mathbf{1}^{\text{Pr}}\text{PO.DMAP}$ (# = DCM, * = H₂O, + = TMS)

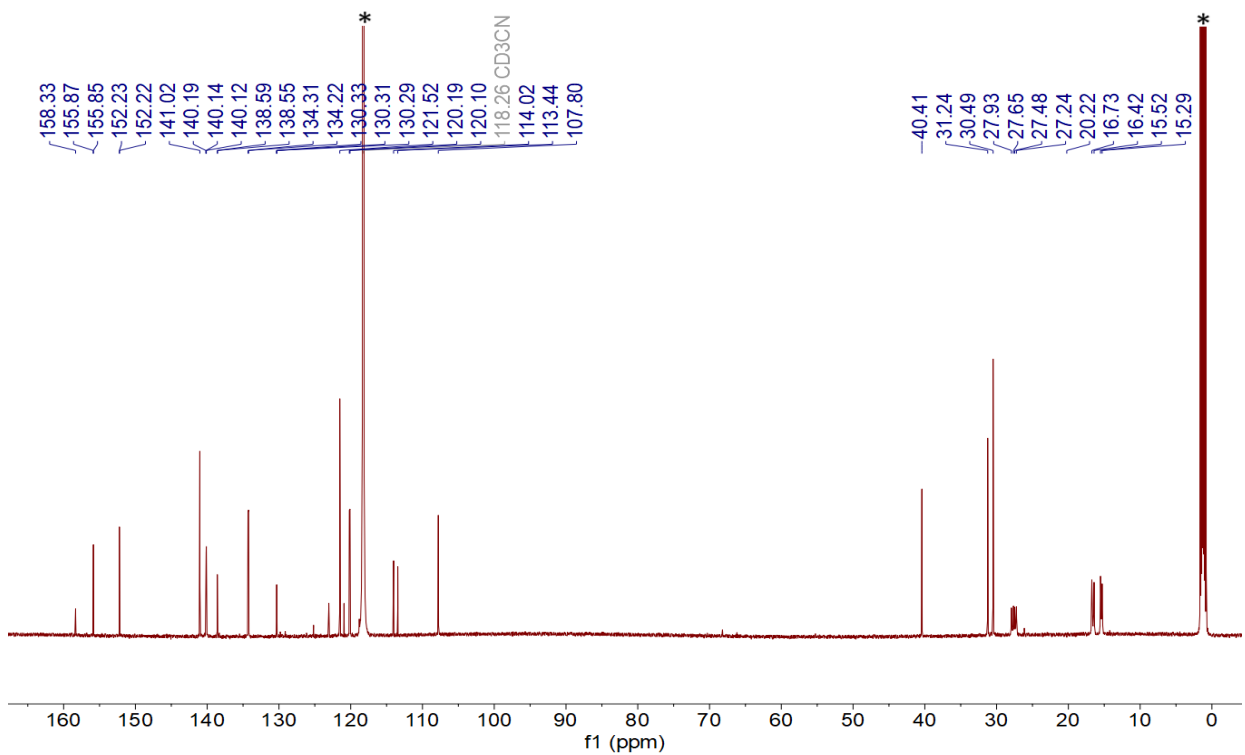


Figure S14. C{¹H} NMR spectrum (101 MHz, CD₃CN, 298 K) of **1*i*PrPO·DMAP** (* = CD₃CN)

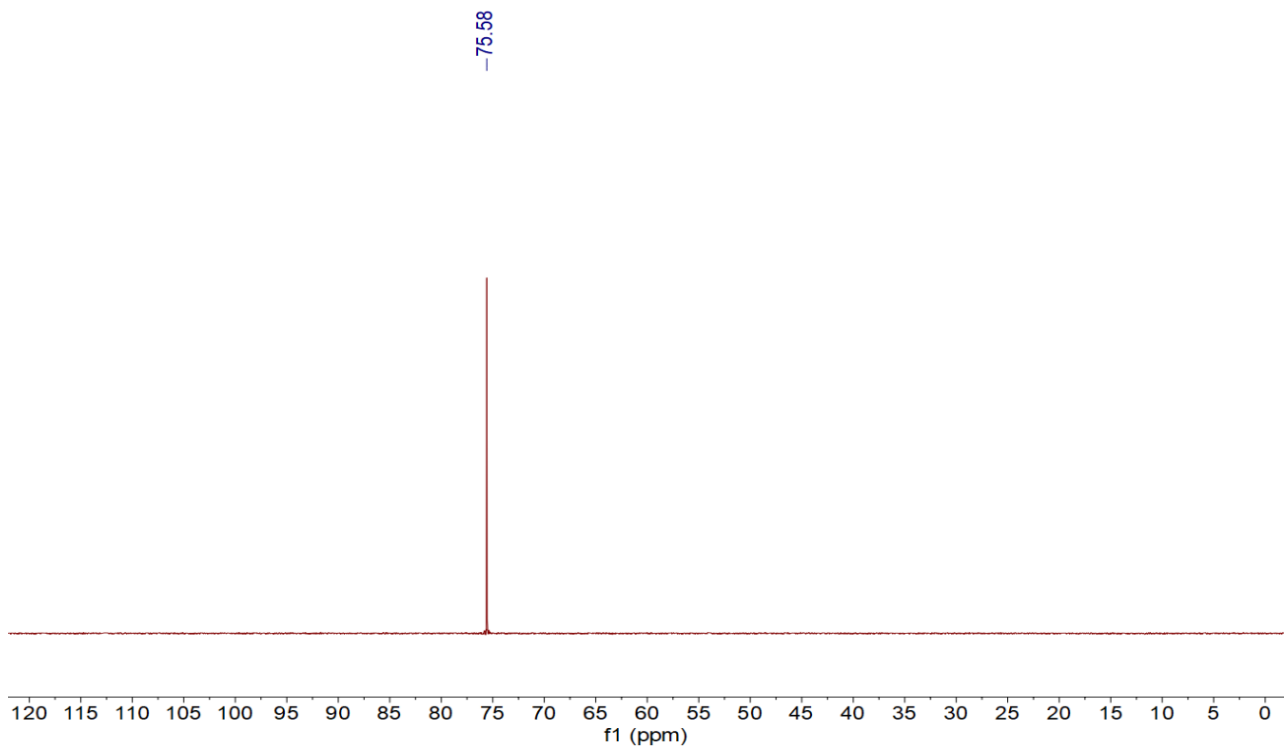


Figure S15. ³¹P{¹H} NMR spectrum (162 MHz, CD₃CN, 298 K) of **1*i*PrPO·DMAP**

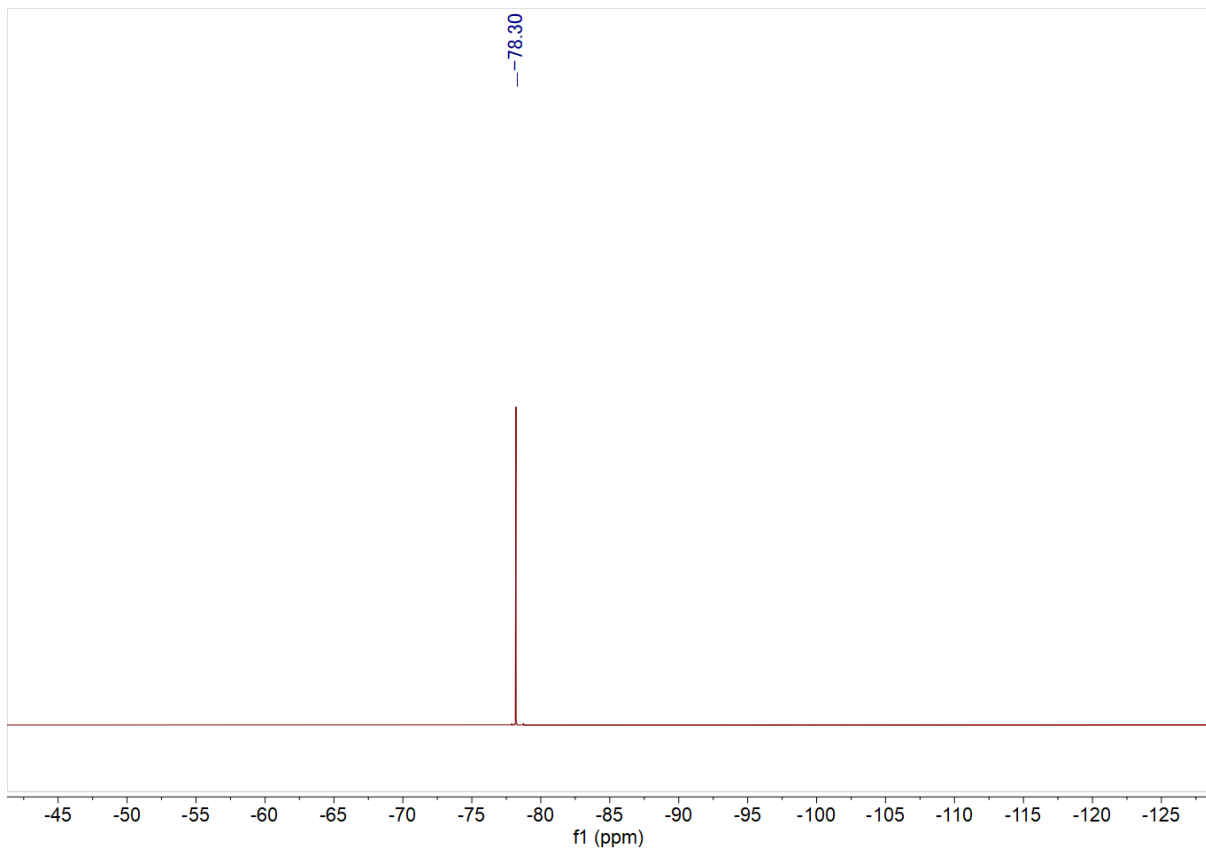


Figure S16. ${}^{19}\text{F}\{{}^1\text{H}\}$ NMR spectrum (377 MHz, CD_3CN , 298 K) of **1ⁱPrPO·DMAP**

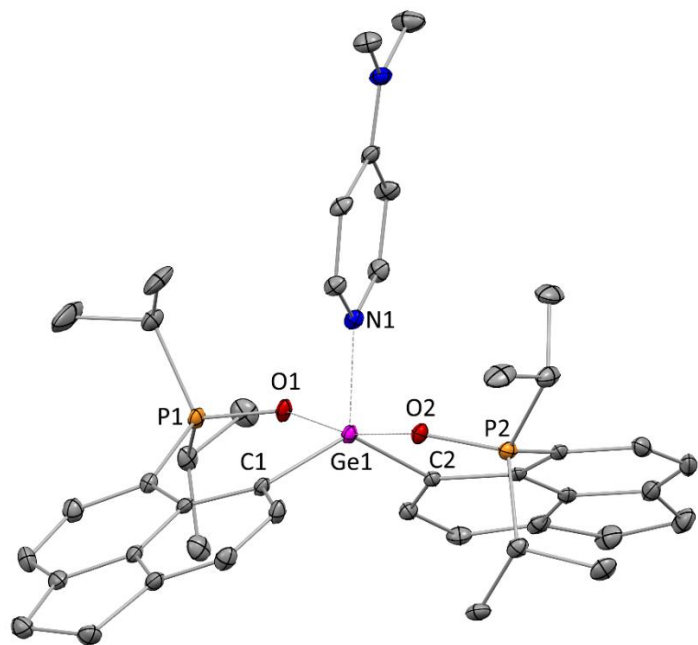


Figure S17. Molecular structure of **1ⁱPrPO·DMAP** in the solid state (thermal ellipsoids at 35%, H atoms and SbF_6^- counter anions are omitted for clarity). Selected bond lengths [\AA] and angle [$^\circ$]: Ge1-N1 = 1.936(3), Ge1-O1 = 1.980(3), Ge1-O2 = 1.981(3), Ge1-C1 = 1.946(4), Ge1-C2 = 1.960(3), P1-O1 = 1.521(3), P2-O2 = 1.523(3), N1-Ge1-C1 = 114.6(2), N1-Ge1-C2 = 114.8(2), N1-Ge1-O1 = 83.4(1), N1-Ge1-O2 = 84.7(1), C1-Ge1-C2 = 130.6(2)

Table S5. Crystal data and structure refinement for Ge- **1^{iPr}PO-DMAP** (CCDC No.: 2416604)

Empirical Formula	C89H114Cl6F24Ge2N4O4P4Sb4	
Color	Colorless	
Formula weight	2728.59 g/mol	
Temperature	150(2) K	
Wavelength	0.71073 Å	
Crystal system	monoclinic	
Space group	C2/c	
Unit cell dimensions	a = 42.865(13) Å b = 16.681(5) Å c = 14.760(4) Å	$\alpha = 90^\circ$ $\beta = 95.368(7)^\circ$ $\gamma = 90^\circ$
Volume	10508.(5) Å ³	
Z	4	
Density (calculated)	1.725 g/cm ³	
Absorption coefficient	1.884 mm ⁻¹	
F(000)	5416	
Size	0.080 x 0.060 x 0.050 mm ³	
Theta range for data collection	0.95 to 25.49°	
Index ranges	-51<=h<=45, -20<=k<=19, -17<=l<=17	
Reflections collected	32893	
Independent reflections	9677 [R(int) = 0.0615]	
completeness to theta = 25.49°	99.2%	
Absorption correction	multi-scan	
Refinement method	Full-matrix least-squares on F2	
Data / restraints / parameters	9677 / 711 / 704	
Goodness-of-fit on F2	1.014	
Final R indices 6688 data; [I>2σ(I)]	R1 = 0.0398, wR2 = 0.0758	
R indices all data	R1 = 0.0784, wR2 = 0.0921	
Largest diff. peak and hole	0.738 and -0.720 eÅ ⁻³	
Extinction coefficient	n/a	

Synthesis of $1^{i\text{Pr}}\text{PO-F}$: To a 20 mL tetrahydrofuran solution of $1^{i\text{Pr}}\text{PO}$ (0.06 g, 0.06 mmol), was added one equivalent of KF (0.003 g, 0.06 mmol) and one equivalent of 18-crown-6 (0.017 g, 0.06 mmol) and stirred overnight at room temperature. The solution was concentrated and layered with hexane or diethyl ether. Colourless single crystals of $1^{i\text{Pr}}\text{PO-F}$ (0.037 g, 60% yield) were obtained from both the solvent combinations. Melting point > 200 °C.

$^1\text{H NMR}$ (400MHz, CDCl_3 , 298 K) 8.36 (d, $J = 7.3$ Hz, 2H, Acn-CH), 7.85-7.80 (dd, $J = 14$ Hz, 7.3 Hz, 2H, Acn-CH), 7.62-7.59 (dd, $J = 7.2$ Hz, 2.0 Hz, 2H, Acn-CH), 7.48 (d, $J = 7.3$ Hz, 2H, Acn-CH) 3.73-3.49 (m, 8H, Acn- CH_2), 2.81-2.74 (m, 4H, $i\text{Pr-CH}$), 1.42-1.15 (m, 24H, $i\text{Pr-CH}_3$).

$^{13}\text{C}\{^1\text{H}\} \text{NMR}$ (101MHz, CDCl_3 , 298 K) 154.74 (d, $J = 3.1$ Hz, Acn-C), 151.88 (d, $J = 1.1$ Hz, Acn-C), 140.55 (s, Acn-C), 139.66 (d, $J = 9.9$ Hz, Acn-CH), 137.74 (d, $J = 5.6$ Hz, Acn-CH), 133.46 (d, $J = 13.2$ Hz, Acn-C), 120.91 (s, Acn-C), 119.84 (d, $J = 14.3$ Hz, Acn-CH), 120.98 (q, $J = 320.2$ Hz, OTf), 113.54 (s, Acn-CH), 112.66 (s, Acn-CH), 70.66 (s, tetrahydrofuran), 30.82 (s, Acn- CH_2), 30.17 (s, Acn- CH_2), 28.10 (d, $J = 9.4$ Hz, $i\text{Pr-CH}$), 27.47 (d, $J = 15.8$ Hz, $i\text{Pr-CH}$), 16.63-16.54 (m, $i\text{Pr-CH}_3$), 15.53-15.42 (m, $i\text{Pr-CH}_3$).

$^{31}\text{P}\{^1\text{H}\} \text{NMR}$ (162 MHz, CDCl_3 , 298 K) = + 77.09 (d, $J = 3.3$ Hz) ppm

$^{19}\text{F}\{^1\text{H}\} \text{NMR}$ (377 MHz, CDCl_3 , 298 K) = - 78.35 (OTf), - 125.17 (s, Ge-F) ppm

MALDI-TOF (CD Matrix): Observed m/z = 663.36 (calculated m/z= 663.20) $[\text{C}_{36}\text{H}_{44}\text{FGeO}_2\text{P}_2]^+$

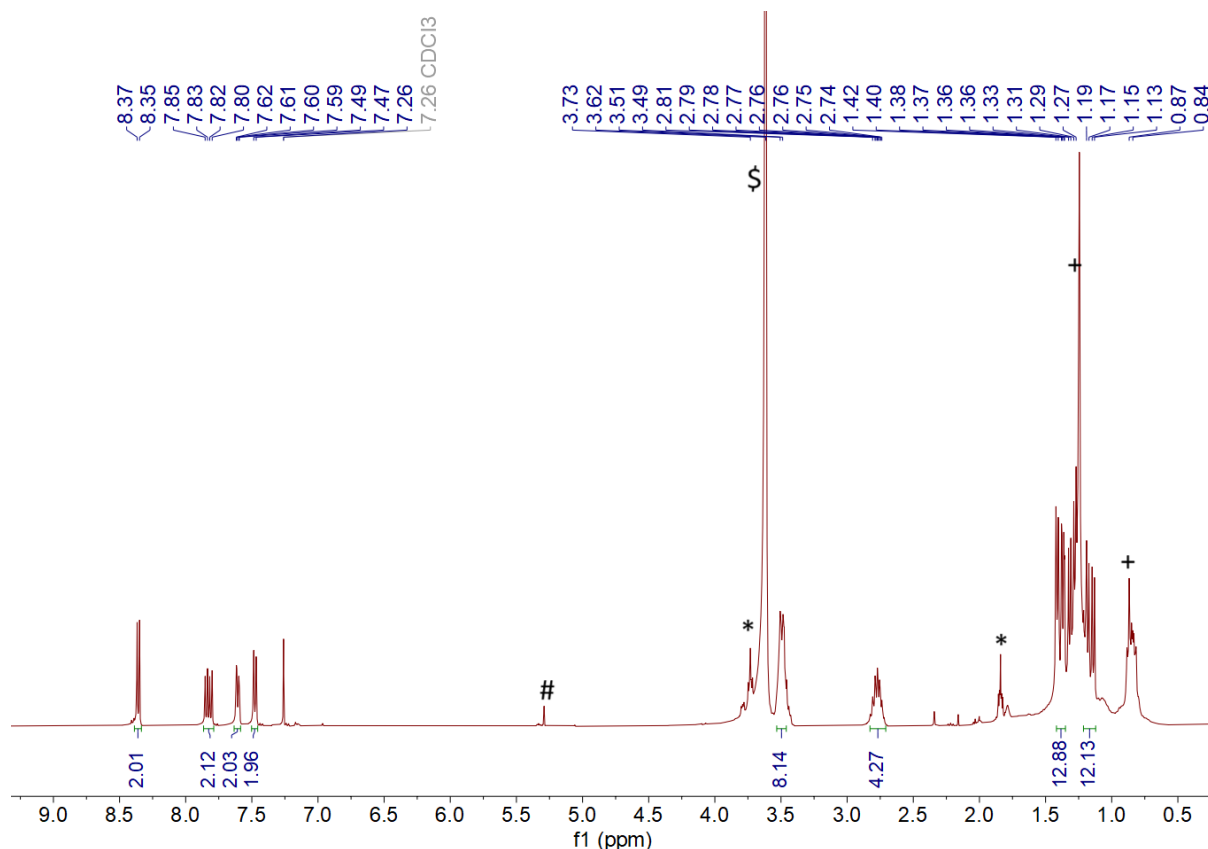


Figure S18. $^1\text{H NMR}$ spectrum (400 MHz, CDCl_3 , 298 K) of $1^{i\text{Pr}}\text{PO-F}$ (# = DCM, * = THF, + = Hexane, \$ = 18-\text{Crown-6})

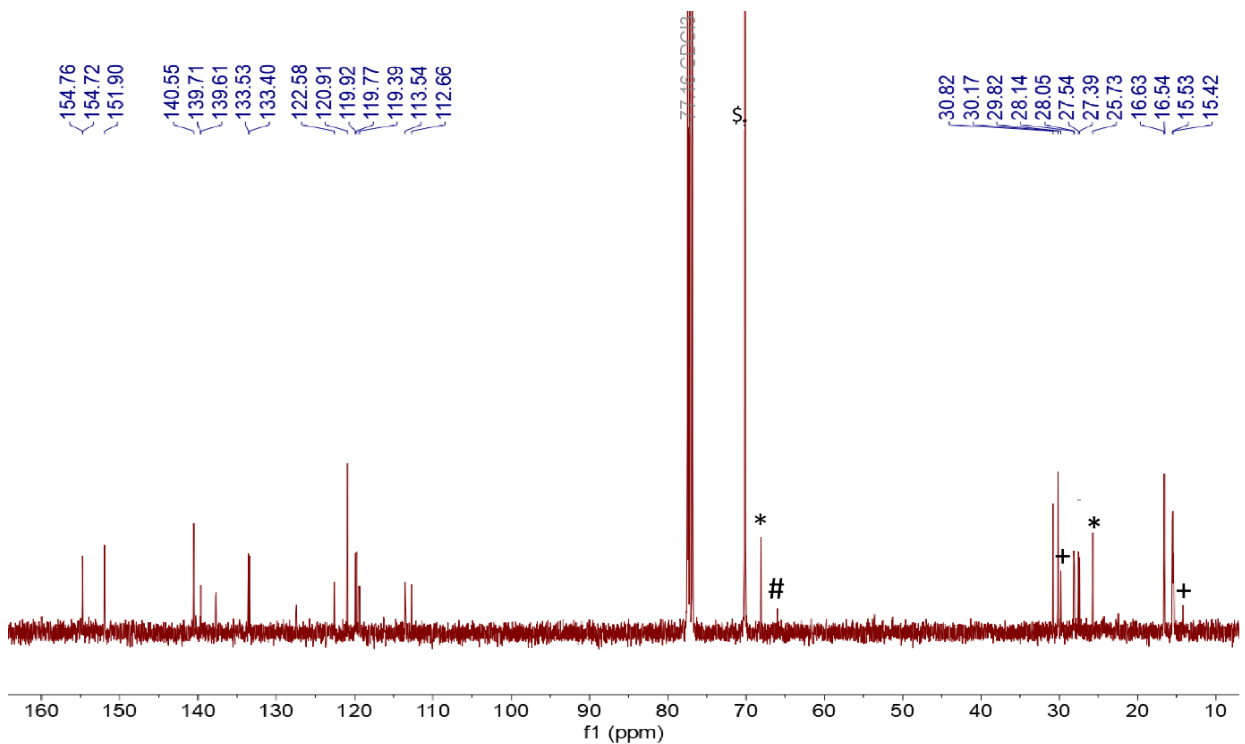


Figure S19. $^{13}\text{C}\{\text{H}\}$ NMR spectrum (101 MHz, CDCl_3 , 298 K) of $\mathbf{1}^{\text{iPr}}\text{PO-F}$ (# = DCM, * = THF, + = Hexane, \$ = 18-Crown-6)

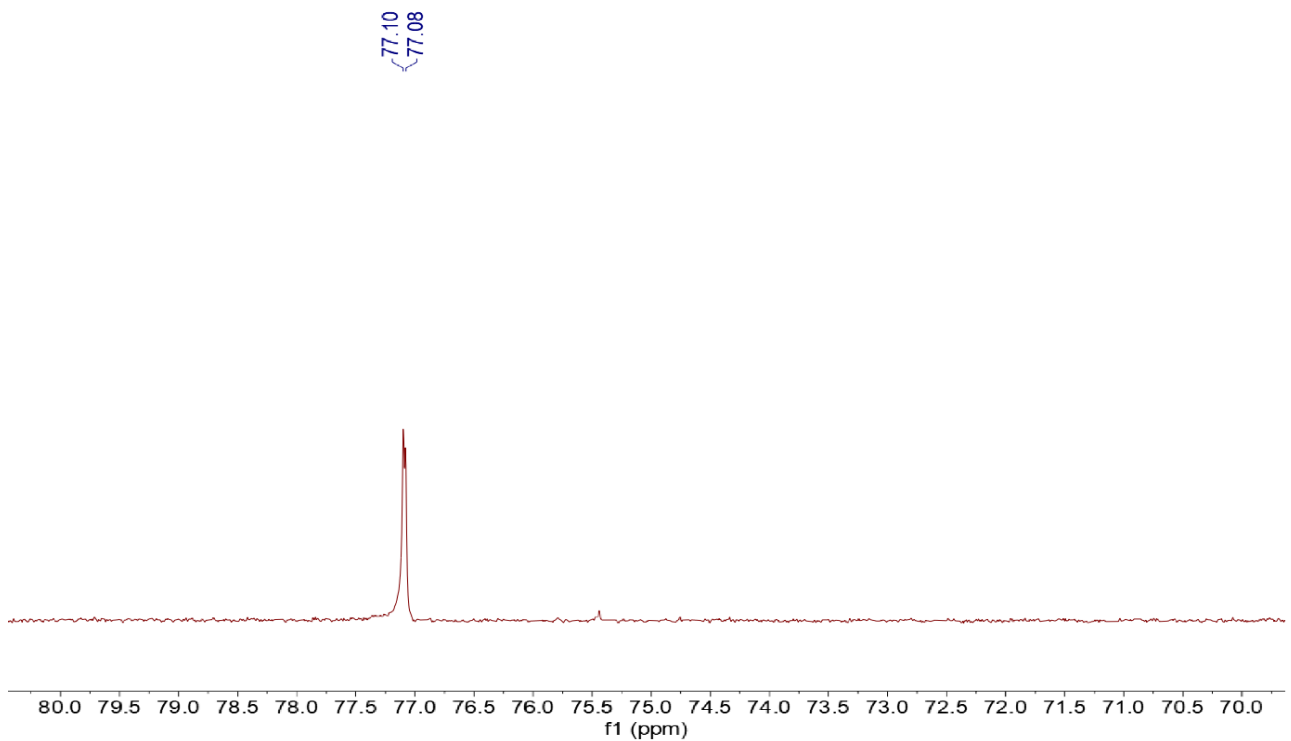


Figure S20. $^{31}\text{P}\{\text{H}\}$ NMR spectrum (162 MHz, CDCl_3 , 298 K) of $\mathbf{1}^{\text{iPr}}\text{PO-F}$

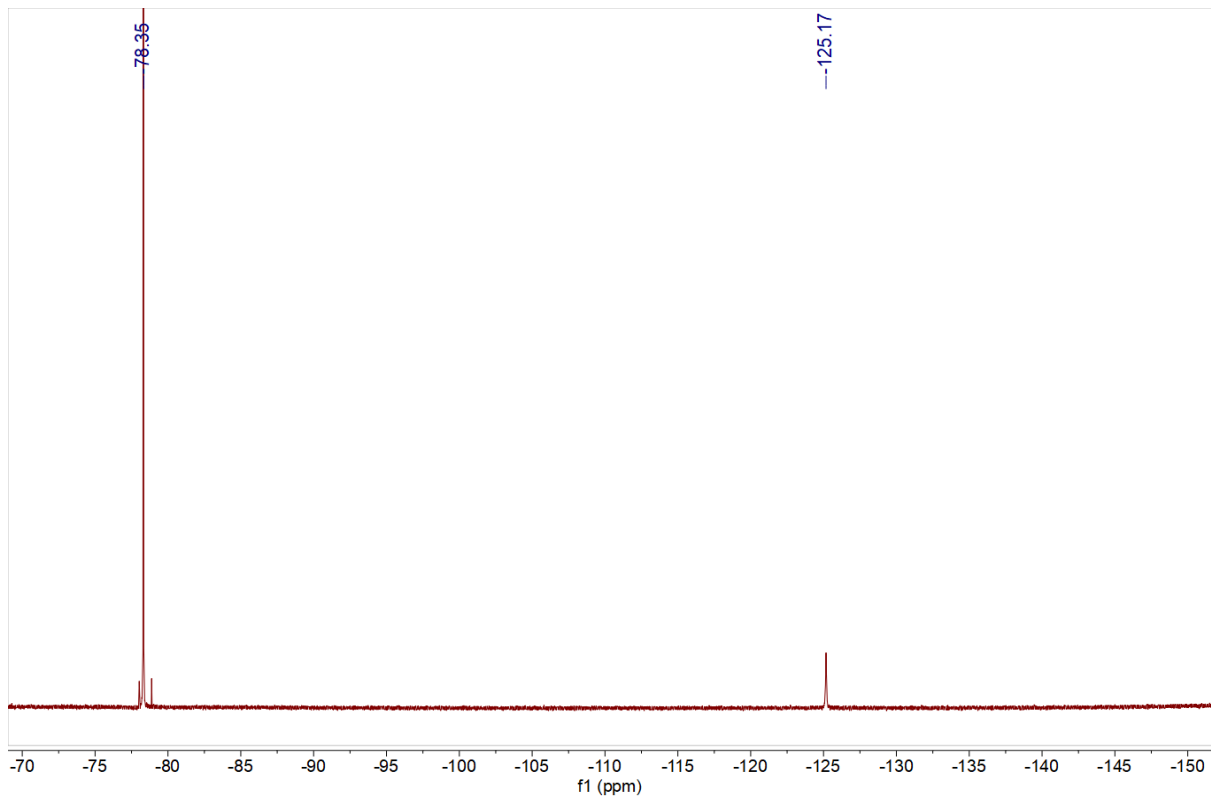


Figure S21. ${}^{19}\text{F}\{{}^1\text{H}\}$ NMR spectrum (377 MHz, CDCl_3 , 298 K) of $\mathbf{1}^{\text{iPr}}\text{PO-F}$

Table S6. Crystal data and structure refinement for **1^{iPr}PO-F** (CCDC No.: 2416606)

Empirical formula	C45 H60 F4 Ge O7 P2 S
Color	Colorless
Formula weight	955.52
Temperature	150(2) K
Wavelength	0.71073 Å
Crystal system	Triclinic
Space group	P $\bar{1}$
Unit cell dimensions	$a = 12.3052(13)$ Å $\alpha = 73.204(3)$ °. $b = 12.8654(14)$ Å $\beta = 72.985(3)$ °. $c = 15.2505(16)$ Å $\gamma = 81.658(3)$ °.
Volume	2205.3(4) Å ³
Z	2
Density (calculated)	1.439 Mg/m ³
Absorption coefficient	0.882 mm ⁻¹
F(000)	1000
Crystal size	0.080 x 0.060 x 0.050 mm ³
Theta range for data collection	1.942 to 25.148°.
Index ranges	-14≤h≤14, -15≤k≤15, -18≤l≤18
Reflections collected	53849
Independent reflections	7874 [R(int) = 0.0594]
Completeness to theta = 25.148°	99.7 %
Absorption correction	multi-scan
Refinement method	Full-matrix least-squares on F2
Data / restraints / parameters	7874 / 0 / 549
Goodness-of-fit on F2	1.056
Final R indices [$I > 2\sigma(I)$]	R1 = 0.0402, wR2 = 0.0857
R indices (all data)	R1 = 0.0595, wR2 = 0.0943
Extinction coefficient	n/a
Largest diff. peak and hole	0.558 and -0.435 e.Å ⁻³

Reaction of $\mathbf{1^{ipr}PO}$ and $\mathbf{TBABF_4}$:

An NMR tube was charged with $\mathbf{1^{ipr}PO}$ (0.015 g, 0.16 mmol) and *n*-tetrabutylammonium tetrafluoroborate ($\mathbf{TBABF_4}$) (0.005 g, 0.24 mmol) taken in 0.5 mL of CD_3CN at room temperature. The reaction was analysed by $^{31}\text{P}\{\text{H}\}$ and $^{19}\text{F}\{\text{H}\}$ NMR spectroscopy at variable temperatures.

^1H NMR (400MHz, CD_3CN , 298 K) δ 8.37- 8.35 (d, J = 7.2 Hz, Acn-C), 8.11- 8.05 (dd, J = 14.5 Hz, 7.5 Hz, Acn-C), 7.99- 7.98 (d, J = 7.1 Hz, Acn-C), 7.88-7.81 (m, Acn-C), 7.71-7.69 (d, J = 7.1 Hz, Acn-C), 7.62-7.61(d, J = 7.4Hz, Acn-C), 7.55- 7.53 (d, J = 7.2Hz, Acn-C), 3.59- 3.44 (m, Acn- CH_2), 3.06-3.01 (m, TBA), 2.78-2.72 (m, $^{i}\text{Pr}-\text{CH}$), 1.57-1.53 (m, TBA), 1.31- 1.02 (m, $^{i}\text{Pr}-\text{CH}_3$), 0.94- 0.91 (m, TBA)

$^{31}\text{P}\{\text{H}\}$ NMR (162 MHz, CD_3CN , 298K) = + 77.86 ppm

$^{31}\text{P}\{\text{H}\}$ NMR (162 MHz, CD_3CN , 248K) = + 78.07 (d, J = 3.6 Hz) ppm

$^{19}\text{F}\{\text{H}\}$ NMR (377 MHz, CD_3CN , 248K) = -79.61 (s, OTf), -125.89 (s, Ge-F), -150.05 (br., $\text{BF}_3\text{CH}_3\text{CN}$), -150.89 (br., $\mathbf{TBABF_4}$)

$^{11}\text{B}\{\text{H}\}$ NMR (128 MHz, CD_3CN , 248K) = -1.05 (br., $\text{BF}_3\text{CH}_3\text{CN}$), -1.20 (br., BF_4^-)

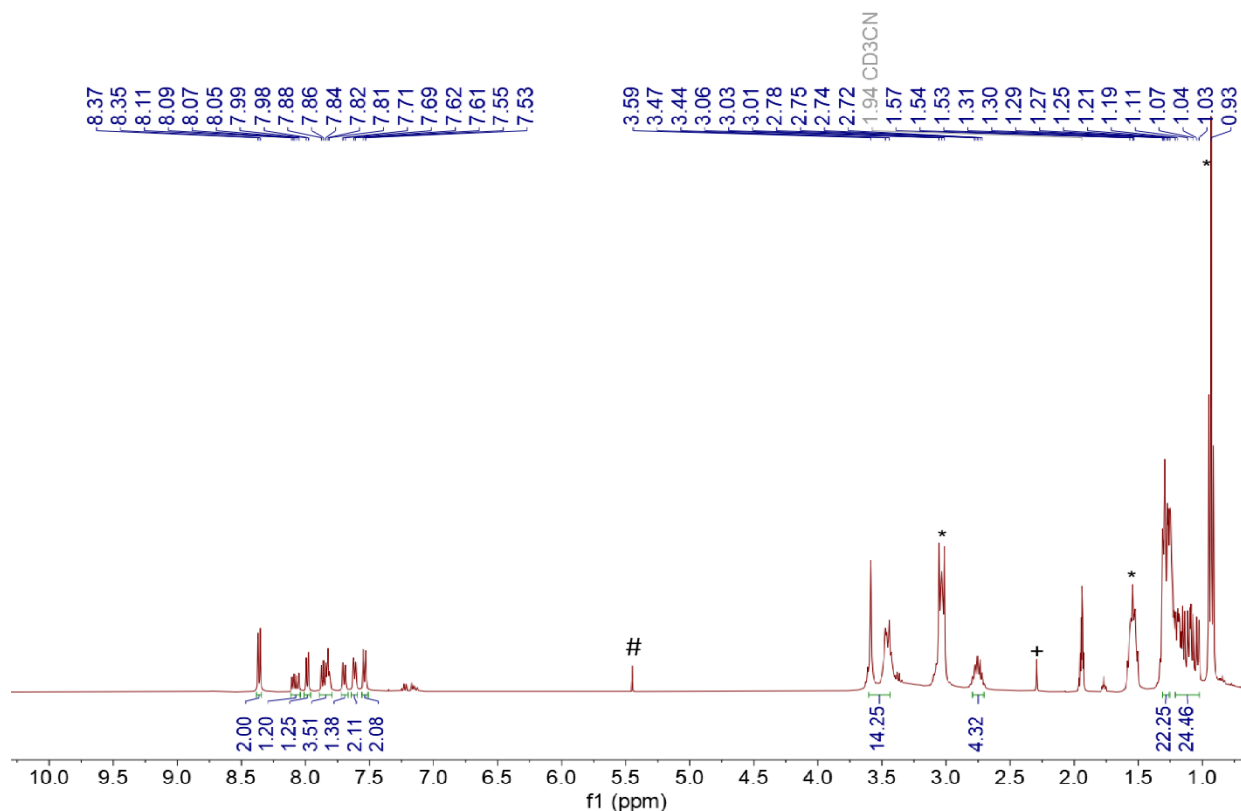


Figure S22. ^1H NMR spectrum (400 MHz, CD_3CN , 248 K) of the reaction mixture $\mathbf{1^{ipr}PO}$ and $\mathbf{TBABF_4}$ [<# = DCM, * = Tetrabutyl ammonium cation, + = Trace amount of H_2O]

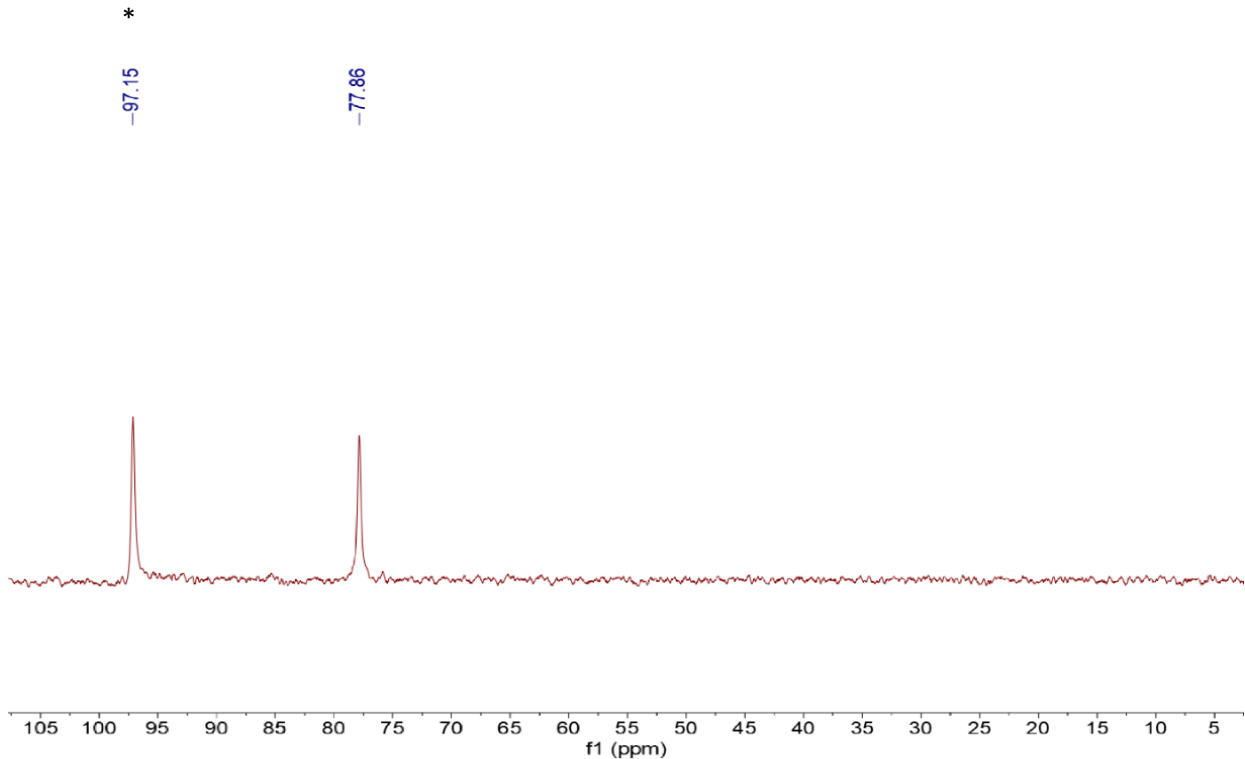


Figure S23. $^{31}\text{P}\{^1\text{H}\}$ NMR spectrum (162 MHz, CD_3CN , 298 K) of the reaction mixture $\mathbf{1}^{\text{iPrPO}}$ and TBABF_4 . (* = $\mathbf{1}^{\text{iPrPO}}$)

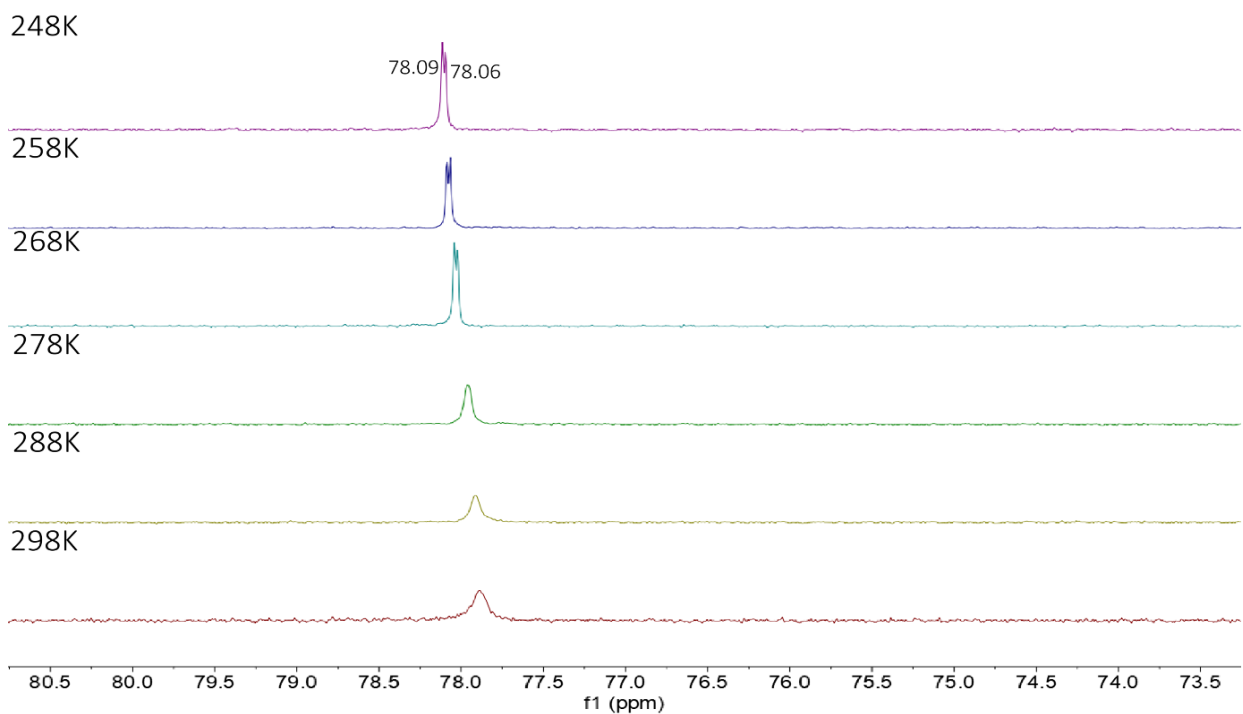


Figure S24. Variable temperature $^{31}\text{P}\{^1\text{H}\}$ NMR spectra (162 MHz, CD_3CN) of the reaction mixture $\mathbf{1}^{\text{iPrPO}}$ and TBABF_4 .

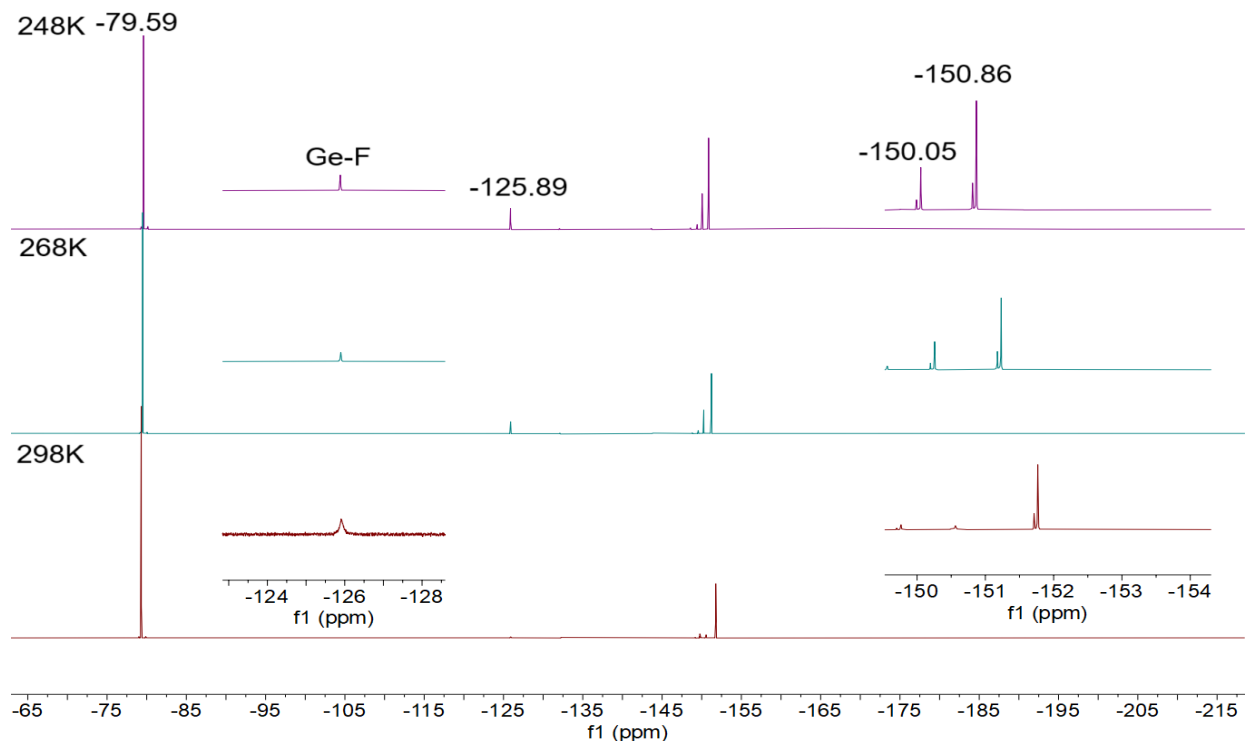


Figure S25. Variable temperature $^{19}\text{F}\{^1\text{H}\}$ NMR spectra (377 MHz, CD_3CN) of the reaction mixture $\mathbf{1}^{\text{iPr}}\text{PO}$ and TBABF_4 .

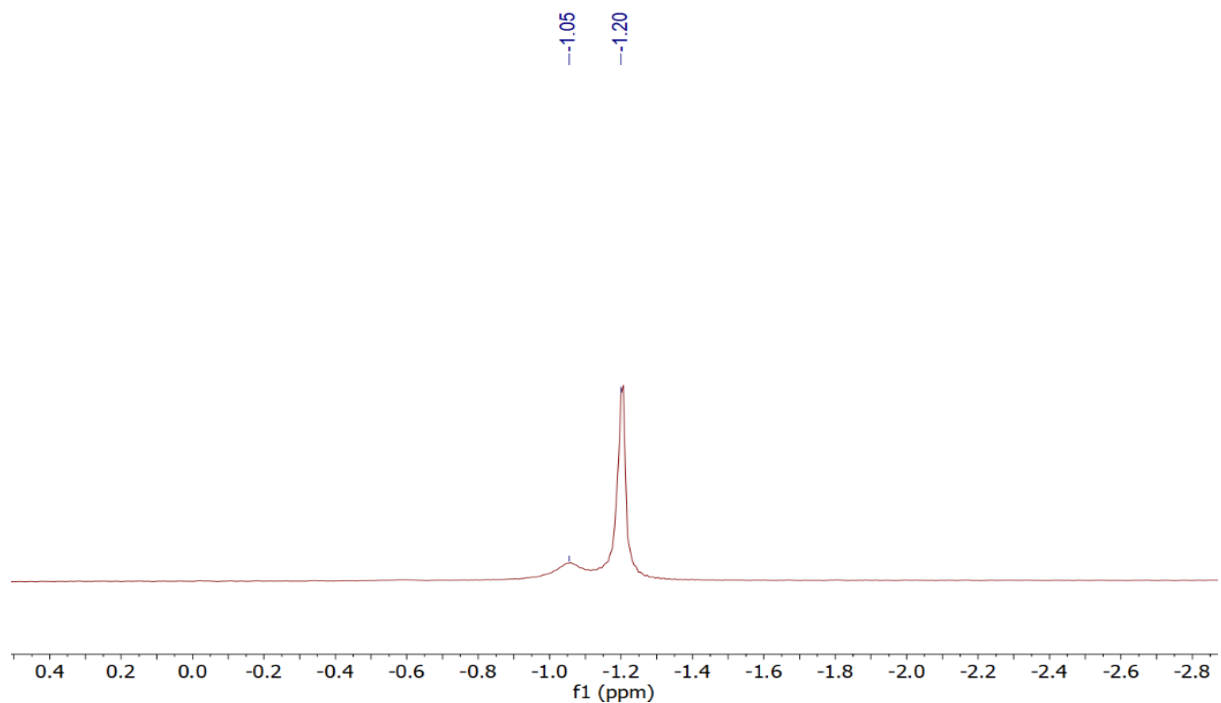


Figure S26. ^{11}B NMR spectra (128 MHz, CD_3CN) of the reaction mixture $\mathbf{1}^{\text{iPr}}\text{PO}$ and TBABF_4 .

Reaction of $1^{i\text{pr}}\text{PO}$ and AgSbF_6 :

An NMR tube was charged with **1^{pr}PO** (0.02 g, 0.02 mmol) and slight excess silver hexafluoroantimonate (AgSbF_6) taken in 0.5 mL of CD_3CN . The solution was heated at 75 °C for 12 hours period and analyzed by $^{31}\text{P}\{^1\text{H}\}$ and $^{19}\text{F}\{^1\text{H}\}$ NMR spectroscopy.

$^{31}\text{P}\{\text{H}\}$ NMR (162MHz, CD₃CN, 298 K) δ = + 97.13, + 77.87 ppm.

³¹P{¹H} NMR (162 MHz, CD₃CN, 248 K) δ = +97.17, 78.07 (d, *J* = 3.5 Hz) ppm.

¹⁹F{¹H} NMR (377MHz, CD₃CN, 248 K) δ = - 79.58 (OTf⁻), -125.88 (s, Ge-F) ppm.

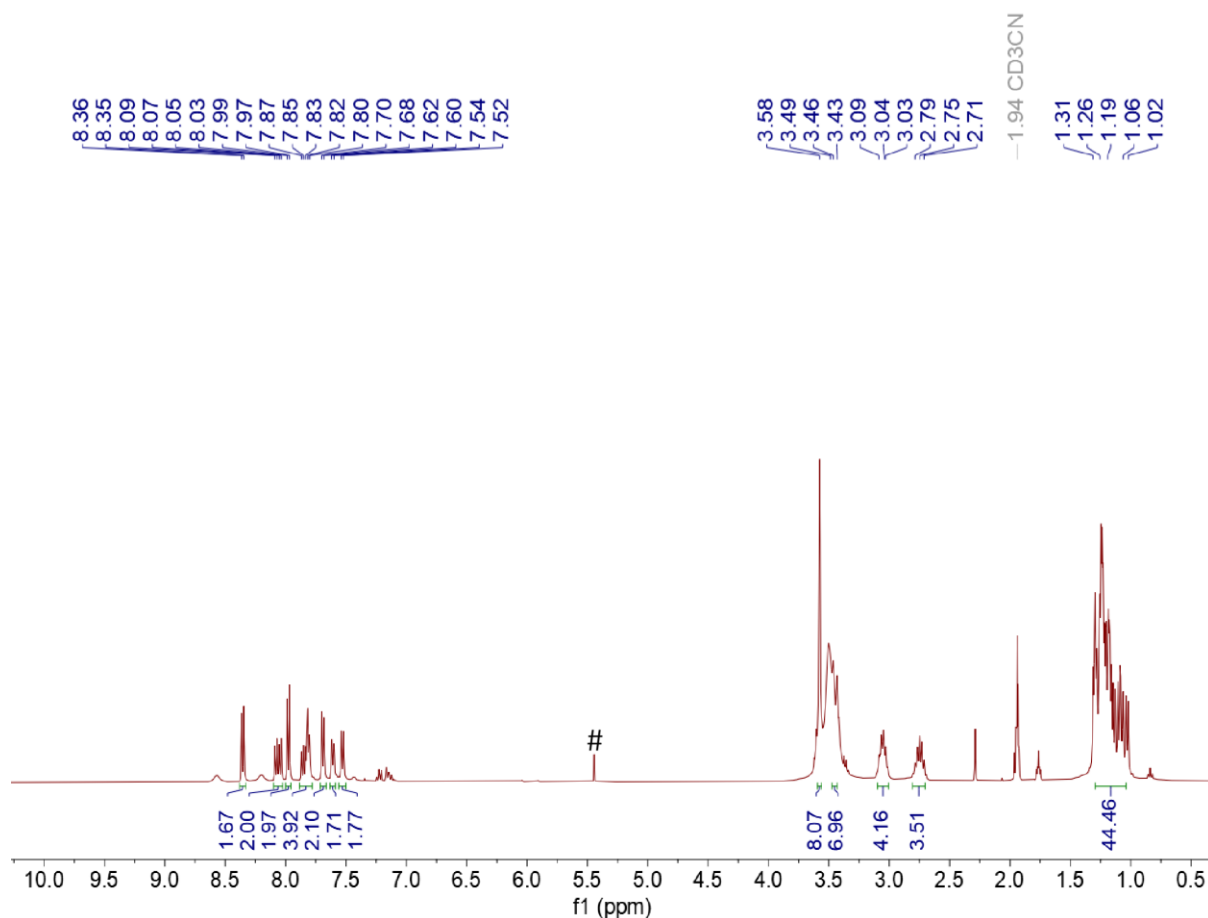


Figure S27. ^1H NMR spectrum (400 MHz, CD_3CN , 248K) of the reaction mixture **1^{iPr}PO** and **AgSbF₆** (# = DCM)

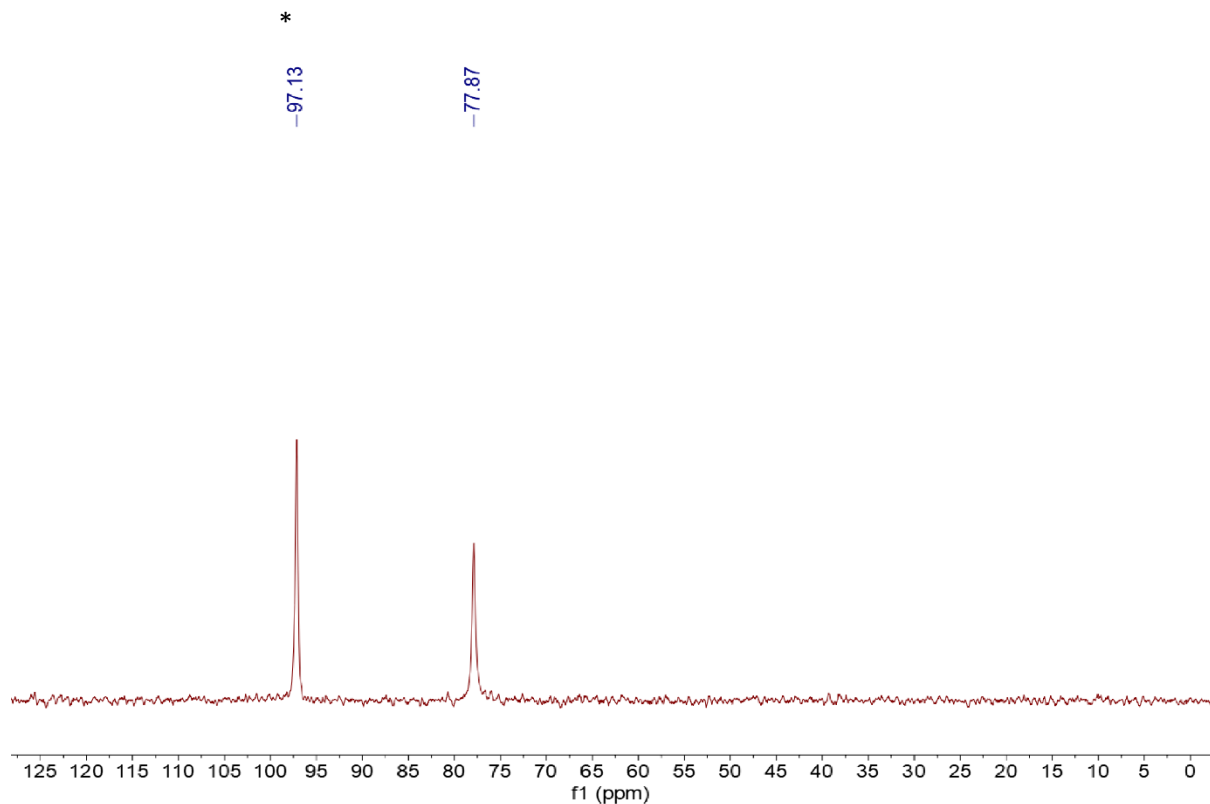


Figure S28 $^{31}\text{P}\{\text{H}\}$ NMR spectrum (162 MHz, CD_3CN , 298 K) of the reaction mixture **1*i*PrPO** and **AgSbF₆**. (* = **1*i*PrPO**)

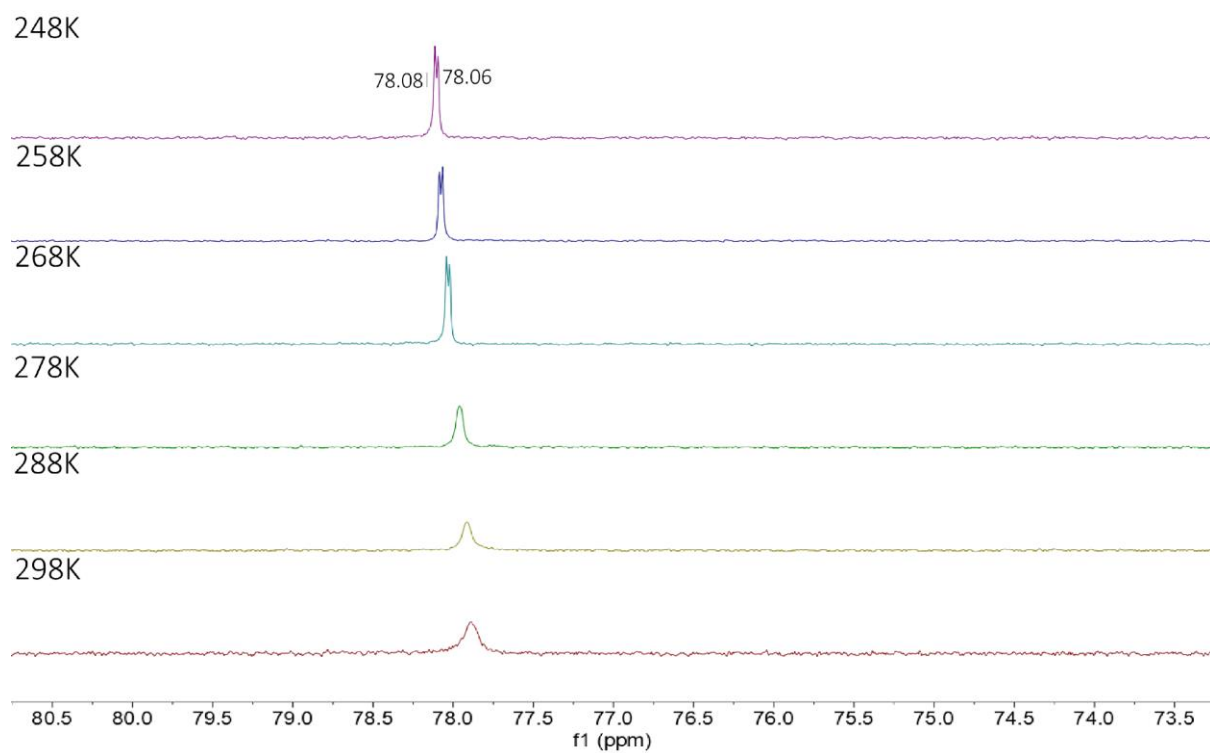


Figure S29. Variable temperature $^{31}\text{P}\{\text{H}\}$ NMR spectra (162MHz, CD_3CN) of the reaction mixture **1*i*PrPO** and **AgSbF₆**.

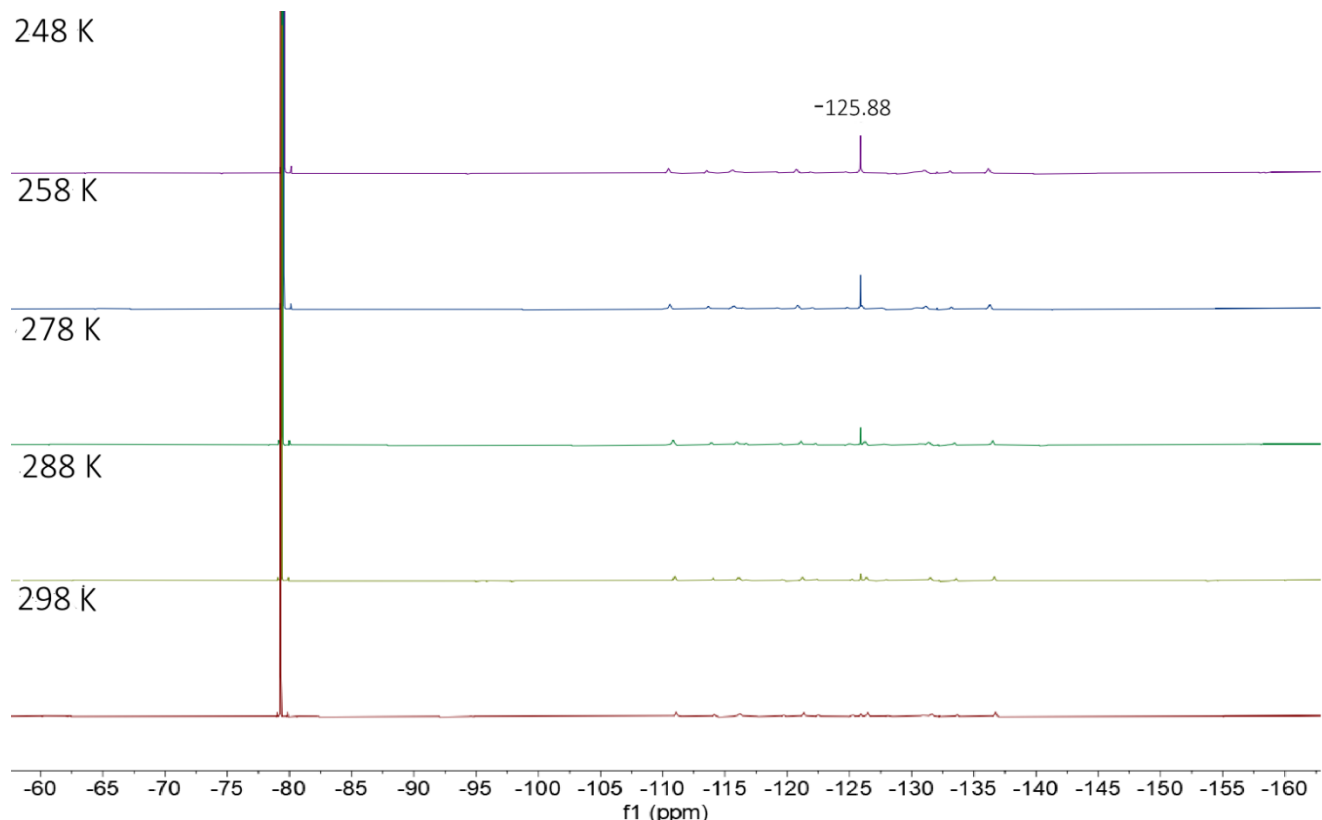


Figure S30. Variable temperature $^{19}\text{F}\{^1\text{H}\}$ NMR spectra (377 MHz, CD_3CN) of the reaction mixture 1^{ipr}PO and AgSbF_6 .

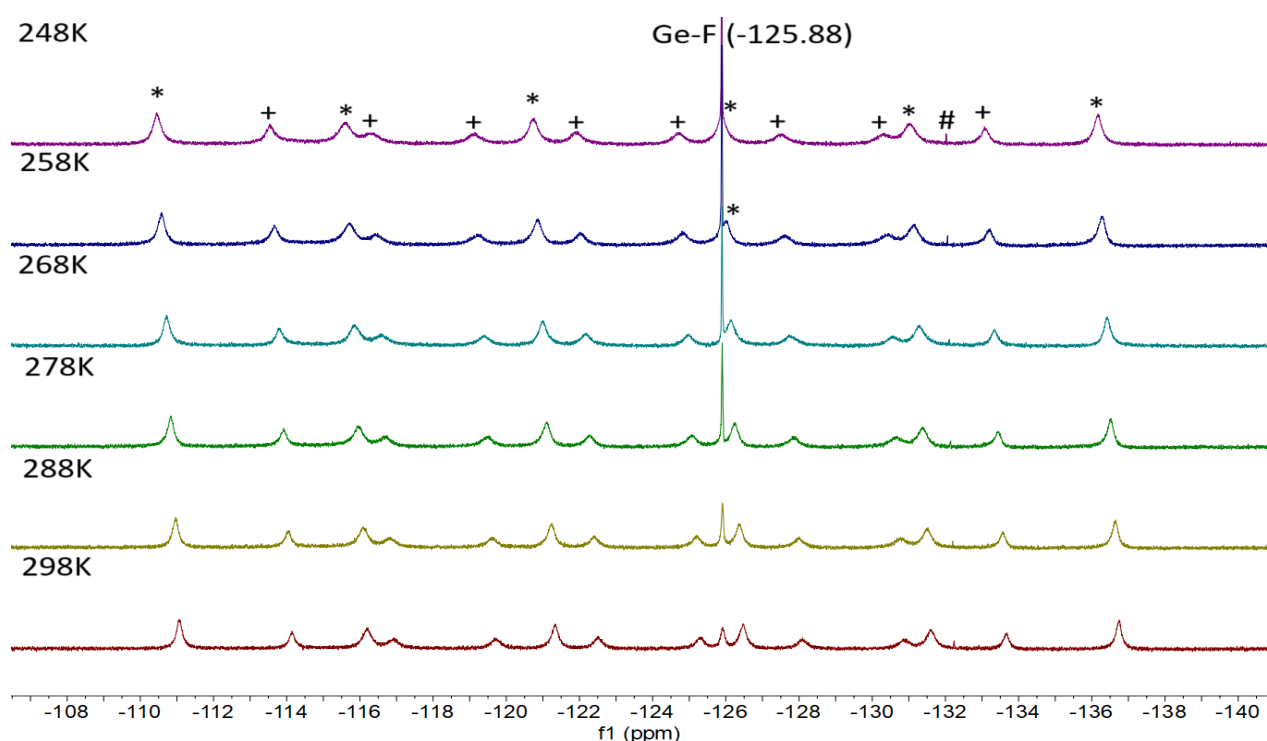


Figure S31. Variable temperature (Zoom-in) $^{19}\text{F}\{^1\text{H}\}$ NMR spectra (377 MHz, CD_3CN) of the reaction mixture 1^{ipr}PO and AgSbF_6 [*, + denote multiplet arising from $^1J(^{19}\text{F}-^{121}\text{Sb})$ and $^1J(^{19}\text{F}-^{123}\text{Sb})$ coupling respectively, # = tentatively assigned to SbF_5]

Synthesis of $\mathbf{1}^{\text{Pr}}\text{PO-H}$: To a 20 mL tetrahydrofuran solution of $\mathbf{1}^{\text{Pr}}\text{PO}$ (0.042 g, 0.04 mmol), was added one equivalent of NaBH_4 (0.016 g, 0.04 mmol) and stirred overnight at room temperature. The solution was filtered and layered with pentane. Colourless single crystals of $\mathbf{1}^{\text{Pr}}\text{PO-H}$ (0.026 g, 76% yield) were obtained at room temperature. Melting point > 200 °C.

^1H NMR (400 MHz, CD_3CN , 298 K) 8.29 (d, $J = 7.3$ Hz, 2H, Acn- CH), 7.85-7.80 (dd, $J = 14.0$ Hz, 7.3 Hz, 2H, Acn- CH), 7.60-7.58 (dd, $J = 7.3$ Hz, 1.6 Hz, 2H, Acn- CH), 7.49 (d, $J = 7.4$ Hz, 2H, Acn- CH), 7.23 (s, 1H, Ge- H), 3.50-3.41 (m, 8H, Acn- CH_2), 2.83-2.69 (m, 4H, $^{\text{Pr}}\text{-CH}$), 1.36-1.07 (m, 24H, $^{\text{Pr}}\text{-CH}_3$).

$^{13}\text{C}\{^1\text{H}\}$ NMR (101MHz, CD_3CN , 298 K) 156.00 (d, $J = 2.9$ Hz, Acn-C), 151.92 (d, $J = 1.4$ Hz, Acn-C), 140.24 (d, $J = 9.9$ Hz, Acn- CH), 140.10 (s, Acn-C), 139.02 (d, $J = 5.4$ Hz, Acn- CH), 134.35 (d, $J = 12.8$ Hz, Acn-C), 121.75 (s, Acn-C) 120.18 (d, $J = 14$ Hz, Acn-C), 114.52 (s, Acn- CH), 113.64 (s, Acn- CH), 31.34 (s, Acn- CH_2), 30.59 (s, Acn- CH_2), 28.18 (d, $J = 24.2$ Hz, $^{\text{Pr}}\text{-CH}$), 27.54 (d, $J = 29.7$ Hz, $^{\text{Pr}}\text{-CH}$), 17.47 (d, $J = 2.1$ Hz, $^{\text{Pr}}\text{-CH}_3$), 16.52 (d, $J = 3$ Hz, $^{\text{Pr}}\text{-CH}_3$), 15.93 (d, $J = 3$ Hz, $^{\text{Pr}}\text{-CH}_3$) 15.44 (d, $J = 3.7$ Hz, $^{\text{Pr}}\text{-CH}_3$)

$^{31}\text{P}\{^1\text{H}\}$ NMR (161 MHz, CD_3CN , 298 K) $\delta = + 73.55$ ppm

$^{19}\text{F}\{^1\text{H}\}$ NMR (377 MHz, CD_3CN , 298 K) $\delta = - 79.34$ ppm

MALDI-TOF (CD Matrix): Observed m/z = 645.34 (calculated m/z= 645.21) $[\text{C}_{36}\text{H}_{45}\text{GeO}_2\text{P}_2]^+$

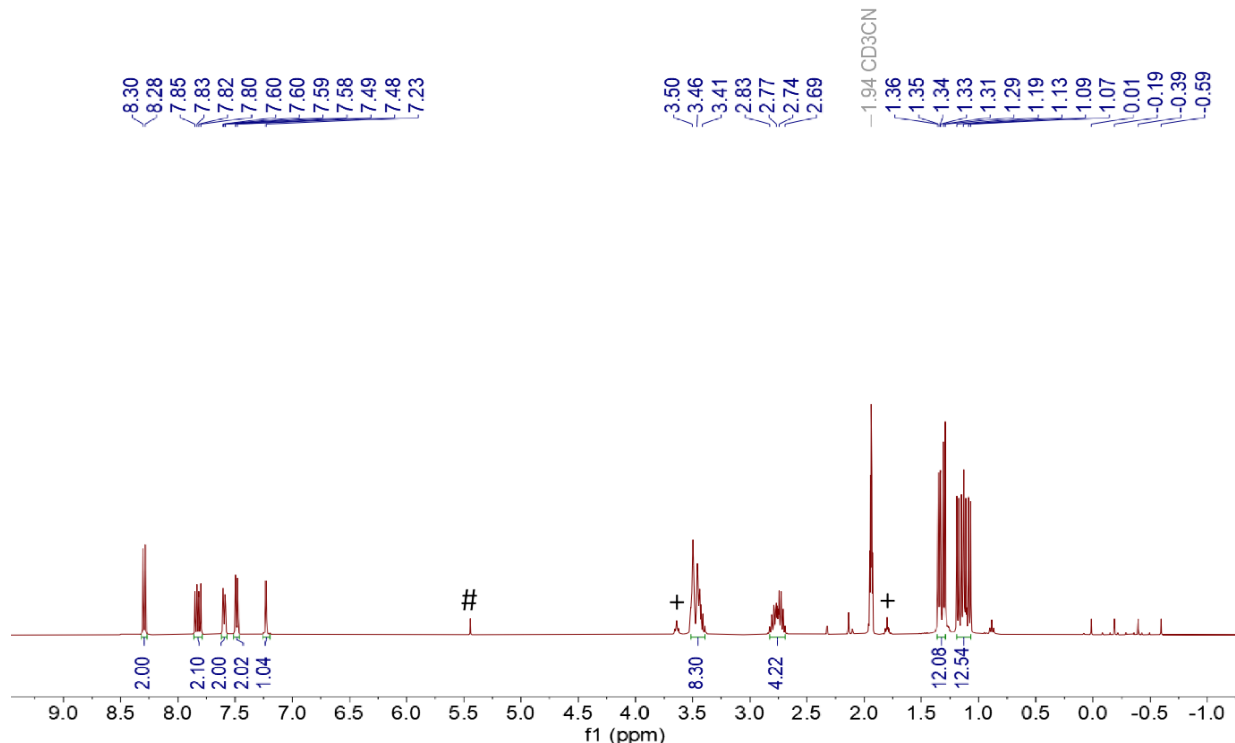


Figure S32. ^1H NMR spectrum (400 MHz, CD_3CN , 298 K) of $\mathbf{1}^{\text{Pr}}\text{PO-H}$ (# = DCM, + = THF)

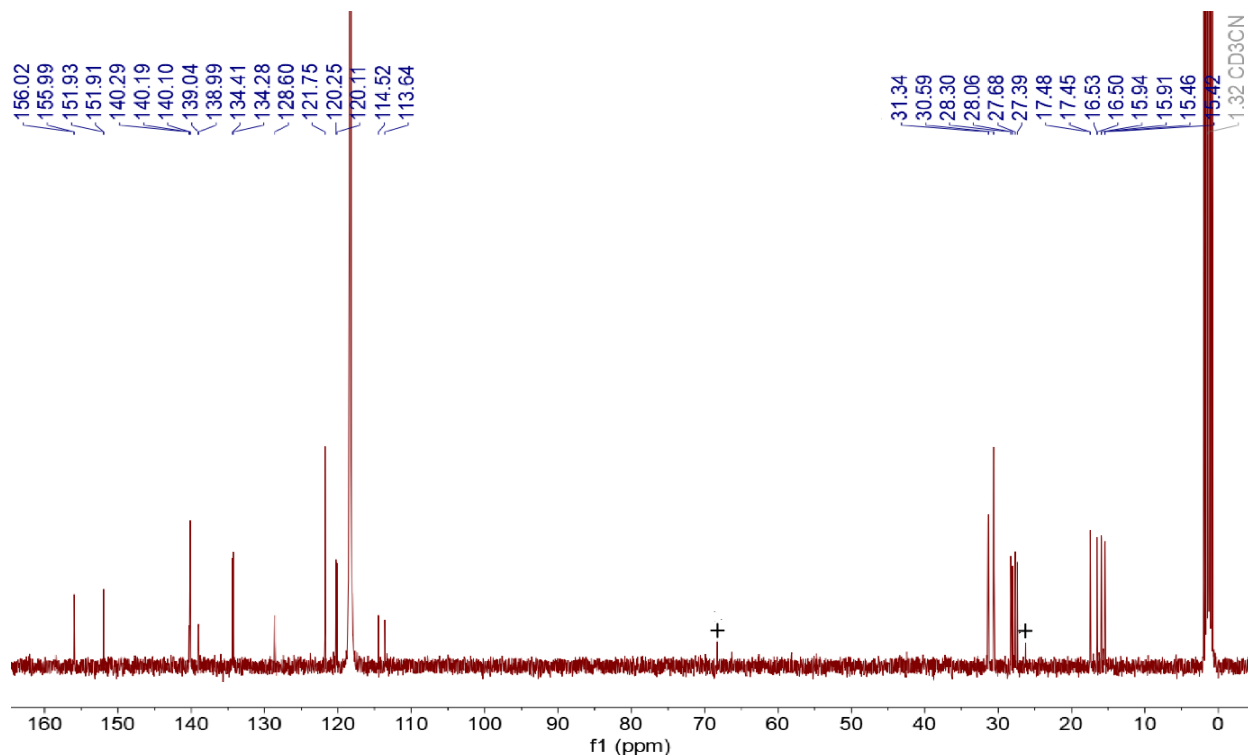


Figure S33. $^{13}\text{C}\{\text{H}\}$ NMR spectrum (101 MHz, CD_3CN , 298 K) of $\mathbf{1}^{\text{iPr}}\text{PO-H}$ (+ = THF)

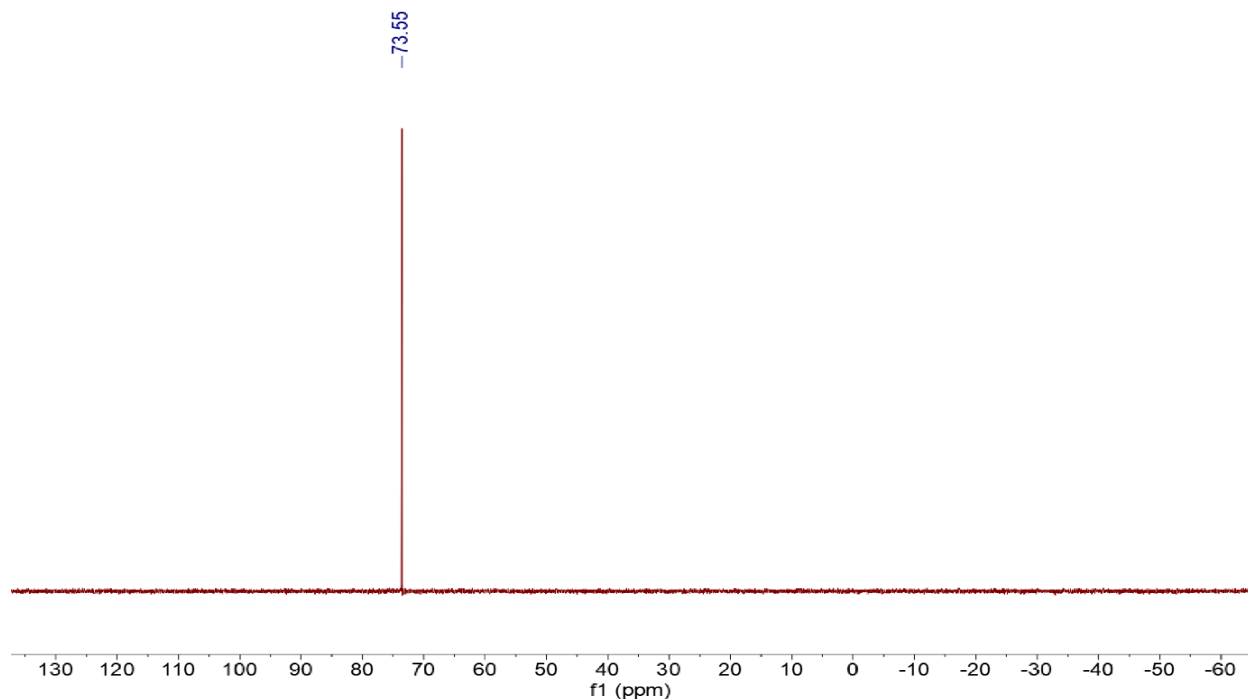


Figure S34. $^{31}\text{P}\{\text{H}\}$ NMR spectrum (162 MHz, CD_3CN , 298 K) of $\mathbf{1}^{\text{iPr}}\text{PO-H}$

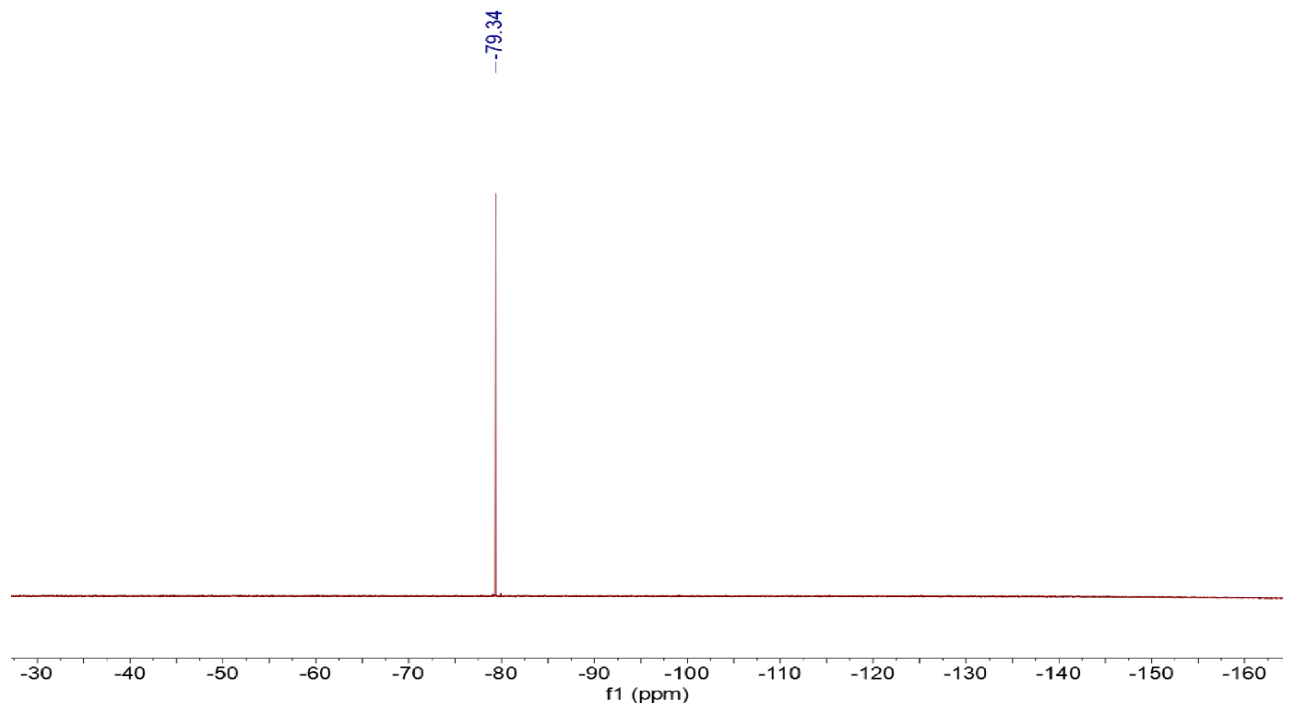


Figure S35. $^{19}\text{F}\{^1\text{H}\}$ NMR spectrum (377 MHz, CD_3CN , 298 K) of **1*i*PrPO-H**

Table S7. Crystal data and structure refinement for **1^{Pr}PO-H** (CCDC No.: 2416610)

Empirical formula	C37 H45 F3 Ge O5 P2 S
Color	Colourless
Formula weight	793.32
Temperature	150(2) K
Wavelength	0.71073 Å
Crystal system	Triclinic
Space group	P $\bar{1}$
Unit cell dimensions	$a = 10.665 \text{ \AA}$ $b = 11.806 \text{ \AA}$ $c = 14.963 \text{ \AA}$ $\alpha = 94.40^\circ$. $\beta = 96.59^\circ$. $\gamma = 98.32^\circ$.
Volume	1843.4 Å ³
Z	2
Density (calculated)	1.429 Mg/m ³
Absorption coefficient	1.031 mm ⁻¹
F(000)	824
Crystal size	0.100 x 0.060 x 0.050 mm ³
Theta range for data collection	2.122 to 25.193°.
Index ranges	-12<=h<=12, -14<=k<=14, -17<=l<=17
Reflections collected	16107
Independent reflections	6572 [R(int) = 0.0573]
Completeness to theta = 25.193°	98.9 %
Absorption correction	multi-scan
Refinement method	Full-matrix least-squares on F ₂
Data / restraints / parameters	6572 / 0 / 460
Goodness-of-fit on F ₂	1.037
Final R indices [I>2sigma(I)]	R1 = 0.0426, wR2 = 0.0892
R indices (all data)	R1 = 0.0689, wR2 = 0.0993
Extinction coefficient	n/a
Largest diff. peak and hole	0.406 and -0.470 e.Å ⁻³

Reaction of $\mathbf{1^{ipr}PO}$ and $\mathbf{Et_3SiH}$:

An NMR tube was charged with $\mathbf{1^{ipr}PO}$ (0.02 g, 0.02 mmol) and triethylsilane (3.3 μL , 0.02 mmol) taken in 0.5 mL of CD_3CN . The reaction mixture was analyzed by $^{31}\text{P}\{^1\text{H}\}$ and $^{19}\text{F}\{^1\text{H}\}$ NMR spectroscopy after 12 hours at room temperature.

$^{31}\text{P}\{^1\text{H}\}$ NMR (162 MHz, CD_3CN , 298 K) = + 97.20 ppm, + 73.55 ppm

$^{19}\text{F}\{^1\text{H}\}$ NMR (377 MHz, CD_3CN , 298 K) = - 79.34 ppm

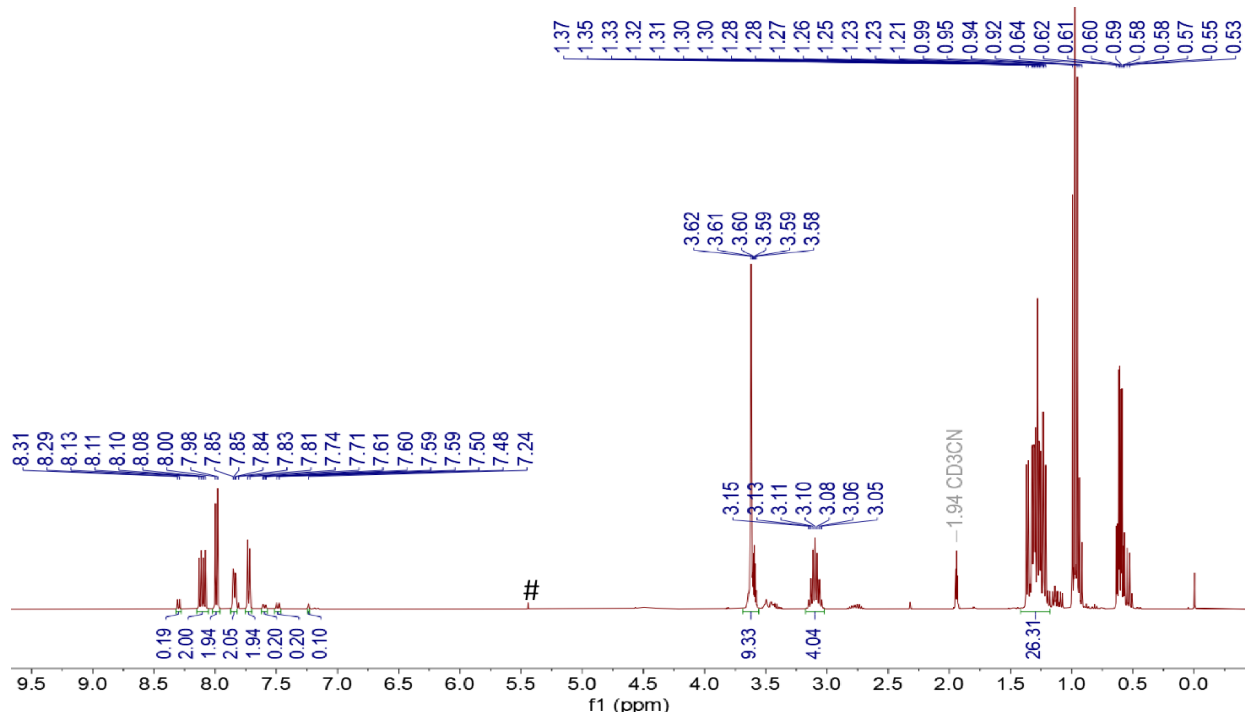


Figure S36. ^1H NMR spectrum (400 MHz, CD_3CN , 298 K) of the reaction mixture (# = DCM)

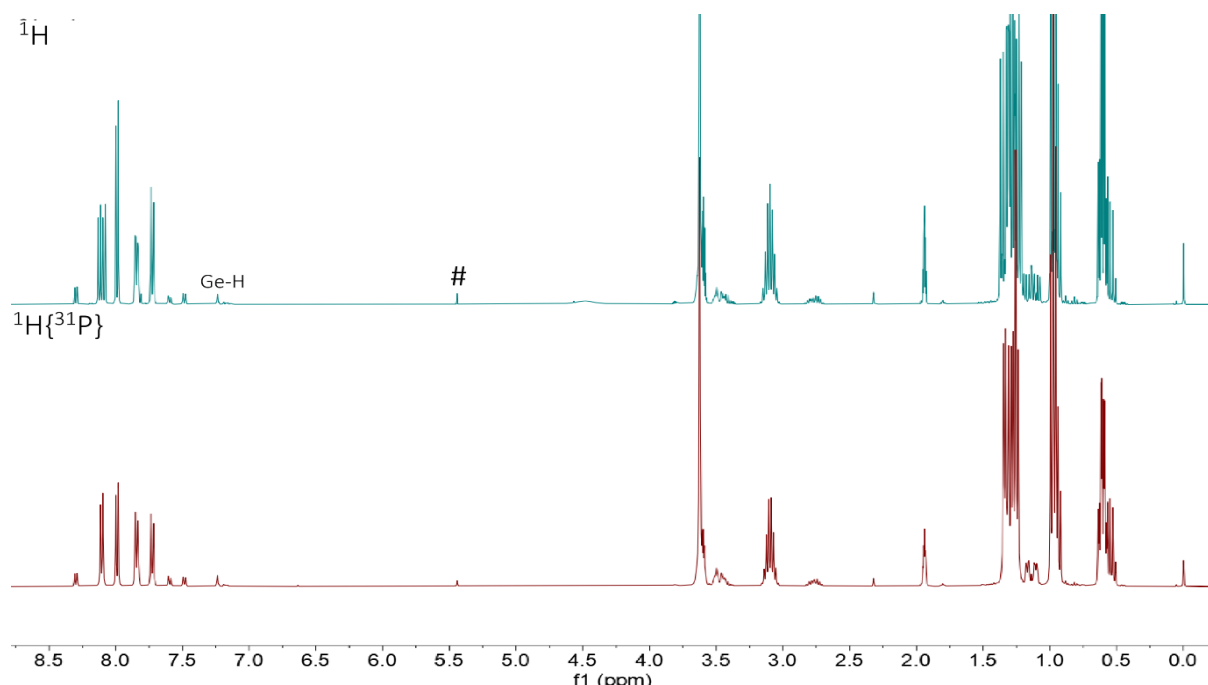


Figure S37. ^1H and $^1\text{H}\{^{31}\text{P}\}$ NMR spectra (CD_3CN , 298 K) of the reaction mixture (# = DCM)

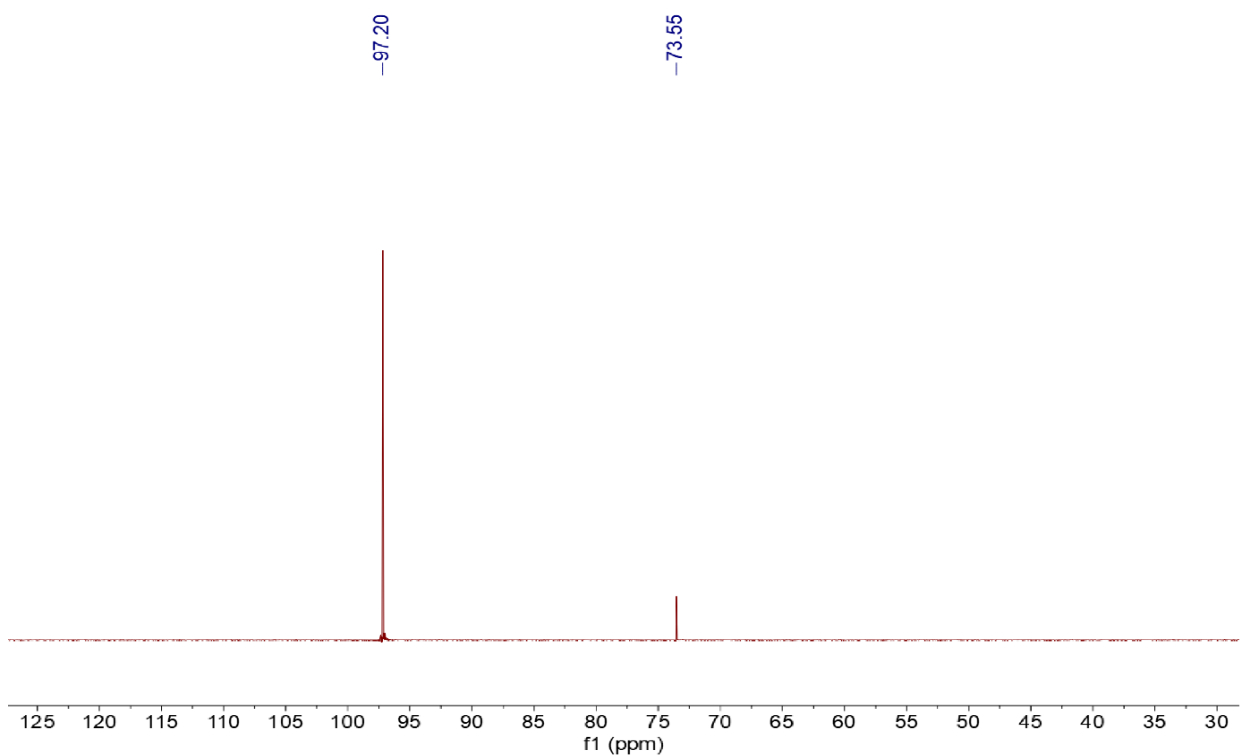


Figure S38. $^{31}\text{P}\{\text{H}\}$ NMR spectrum (162 MHz, CD_3CN , 298 K) of the reaction mixture

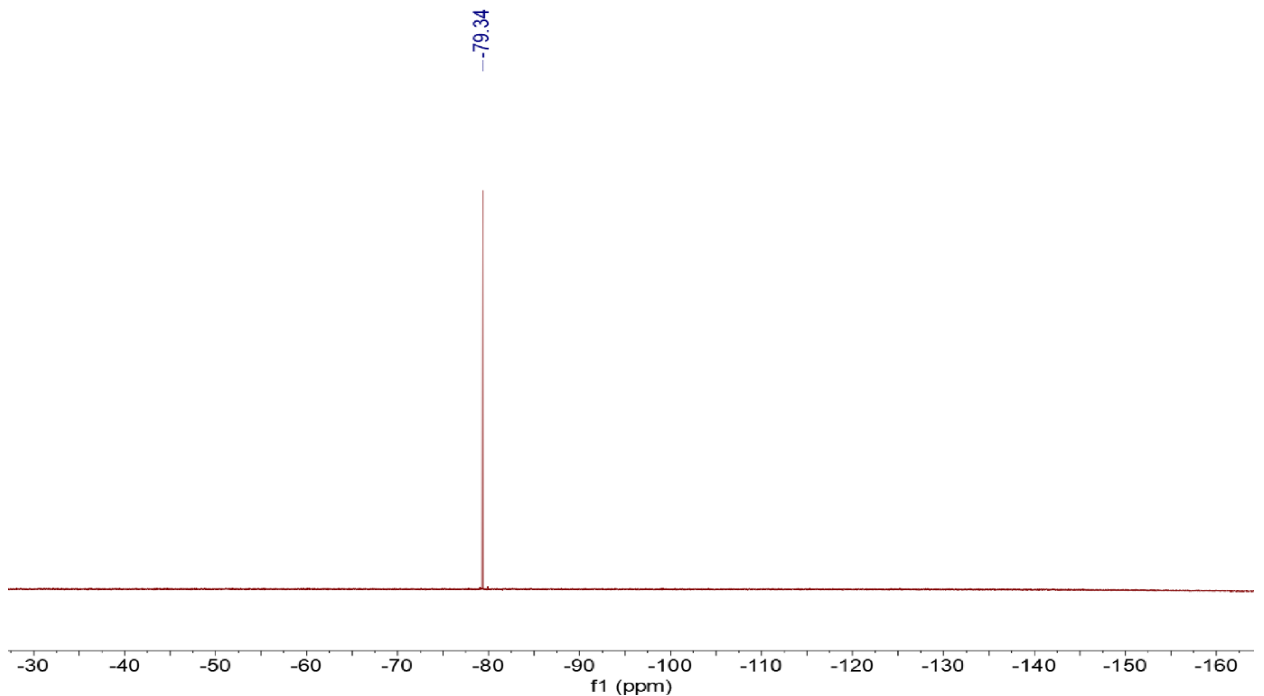


Figure S39. $^{19}\text{F}\{\text{H}\}$ NMR spectrum (377 MHz, CD_3CN , 298 K) of the reaction mixture

Catalytic Applications

Hydrodefluorination of 1-Adamantyl Fluoride using Ph₃SiH as the hydride source:

An NMR tube was charged with 1-Fluoroadamantane (0.015 g, 0.1 mmol), Ph₃SiH (26 μ L, 0.1 mmol), catalyst **1^PrPO** (0.0005 mmol) in CD₃CN (0.5 mL). The reaction mixture was heated at 75 °C. ¹H NMR measurements were carried out at various time intervals and the conversion was calculated by integration against internal standard hexafluorobenzene.

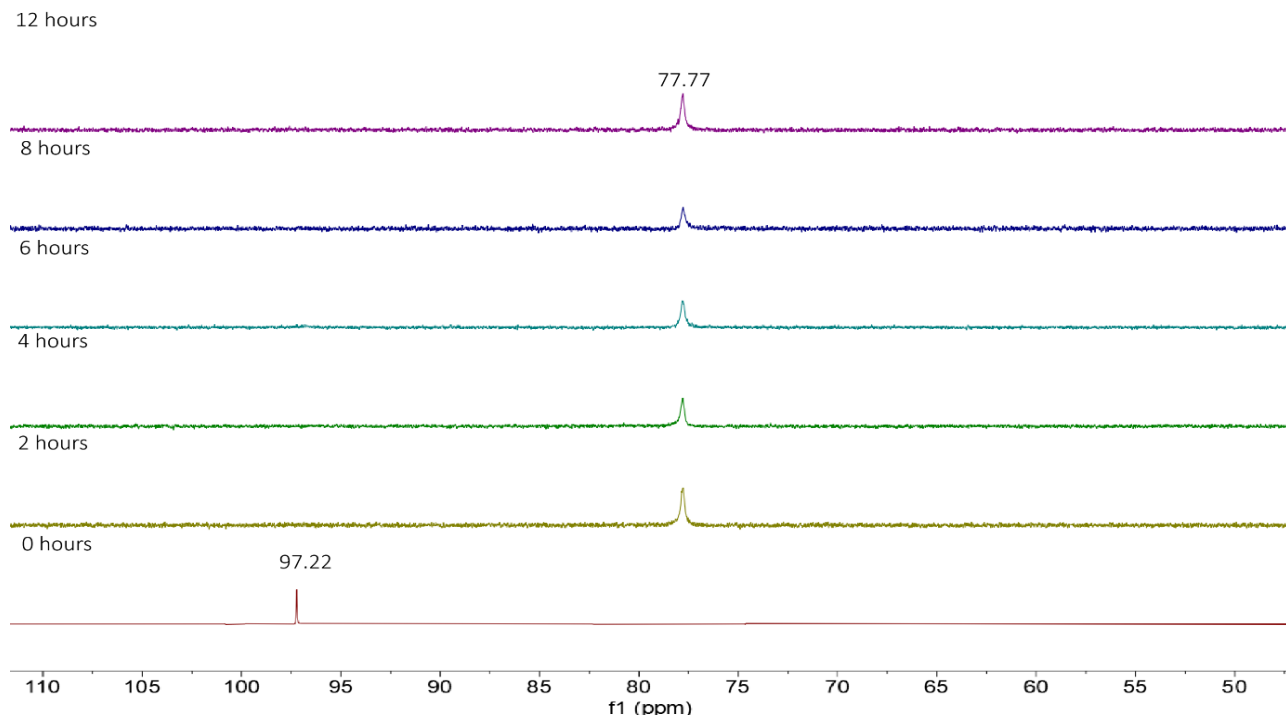


Figure S40. Time-dependent ³¹P{¹H} NMR spectra (162 MHz, CD₃CN, 298 K) of the catalytic reaction mixture depicting the formation of the Ge-F bond (**1^PrPO-F** as an intermediate).

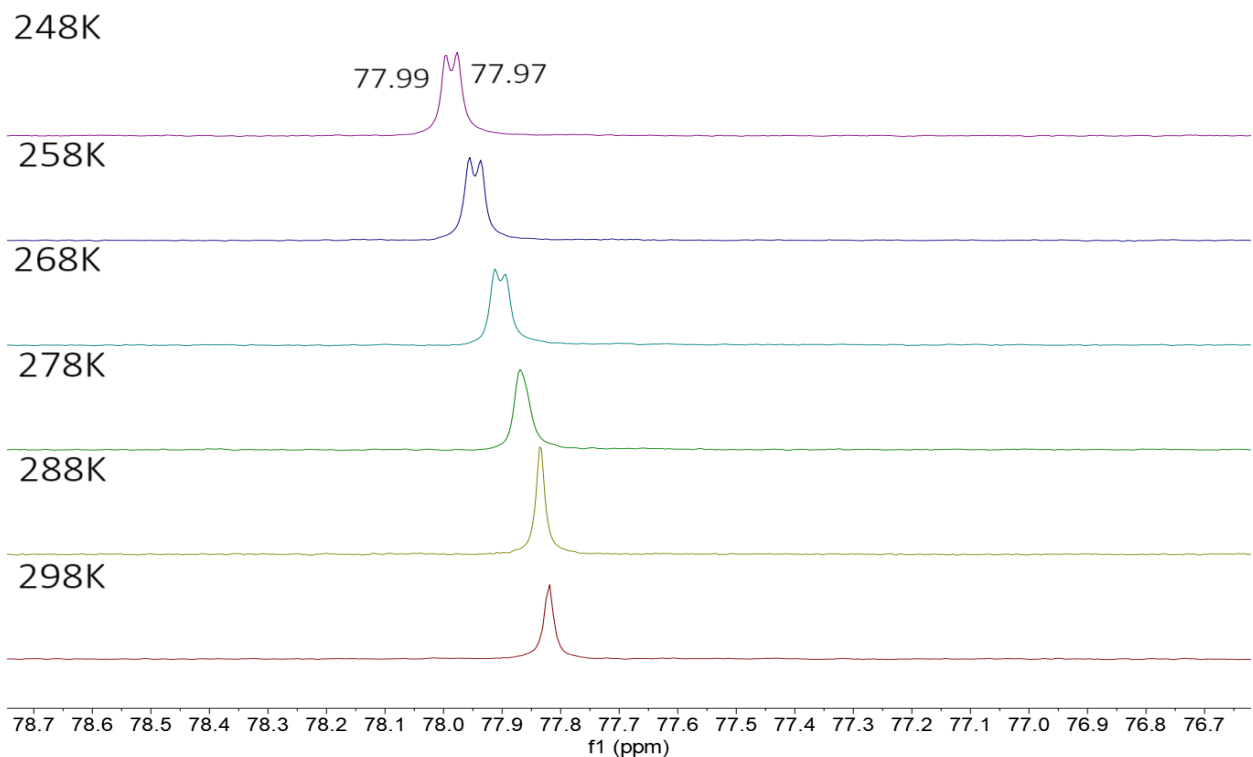


Figure S41. Variable temperature $^{31}\text{P}\{\text{H}\}$ NMR spectra (162 MHz, CD_3CN) of the catalytic reaction mixture depicting the formation of the Ge-F bond (1^{Pr}PO-F as an intermediate).

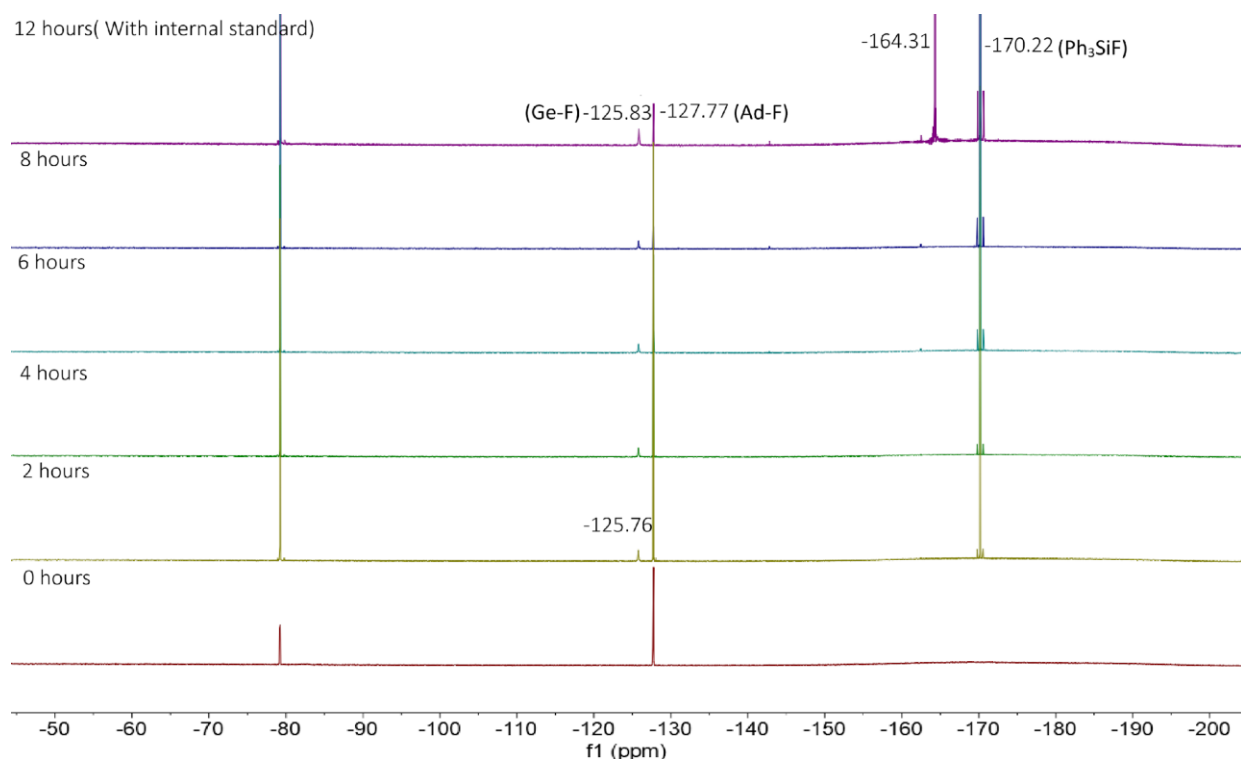


Figure S42. Time-dependent $^{19}\text{F}\{\text{H}\}$ NMR spectra (377 MHz, CD_3CN , 298 K) of the catalytic reaction mixture depicting the formation of the Ge-F bond (1^{Pr}PO-F as an intermediate), by-product Ph_3SiF , internal standard (-164.31 ppm) and triflate

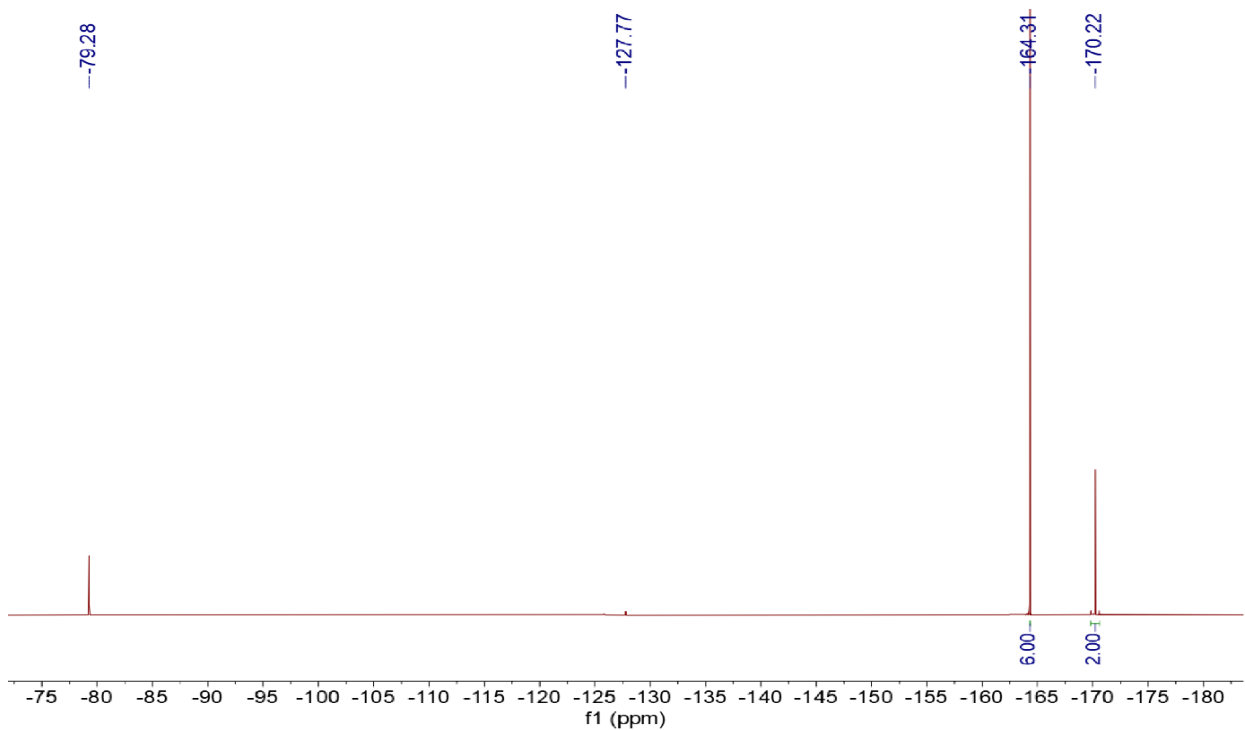


Figure S43. ${}^{19}\text{F}\{{}^1\text{H}\}$ NMR spectrum (377 MHz, CD_3CN , 298 K) showing 76% conversion of AdF to AdH (w. r. t. Ph_3SiF formation)

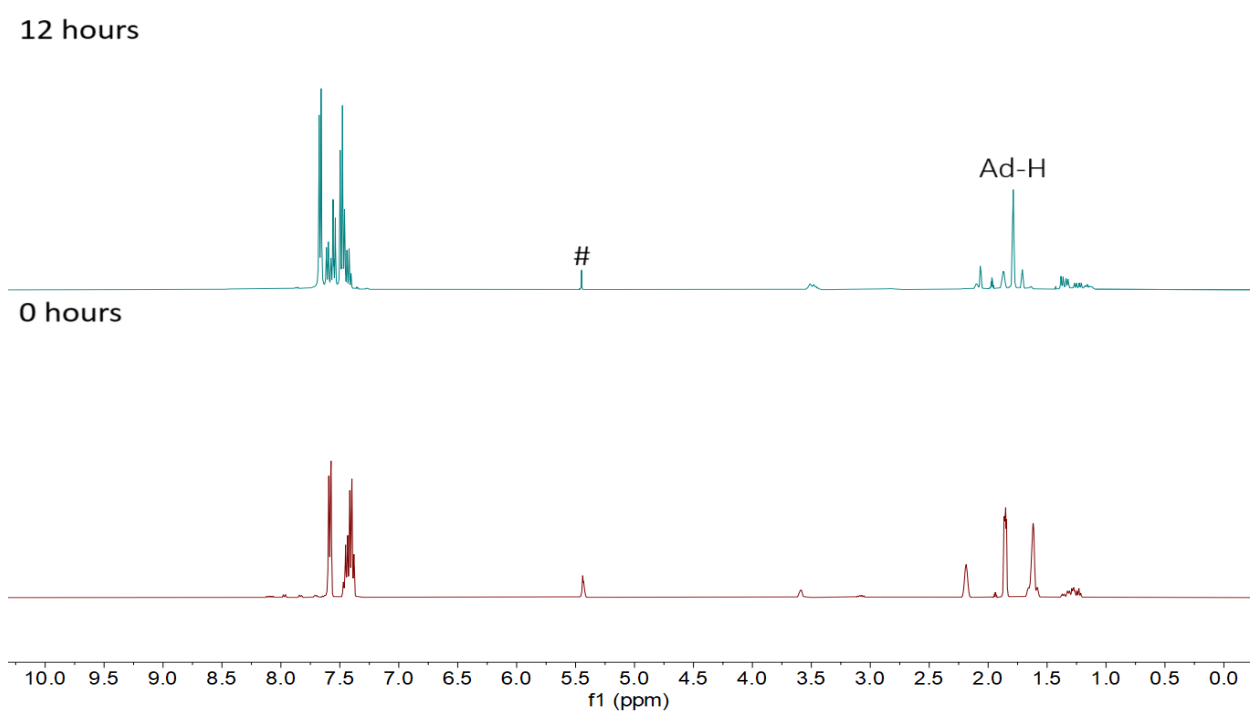


Figure S44. ${}^1\text{H}$ NMR spectra (400 MHz, CD_3CN , 298 K) showing the conversion of AdF to AdH (# = DCM)

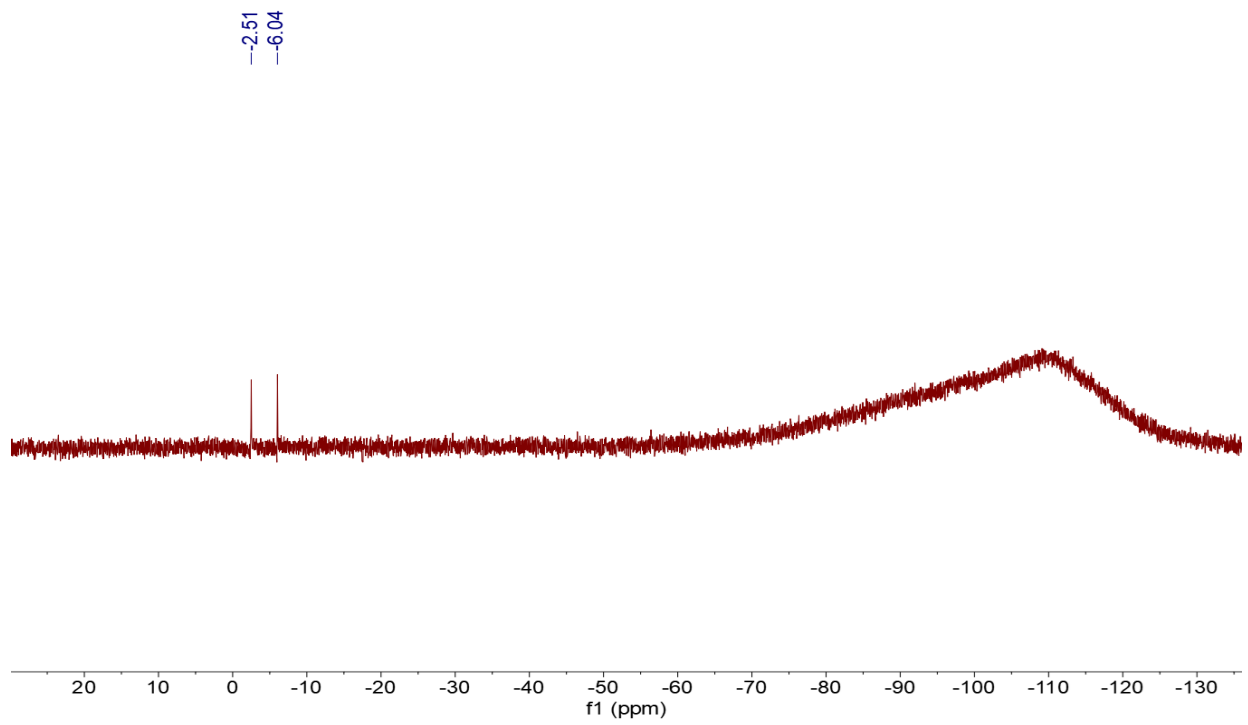


Figure S45. $^{29}\text{Si}\{^1\text{H}\}$ NMR spectra (80 MHz, CD₃CN, 298 K) showing the conversion of Ph₃SiH to Ph₃SiF ($J_{\text{Si}-\text{F}} = 280.6$ Hz)

Control Experiment

An NMR tube was charged with 1 equiv. of **1*i*PrPO** (0.02 mmol, 0.020 g) and 1-Fluoroadmantane (0.02 mmol, 0.003 g, 1 equiv.) in 0.4 mL CD₃CN. ¹H, ³¹P{¹H} and ¹⁹F{¹H} have been recorded after mild heating for 2 hours.

³¹P{¹H} NMR (162 MHz, CD₃CN, 298 K) = + 97.11 ppm, + 77.93 ppm

¹⁹F{¹H} NMR (377 MHz, CD₃CN, 298 K) = - 79.63 ppm, -125.88 ppm, -127.30 ppm

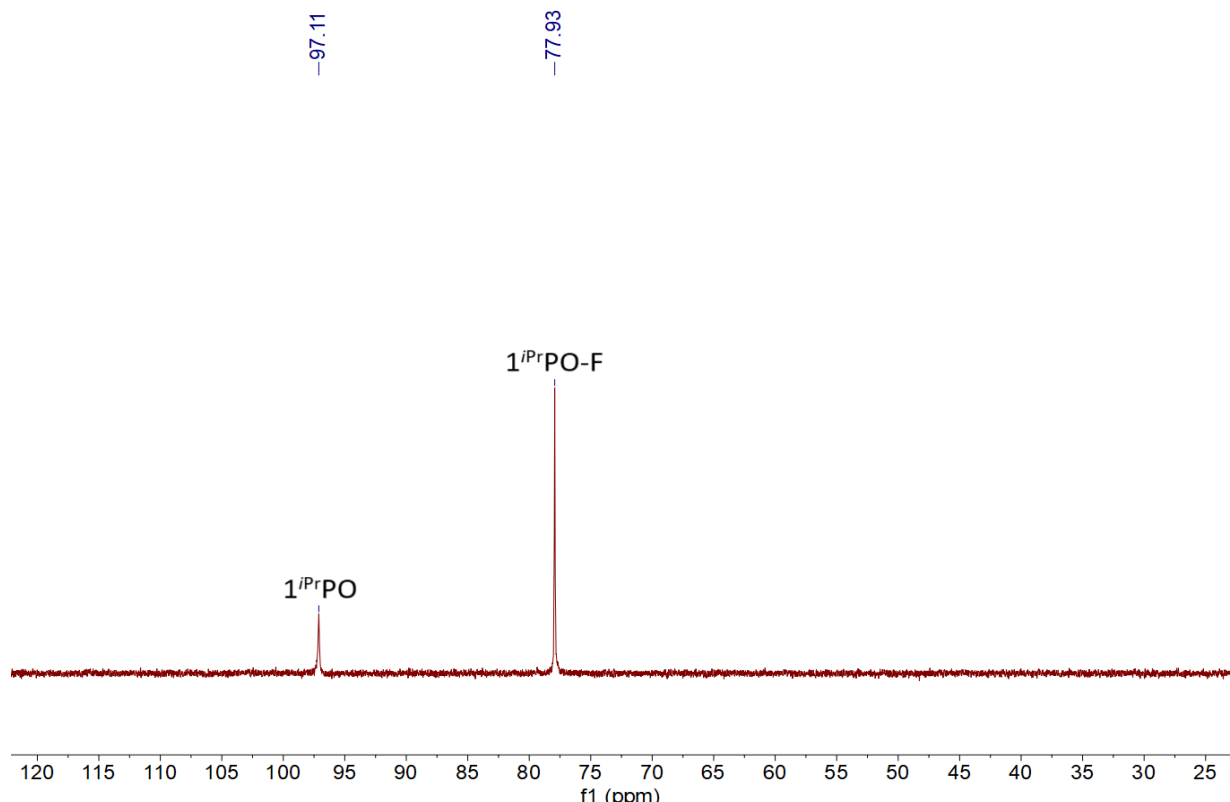


Figure S46. ³¹P{¹H} NMR spectra (162 MHz, CD₃CN, 298 K) showing the conversion of **1*i*PrPO** to **1*i*PrPO-F**

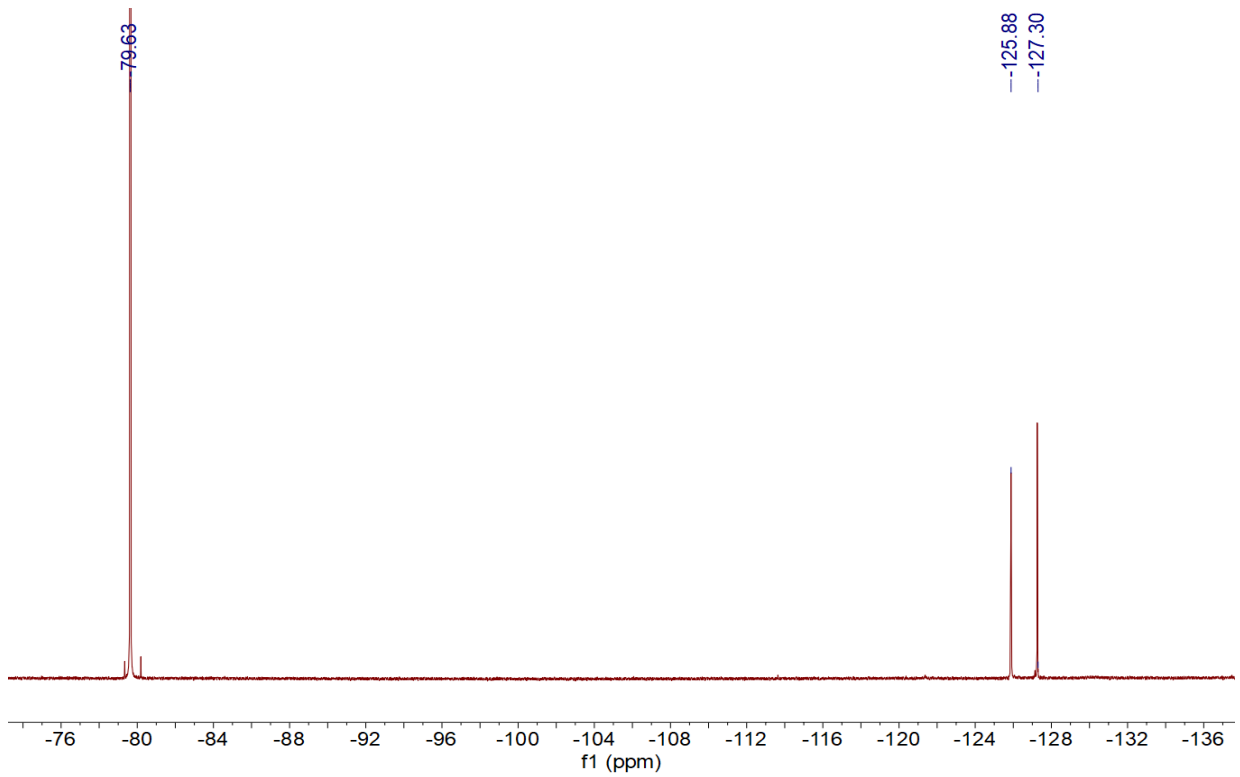


Figure S47. $^{19}\text{F}\{\text{H}\}$ NMR spectra (377 MHz, CD_3CN , 298 K) showing the conversion of 1^{Pr}PO to 1^{Pr}PO-F

Hydrodefluorination of 1-Adamantyl Fluoride using Et₃SiH as the hydride source:

An NMR tube was charged with 1-Fluoroadamantane (0.015 g, 0.1 mmol), Et₃SiH (16 μ L, 0.1 mmol), catalyst **1*i*PrPO** (0.0005 mmol) in CD₃CN (0.5 mL). The reaction mixture was heated at 75 °C. ¹H NMR measurements were carried out at various time intervals and the conversion was calculated by integration against internal standard hexafluorobenzene.

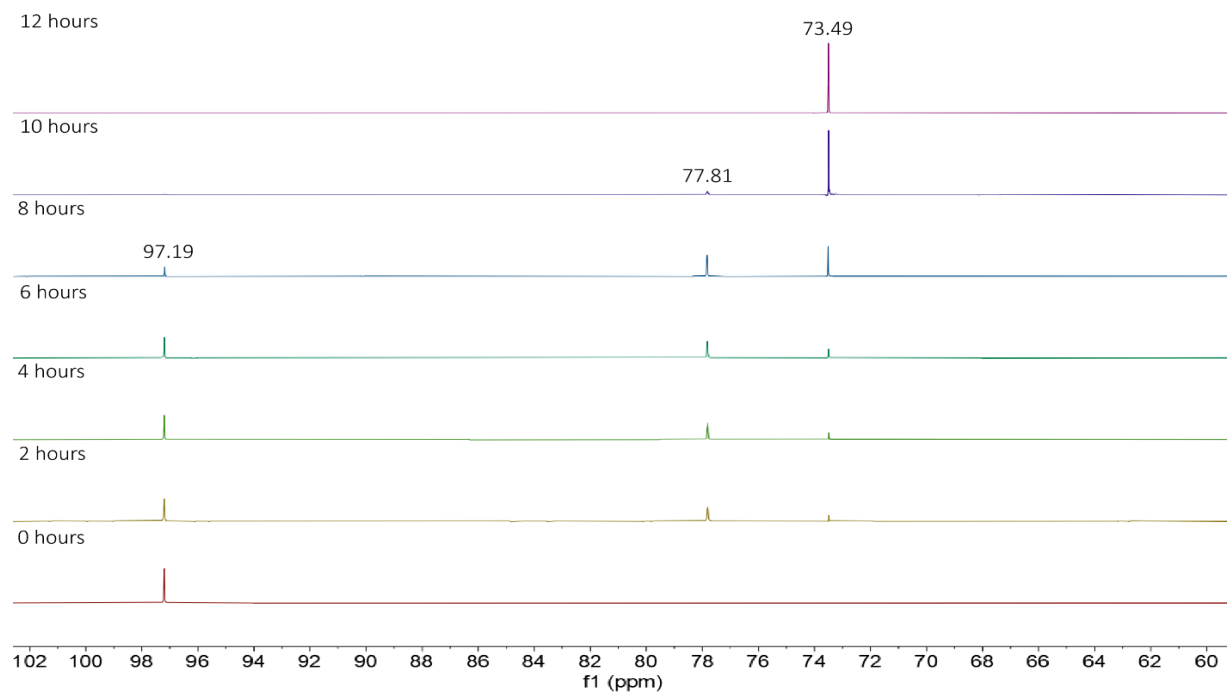


Figure S48. Time-dependent ³¹P{¹H} NMR spectra (162 MHz, CD₃CN, 298 K) of the catalytic reaction mixture depicting the formation of the Ge-F bond(77.81ppm) (**1*i*PrPO**-F as an intermediate). Note: Ge-H bond formation (as **1*i*PrPO**-H) is observed (73.49 ppm) which deactivates the catalyst.

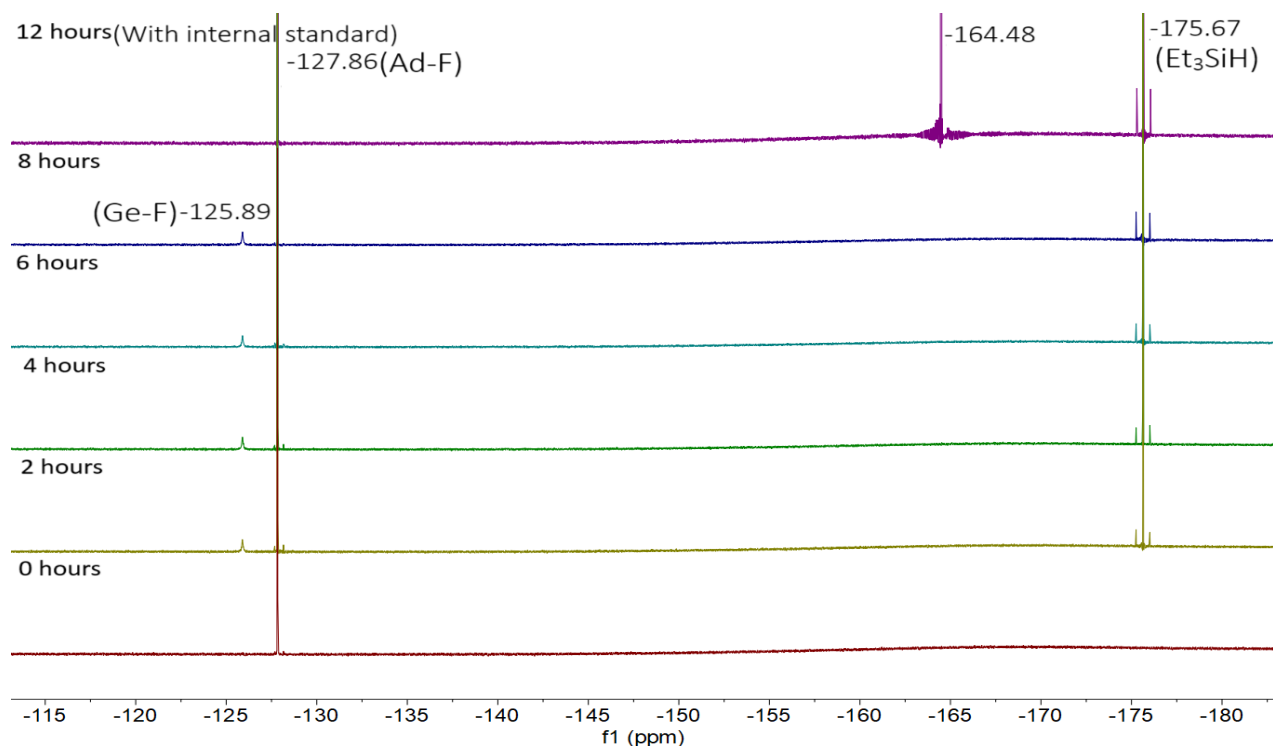


Figure S49. Time-dependent $^{19}\text{F}\{\text{H}\}$ NMR spectra (377 MHz, CD₃CN, 298 K) of the catalytic reaction mixture depicting the formation of the Ge-F bond ($\mathbf{1}^{\text{Pr}}\text{PO-F}$ as an intermediate), product Ph₃SiF and internal standard.

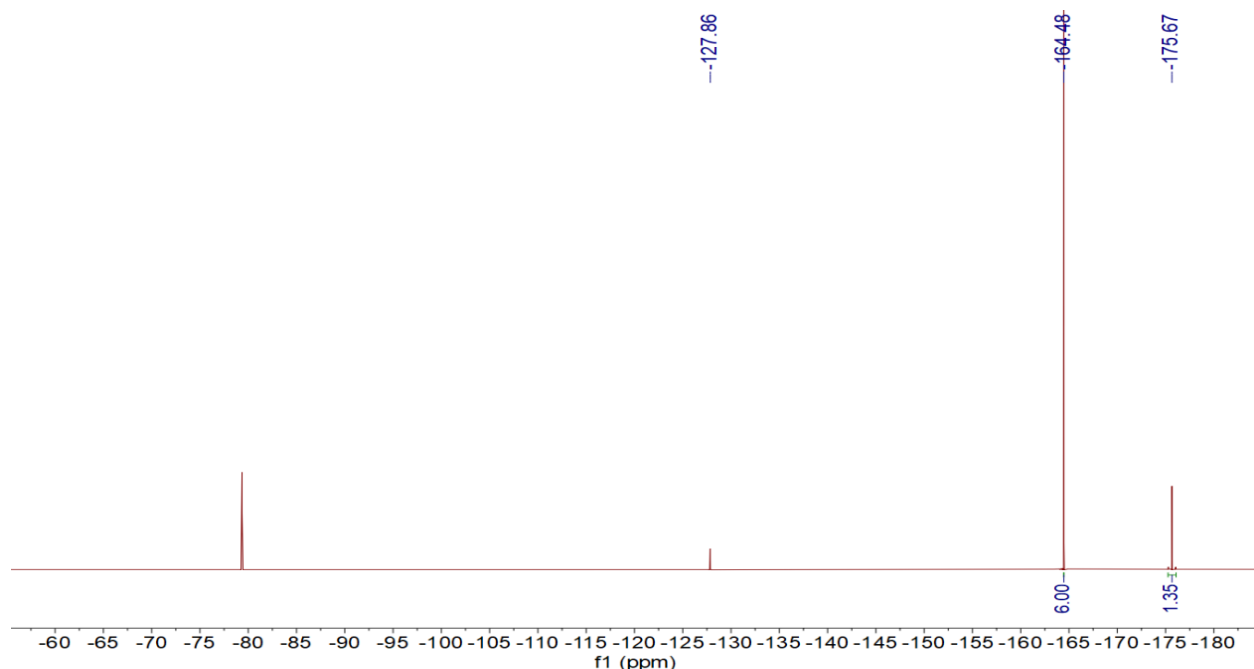


Figure S50. $^{19}\text{F}\{\text{H}\}$ NMR spectrum (377 MHz, CD₃CN, 298 K) showing 76% conversion of AdF to AdH.

12 hours

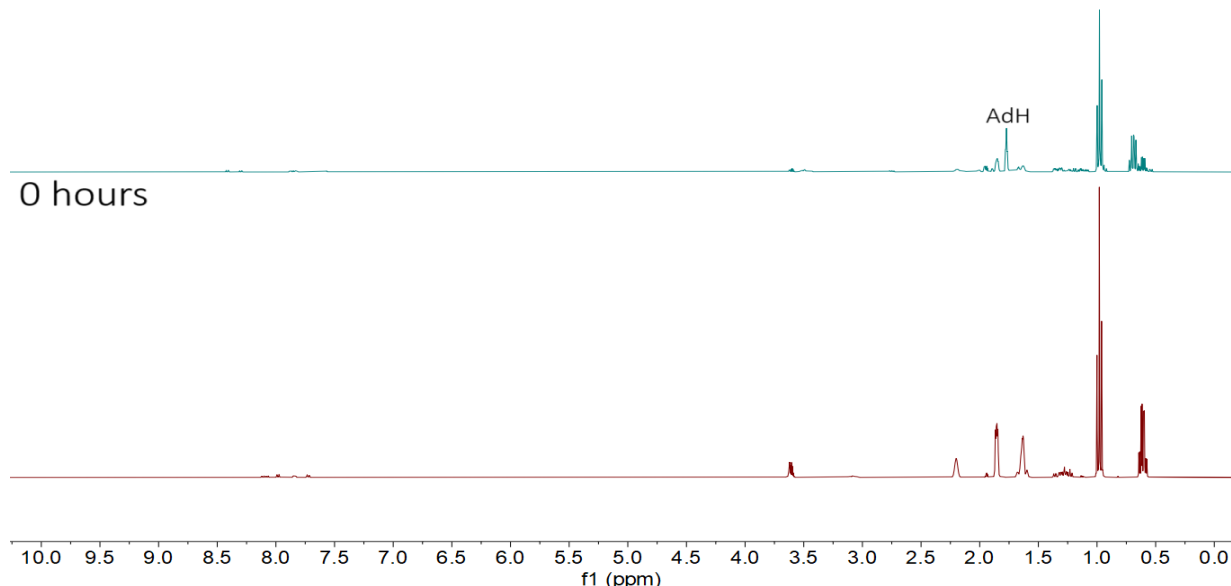
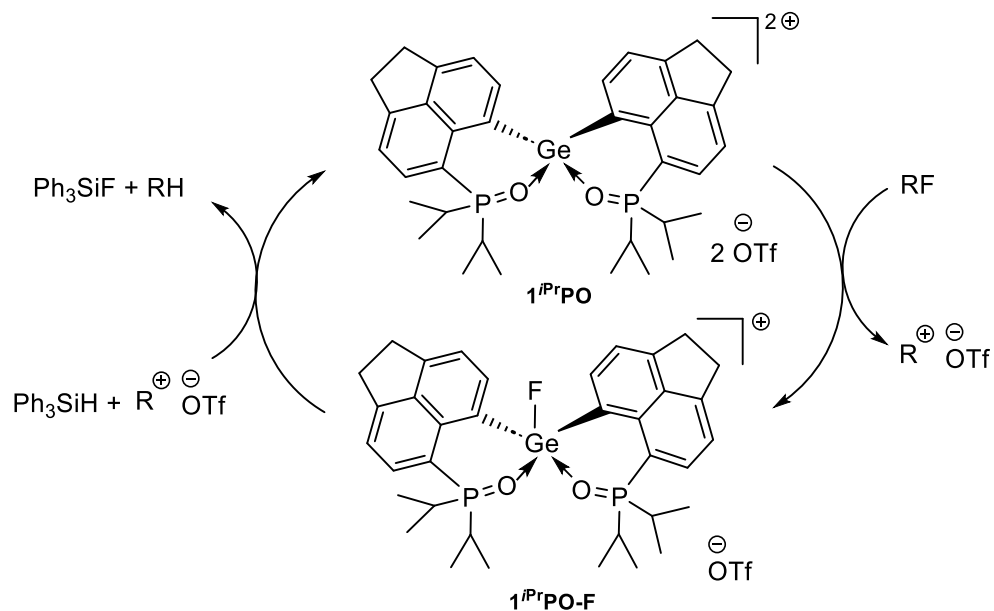


Figure S51. ¹H NMR spectra (400 MHz, CD₃CN, 298 K) showing the formation of AdH from AdF



Scheme S1. Proposed catalytic cycle for the hydrodefluorination of 1-adamantyl fluoride (RF = AdF) using **1*i*PrPO** as catalyst.

Hydrosilylation of aldehydes by 1^{Pr}PO as catalyst:

General Procedure: An NMR tube was charged with the aldehyde (0.10 mmol), Et₃SiH (0.10 mmol), catalyst 1^{Pr}PO (5 mol%) in CD₃CN (0.5 mL). The reaction mixtures were heated overnight at 75 °C. The reaction mixtures were analysed by ¹H NMR measurement and conversion was calculated by integration against internal standard mesitylene.

NMR Data for the hydrosilylation of *p*-nitro benzaldehyde:

Final(12 hours) With internal standard

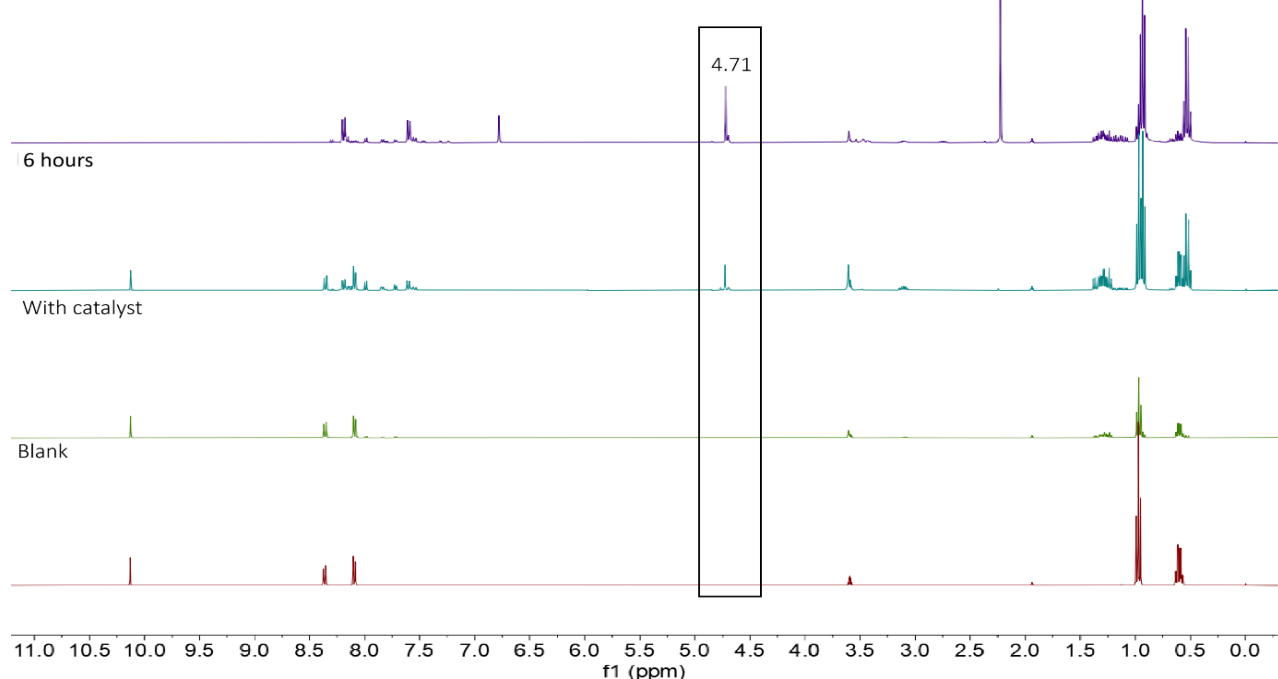


Figure S52. ¹H NMR spectra (400 MHz, CD₃CN, 298 K) of the reaction mixture with and without catalyst added.

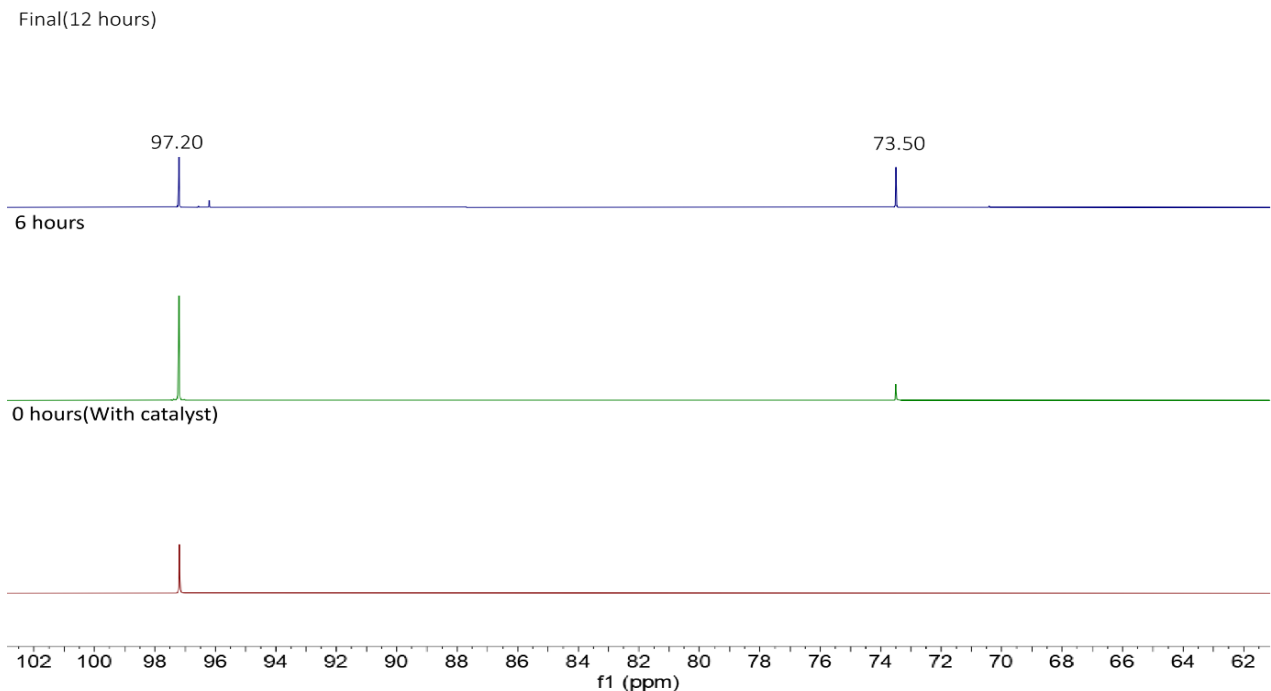


Figure S53. Time-dependent $^{31}\text{P}\{\text{H}\}$ NMR spectra (162 MHz, CD_3CN , 298 K) of the catalytic reaction mixture.

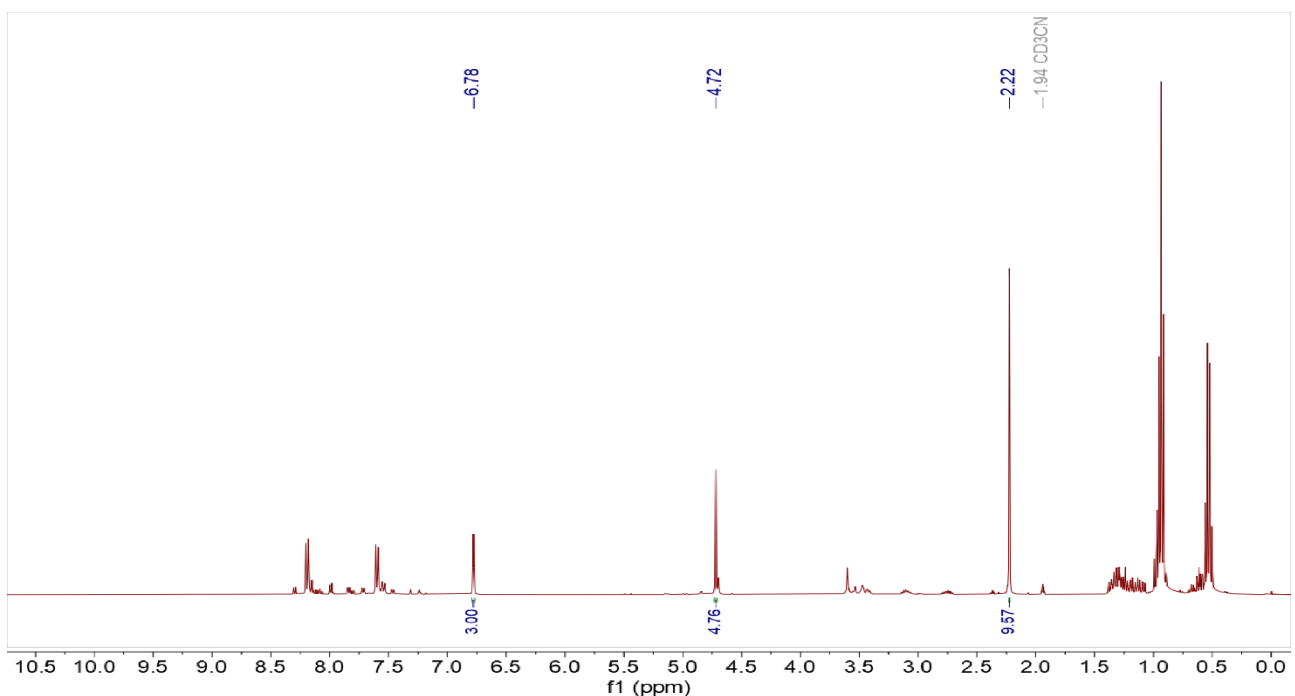


Figure S54. ^1H NMR spectra (400 MHz, CD_3CN , 298 K) of the reaction mixture after 12 hours showing the product formation.

NMR Data for the hydrosilylation of 4-(Trifluoromethyl) benzaldehyde:

Final(12 hours)

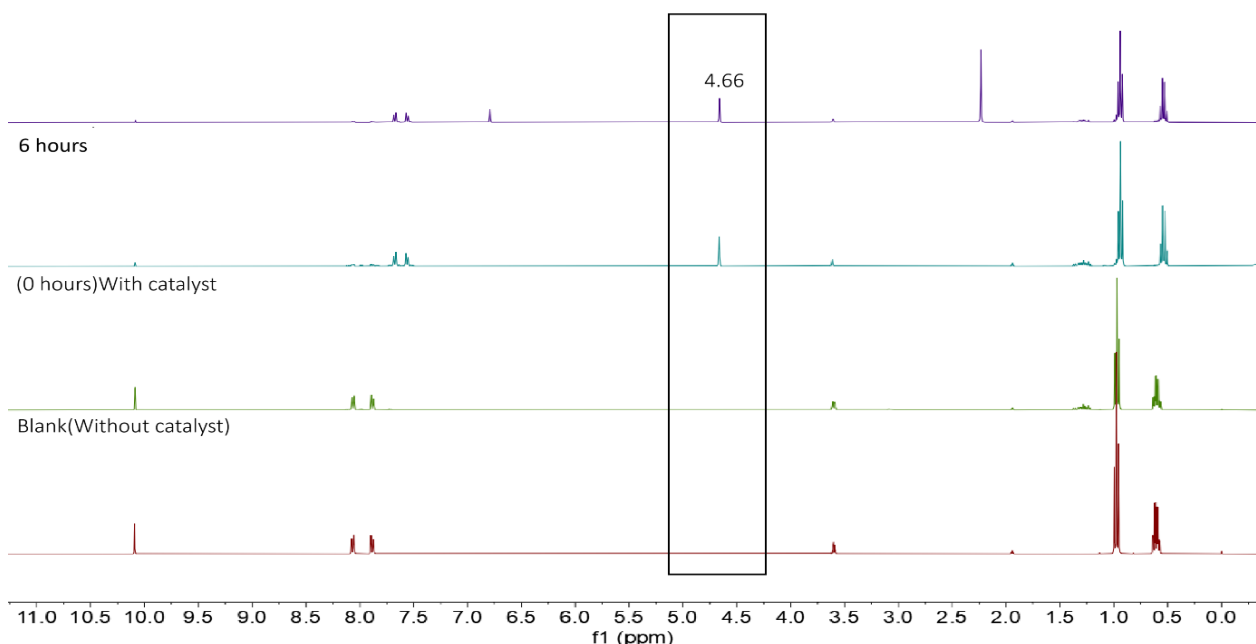


Figure S55. ^1H NMR spectra (400 MHz, CD_3CN , 298 K) of the reaction mixture with and without catalyst added.

12 hours(Final)

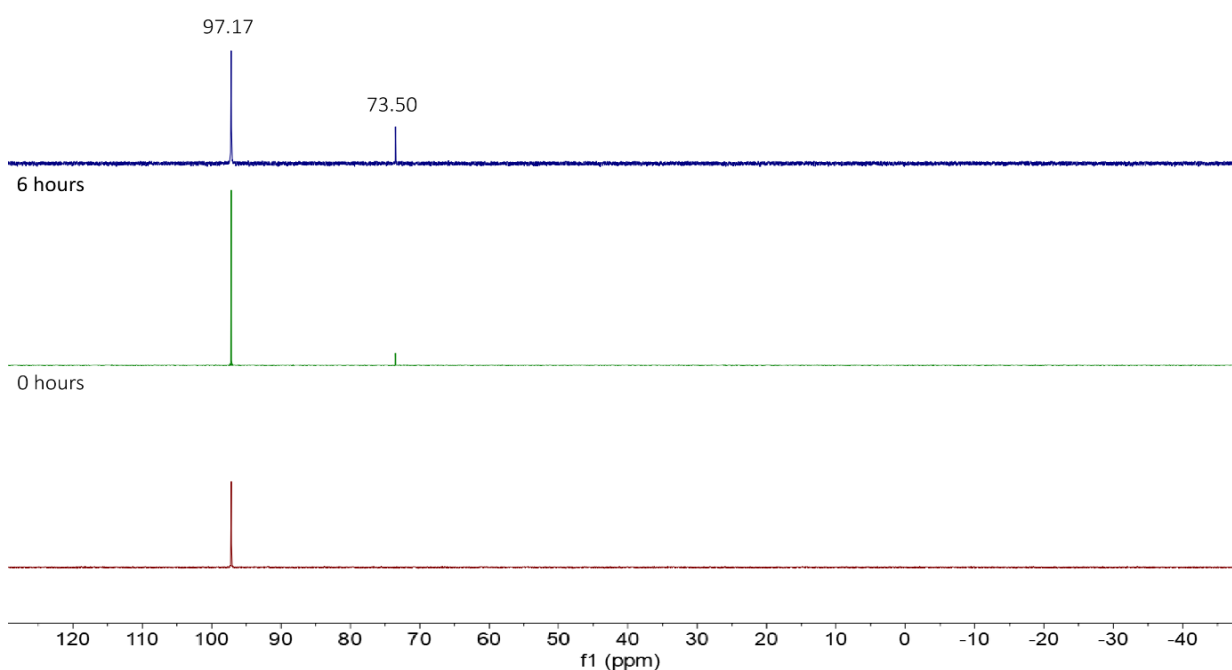


Figure S56. Time-dependent $^{31}\text{P}\{\text{H}\}$ NMR spectra (162 MHz, CD_3CN , 298 K) of the catalytic reaction mixture.

12 hours

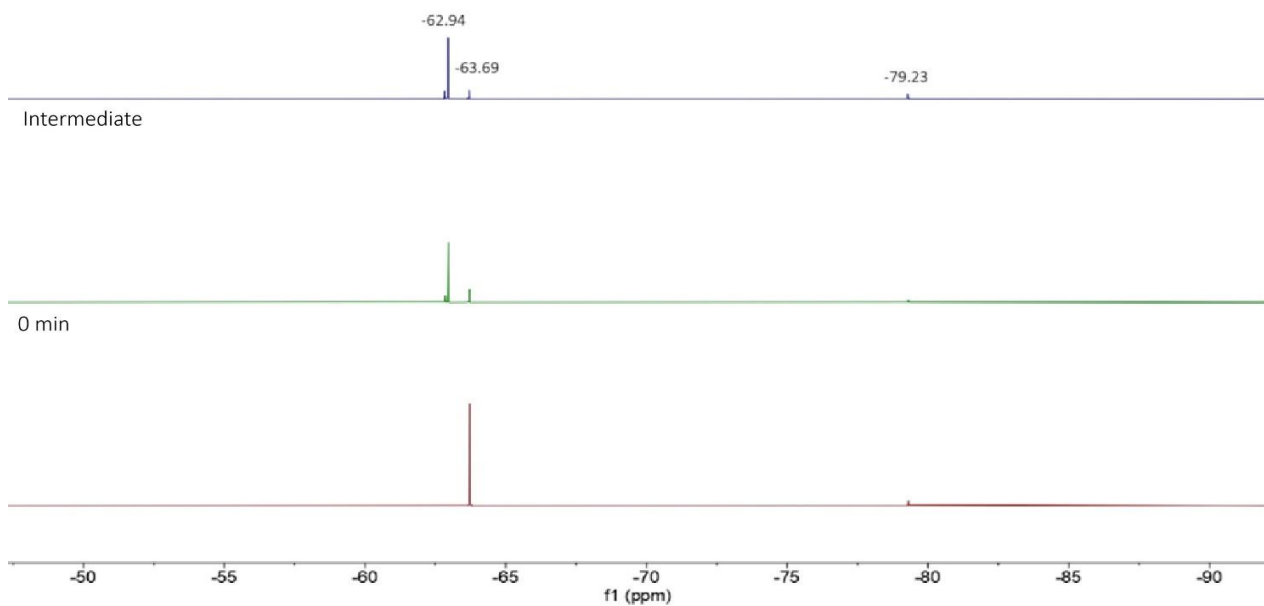


Figure S57. Time-dependent $^{19}\text{F}\{\text{H}\}$ NMR spectra (162 MHz, CD_3CN , 298 K) of the catalytic reaction mixture.

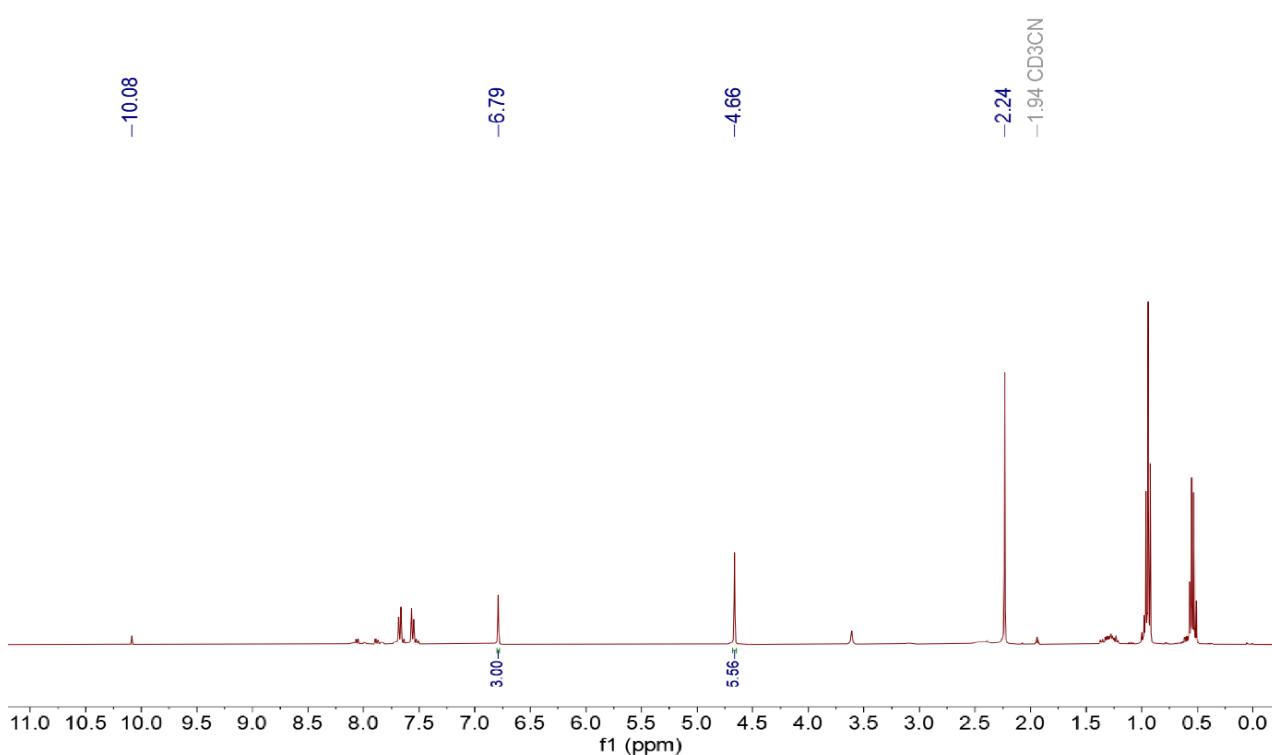


Figure S58. ^1H NMR spectra (400 MHz, CD_3CN , 298 K) of the reaction mixture after 12 hours showing the product formation.

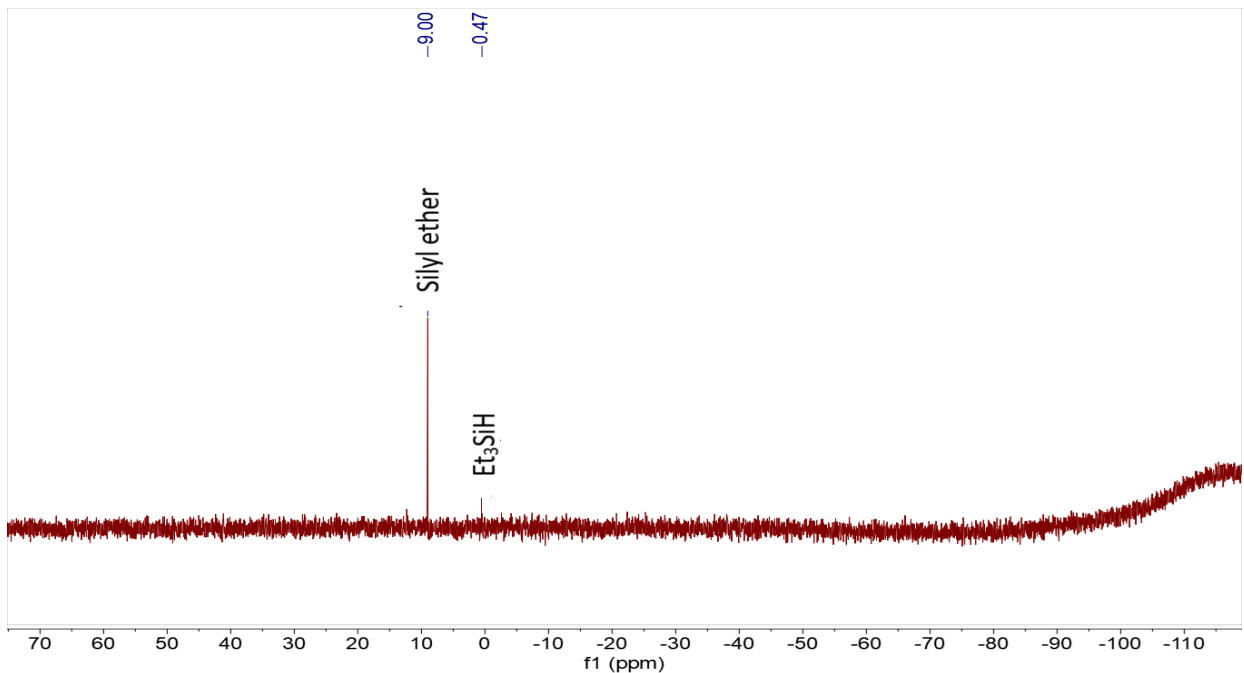


Figure S59. $^{29}\text{Si}\{^1\text{H}\}$ NMR spectra (80 MHz, CD₃CN, 298 K) of the reaction mixture after 24 hours showing the product formation

NMR Data for the hydrosilylation of 4-cyano benzaldehyde:

12 hours

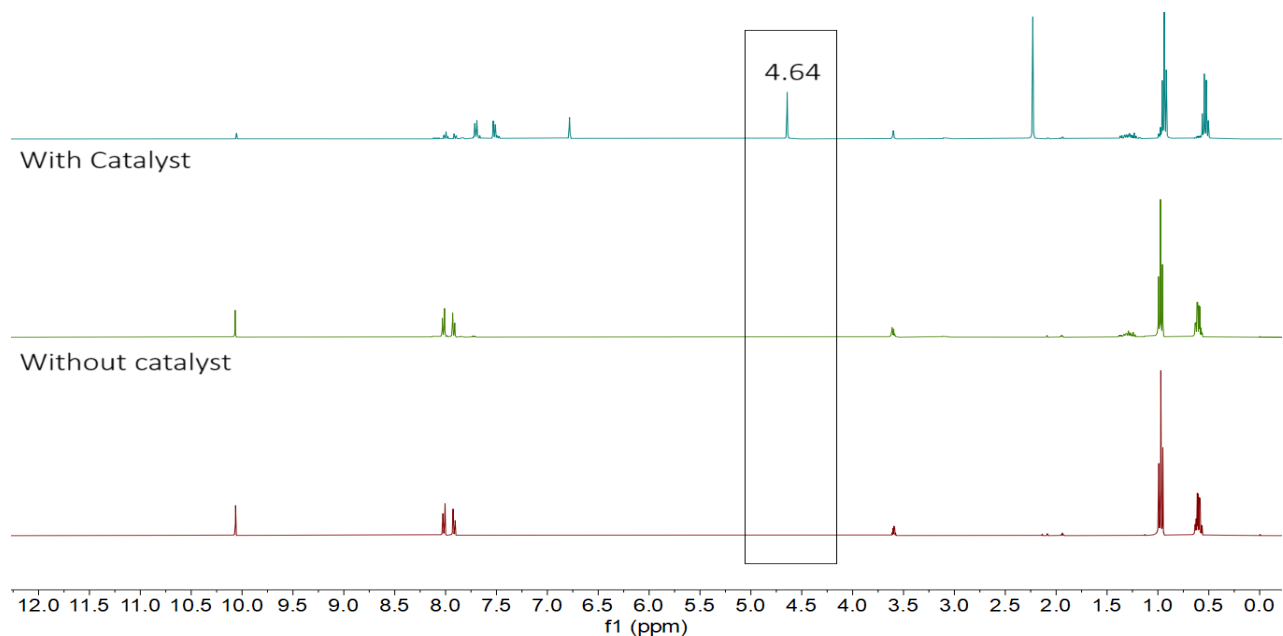


Figure S60. ¹H NMR spectra (400 MHz, CD₃CN, 298 K) of the reaction mixture with and without catalyst added.

12 hours

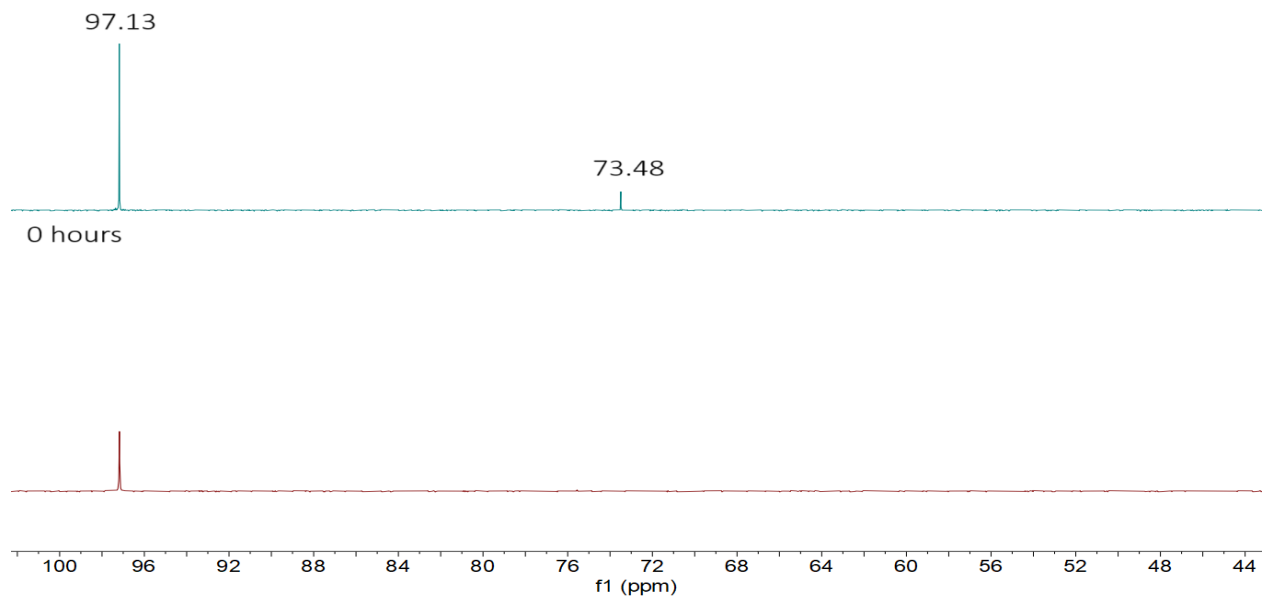


Figure S61. Time-dependent ³¹P{¹H} NMR spectra (162 MHz, CD₃CN, 298 K) of the catalytic reaction mixture.

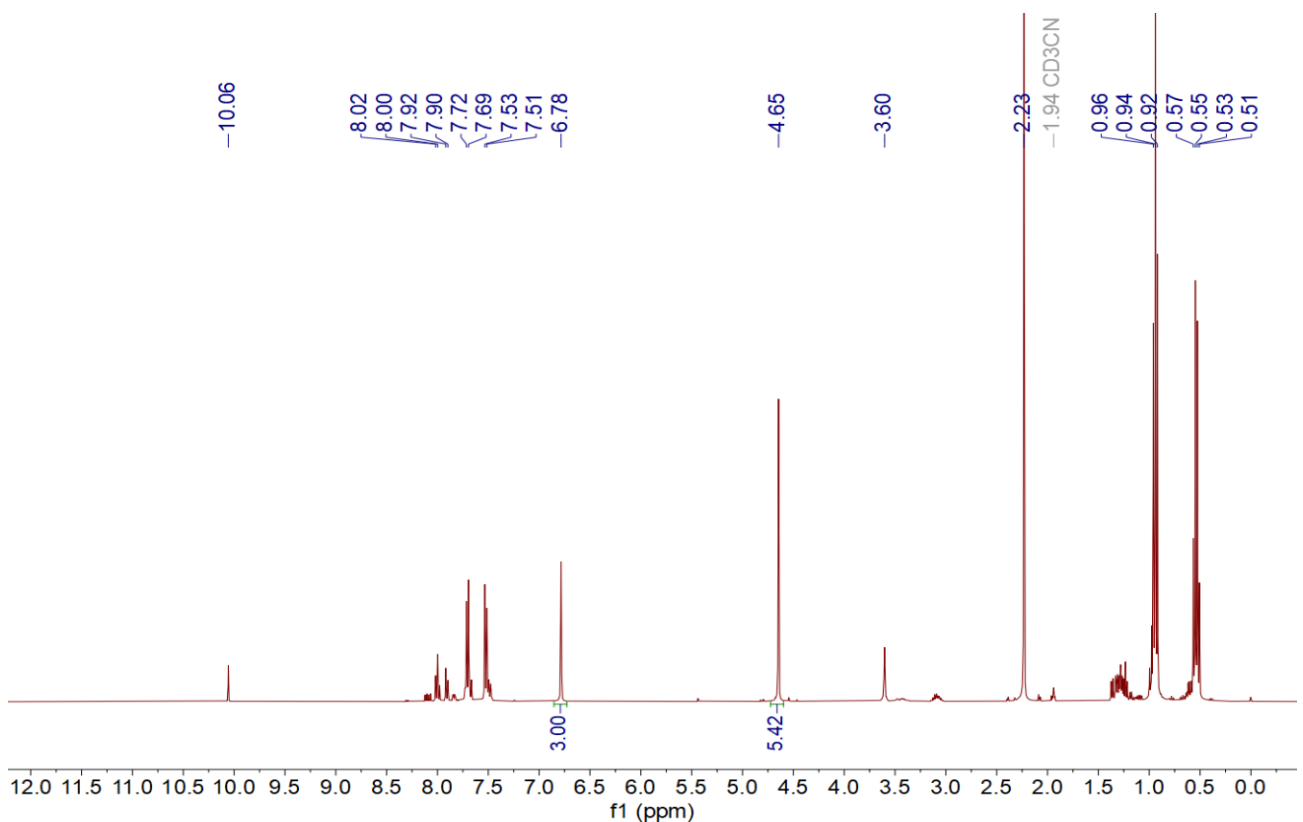


Figure S62. ^1H NMR spectra (400 MHz, CD₃CN, 298 K) of the reaction mixture after 12 hours showing the product formation.

NMR Data for the hydrosilylation of 2-fluoro benzaldehyde:

12 hours

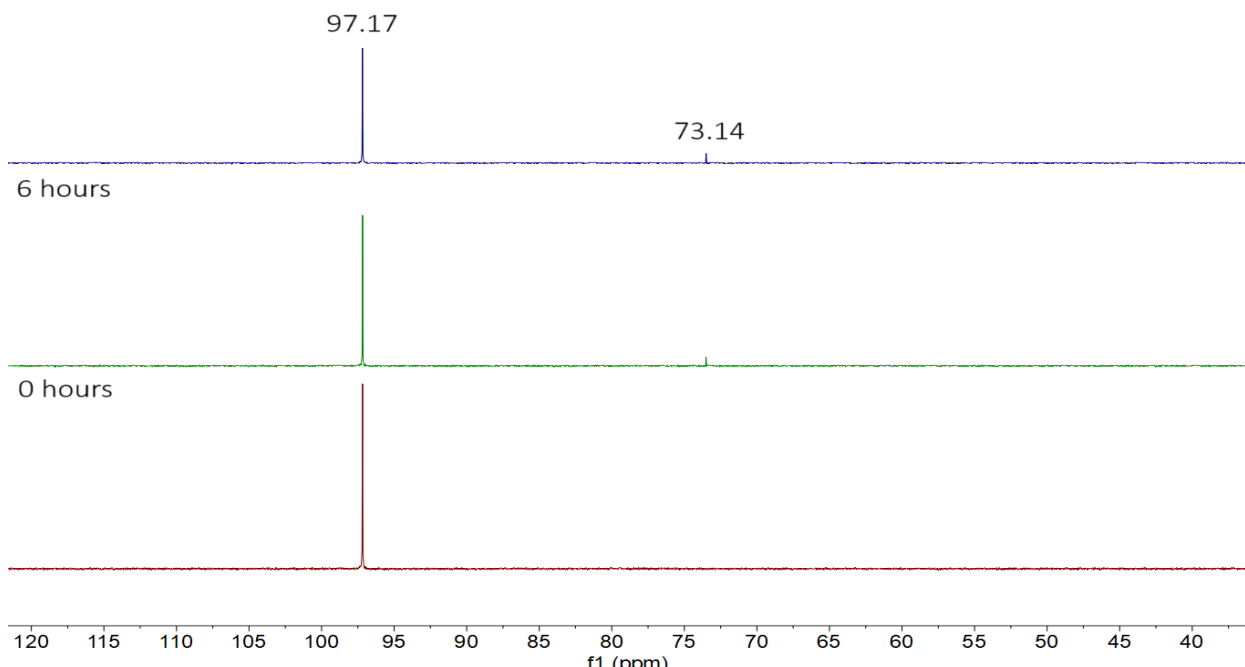


Figure S63. Time-dependent $^{31}\text{P}\{^1\text{H}\}$ NMR spectra (162 MHz, CD₃CN, 298 K) of the catalytic reaction mixture.

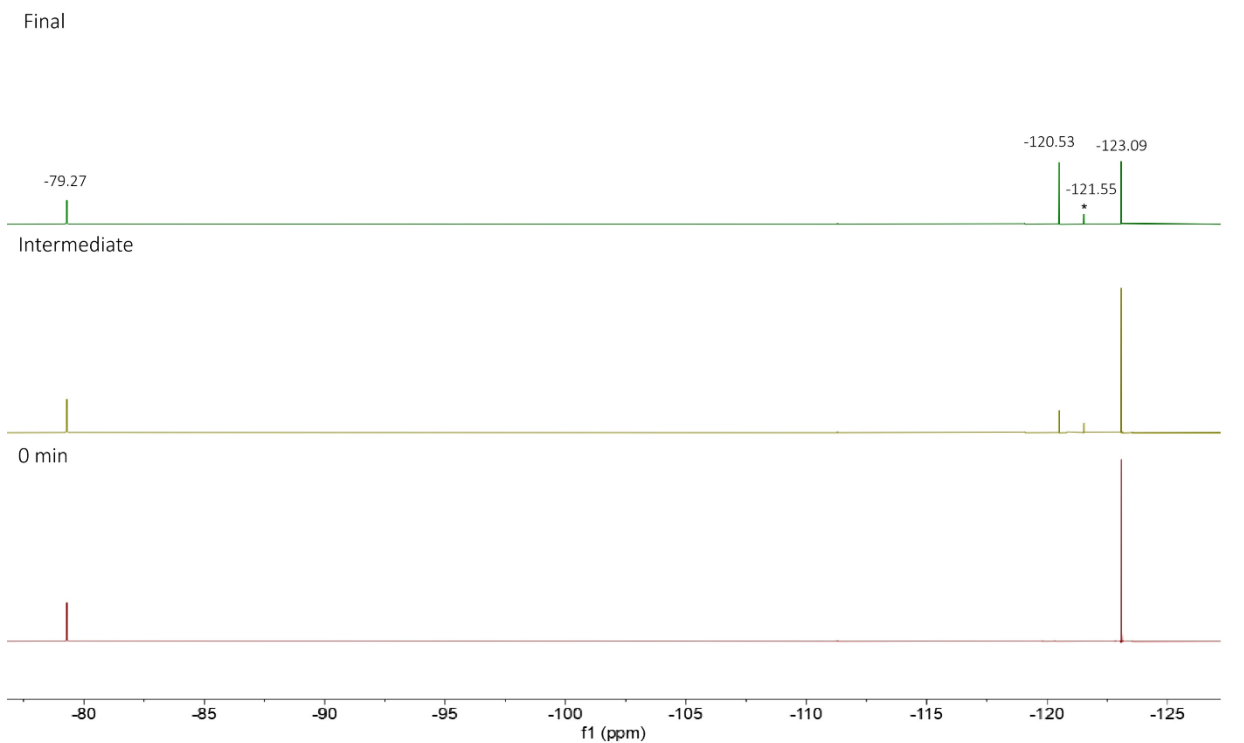


Figure S64. Time-dependent $^{19}\text{F}\{\text{H}\}$ NMR spectra (162 MHz, CD₃CN, 298 K) of the catalytic reaction mixture (* = unidentified intermediate)

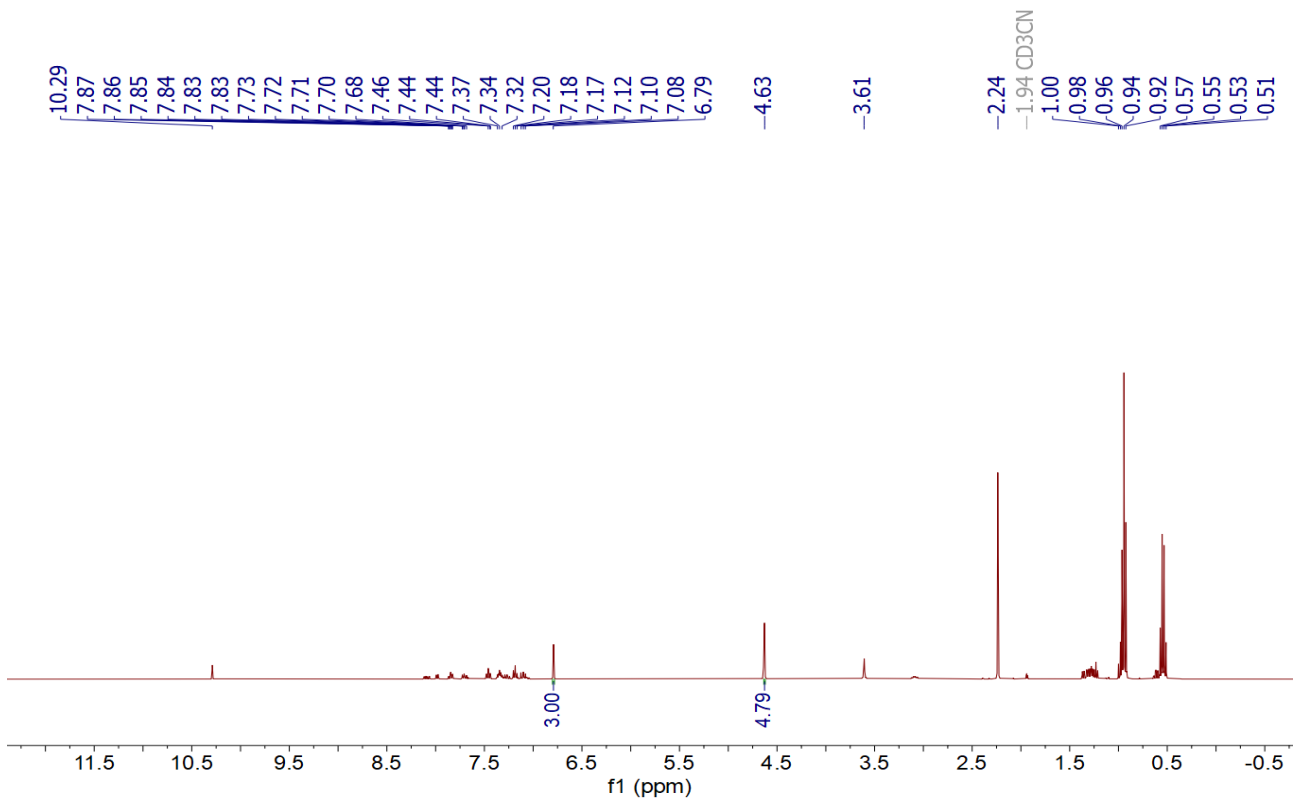


Figure S65. ^1H NMR spectra (400 MHz, CD₃CN, 298 K) of the reaction mixture after 12 hours showing the product formation.

NMR Data for the hydrosilylation of 4-fluoro benzaldehyde:

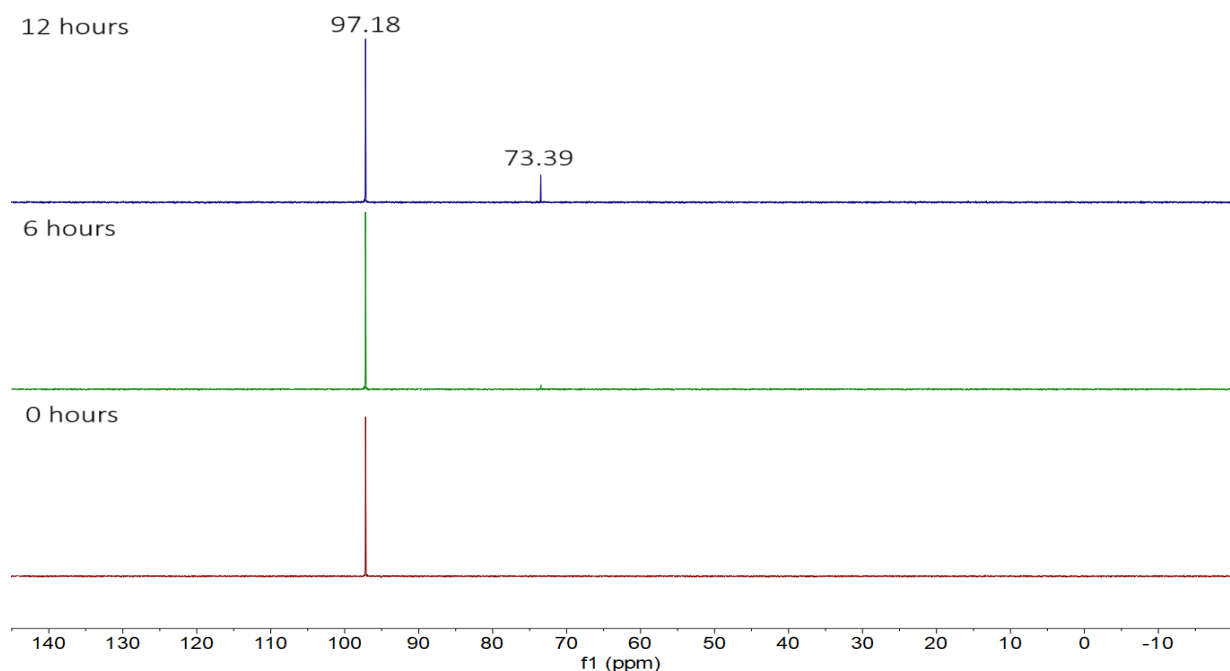


Figure S66. Time-dependent $^{31}\text{P}\{\text{H}\}$ NMR spectra (162 MHz, CD_3CN , 298 K) of the catalytic reaction mixture.

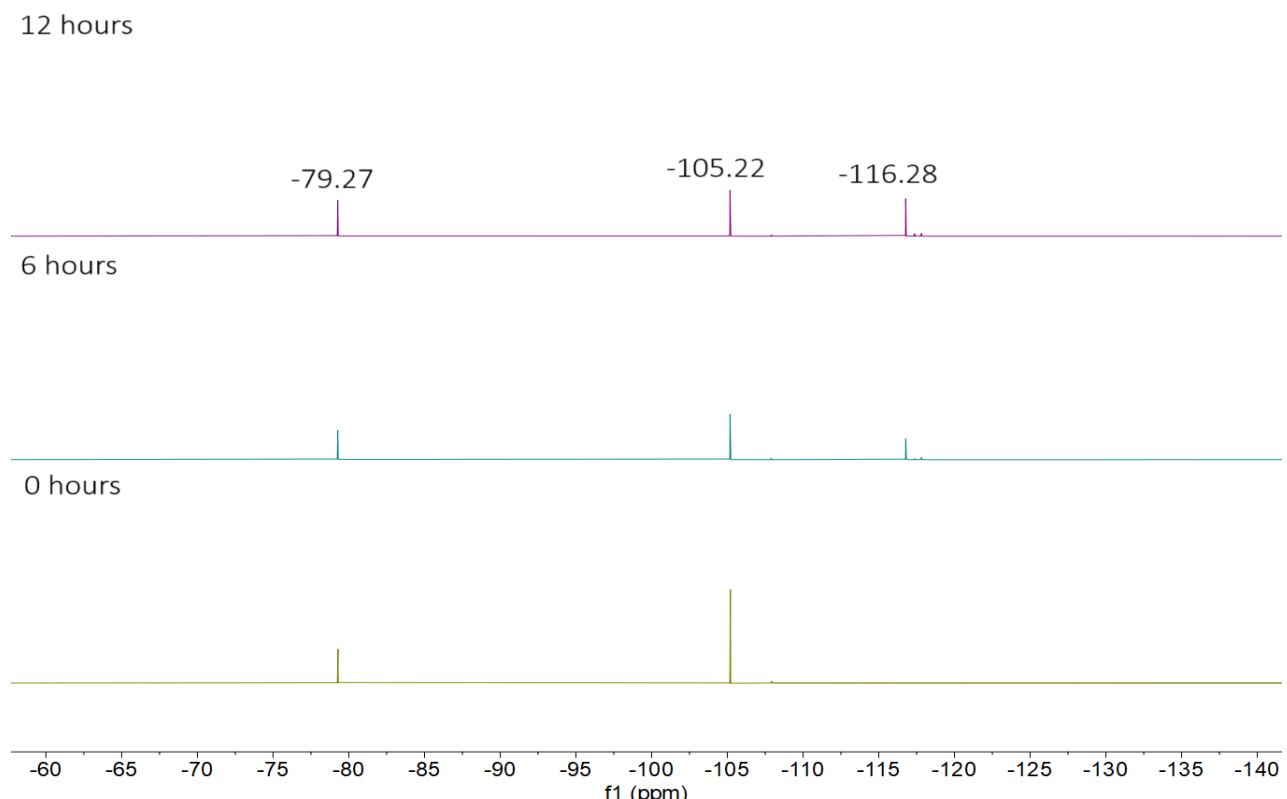


Figure S67. Time-dependent $^{19}\text{F}\{\text{H}\}$ NMR spectra (162 MHz, CD_3CN , 298 K) of the catalytic reaction mixture.

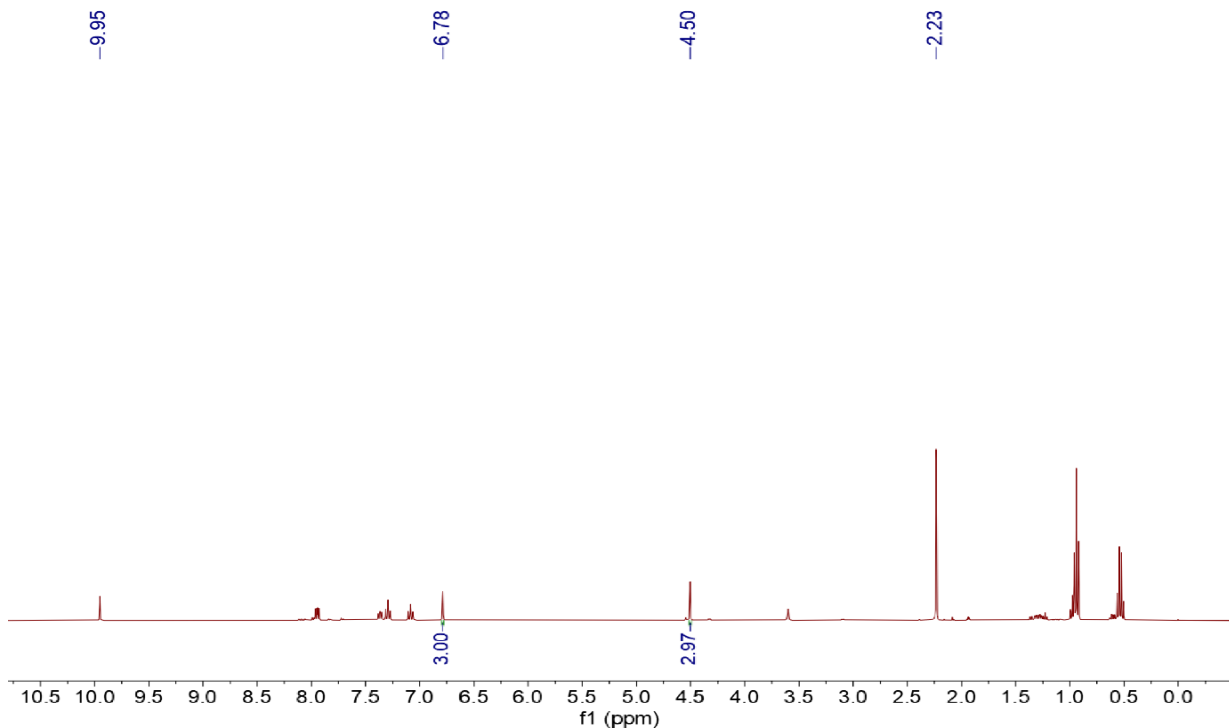
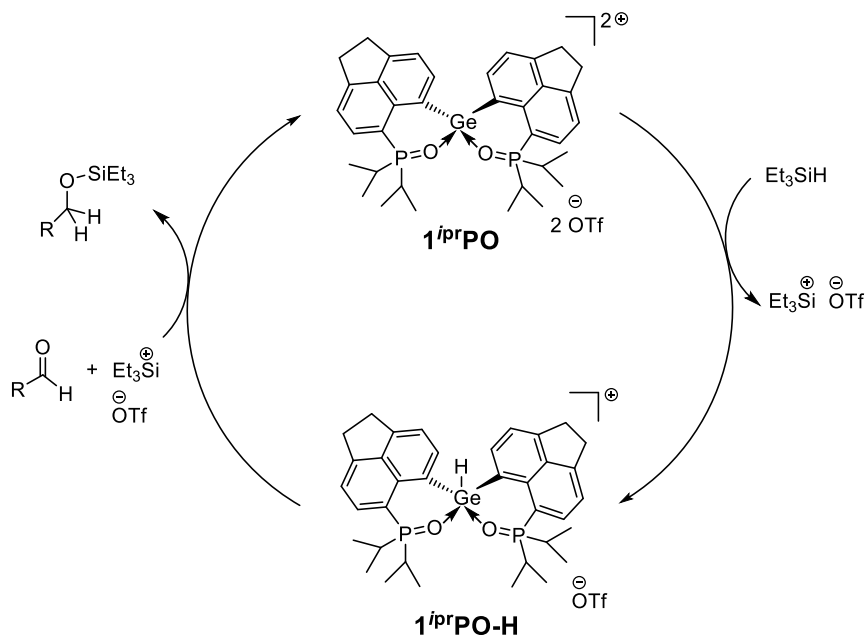


Figure S68. ¹H NMR spectra (400 MHz, CD₃CN, 298 K) of the reaction mixture after 12 hours showing the product formation.



Scheme S2. Proposed catalytic cycle for the hydrosilylation of benzaldehyde with electron-withdrawing groups using $\mathbf{1}^{i\text{Pr}}\text{PO}$ as catalyst.

Table S8. Cartesian coordinates of **1*i*PrPO** at the TPSS-D3(BJ)/def2-TZVPP level of theory.

Ge	2.385349399	5.663674814	1.765702885
P	2.110776411	5.802635019	4.827540389
P	1.239120010	3.209480444	0.304889559
O	1.495657142	5.766367133	3.367432020
O	2.162269954	3.880066283	1.401051365
C	4.659637355	5.812820765	3.583342214
C	0.315482224	8.032563229	-1.768223033
C	1.448950297	6.547420335	0.356813766
C	3.884909126	5.610645714	4.774085046
C	0.864896391	8.704297234	-0.693933686
H	0.881030751	9.787744695	-0.640570848
C	0.789324589	4.404358579	-0.939991881
C	0.873933867	5.822794055	-0.735636634
C	4.209553374	5.961793939	2.235296139
C	1.438846058	7.943601384	0.346232163
H	1.902788950	8.481961036	1.169123073
C	0.240702648	3.906508161	-2.127740661
H	0.200493984	2.831884315	-2.280744121
C	0.335242059	6.618704676	-1.778906083
C	6.063795825	5.856850646	3.767532113
C	1.353599780	4.441349793	5.766220201
H	1.846938181	4.452799032	6.746396598
C	2.215448070	1.851421047	-0.405867054
H	1.592279961	1.412762859	-1.195215313
C	-0.233486844	6.100660552	-2.964341279
C	-0.253003252	2.592033233	1.148539490
H	0.141044977	1.975332408	1.967422922
C	6.991055369	6.088162627	2.725167595
C	6.709586173	5.666927930	5.009067462
C	-0.337810058	8.531937716	-3.035429312
H	-1.228566897	9.125709773	-2.806740302
H	0.338054954	9.186795560	-3.594003559
C	5.131625312	6.196444900	1.214234478
H	4.7711357284	6.315479922	0.194871642
C	1.668568906	7.426886626	5.520571060
H	0.575026557	7.466182730	5.427316055
C	-1.115617432	1.717406264	0.220761591
H	-1.519257504	2.305746030	-0.607609327
H	-1.960744815	1.325915438	0.792820698
H	-0.564093634	0.865220735	-0.184386536
C	-0.693592821	7.242306162	-3.838859651
H	-1.766534342	7.171011500	-4.043155756
H	-0.189692429	7.216422660	-4.810252632
C	4.539772048	5.402916130	5.994735155
H	3.949390500	5.233776360	6.890611742
C	-0.270246990	4.731849623	-3.148394329
H	-0.678984838	4.281666136	-4.046670896
C	5.942123460	5.414491289	6.130669560
H	6.385747294	5.241176840	7.105273780
C	8.203280255	5.777551684	4.815989782
H	8.703790730	4.850656904	5.113695749
H	8.621840847	6.571695640	5.442163071
C	-1.055532400	3.768911672	1.729949552
H	-0.461702702	4.375603267	2.418412731
H	-1.914834366	3.375063009	2.279506475
H	-1.433140147	4.414072316	0.931702070
C	6.523243597	6.278070463	1.439457958
H	7.192363678	6.470213283	0.607298898

C	2.504346114	0.784264139	0.667248640
H	3.057438478	1.214728290	1.506721944
H	3.120601581	-0.002630266	0.225121775
H	1.591084880	0.319229185	1.046506617
C	8.390619577	6.074875563	3.294622393
H	8.887719159	7.035964393	3.128794235
H	9.008204116	5.316197641	2.804135345
C	-0.157591245	4.669597289	5.953312966
H	-0.372742573	5.570601649	6.532295261
H	-0.579763844	3.817608781	6.492422327
H	-0.665423585	4.743720358	4.987680237
C	2.062911143	7.550251997	7.002376459
H	3.149684750	7.538744705	7.119928274
H	1.630274637	6.758727403	7.620309597
H	1.697165770	8.506757556	7.384540213
C	2.291386840	8.542948340	4.664061988
H	1.993069248	9.512907190	5.070050435
H	1.948893809	8.494393356	3.627368212
H	3.383646498	8.488472587	4.681303550
C	1.663002474	3.107890084	5.060989979
H	1.173973296	3.072060471	4.084088353
H	1.279804893	2.284452609	5.668664595
H	2.736850736	2.960704989	4.918799973
C	3.503837446	2.420236232	-1.028622388
H	4.062989340	1.605101282	-1.494579610
H	4.136783893	2.870786271	-0.259053763
H	3.289675690	3.169705341	-1.795011765

Table S9. Cartesian coordinates of **1*i*PrPO_HIA** at the TPSS-D3(BJ)/def2-TZVPP level of theory.

Ge	2.324609582	8.277375283	10.469265535
P	0.440716992	8.879407983	8.032440082
P	4.368145528	8.664910086	12.917739887
O	0.531102289	8.303516487	9.456817154
O	4.108385992	8.564613106	11.406754665
C	2.181965261	6.904709751	13.198668633
C	3.372306235	7.464683524	13.785023767
C	1.596118463	7.136674879	11.904723582
C	0.319341910	5.293396123	13.681898146
C	1.724939327	8.161950341	7.007712604
C	3.210848448	7.364313711	8.976758537
C	1.499646321	5.980653118	14.043278124
C	3.773660680	7.095309277	15.069240563
H	4.686261103	7.521606984	15.476162518
C	4.299930400	6.562908327	9.306887376
H	4.566144873	6.471996674	10.354159320
C	2.842280458	7.473998255	7.596501883
C	-0.214549370	5.518071059	12.435470062
H	-1.115006850	5.014689996	12.096011526
C	1.567594645	8.184995098	5.622002116
H	0.705512498	8.692872104	5.198787752
C	3.686695663	6.808301253	6.664480403
C	1.914853157	5.624824903	15.347187197
C	0.668603943	10.701719127	8.050937173
H	1.749821122	10.791950670	8.225454904
C	3.962396642	10.330614791	13.564005814
H	4.465664678	11.018697045	12.872083347
C	3.515598924	6.845288585	5.262702527
C	0.436844084	6.433309208	11.578335970

H	0.000536441	6.600081719	10.601325803
C	0.340485965	11.356584225	6.699828868
H	0.921342301	10.922977597	5.881550279
H	0.579718881	12.422892237	6.748469213
H	-0.723934657	11.266825570	6.462284035
C	6.509406094	6.928502619	12.724071271
H	5.896076117	6.159899296	13.201459672
H	7.558623017	6.727213977	12.958536425
H	6.383626938	6.853617925	11.640939849
C	-1.171206642	8.389470330	7.320987772
H	-1.188899312	8.766293937	6.291063474
C	2.458160245	7.552061050	4.730046877
H	2.281585505	7.609201518	3.660727887
C	3.061731923	6.181400094	15.870655325
H	3.426076517	5.931703849	16.861966443
C	6.141947571	8.340312408	13.209986690
H	6.307614342	8.403889268	14.292018724
C	0.944619615	4.625187369	15.935156752
H	0.493292897	5.013312626	16.854079989
H	1.455132674	3.695261669	16.205337132
C	5.096420126	5.873057873	8.363643175
H	5.927320231	5.262659314	8.705213564
C	4.799899478	6.017998926	7.027581271
C	-0.121208805	4.398728164	14.818903211
H	-0.159326146	3.351065107	14.503875730
H	-1.127059015	4.661487151	15.161533418
C	4.603903590	6.029962361	4.600282362
H	5.205134500	6.651822303	3.929090082
H	4.177043336	5.229273147	3.987872352
C	6.983687880	9.420655892	12.504822714
H	6.772994878	9.430969900	11.431958425
H	8.045470339	9.198366474	12.643875943
H	6.794191464	10.419966452	12.905888527
C	5.455675129	5.464912264	5.780886529
H	5.456772165	4.370246966	5.788122769
H	6.501432664	5.780582816	5.710596486
C	-1.251134050	6.851745016	7.297199212
H	-0.423678445	6.408628326	6.738153708
H	-2.190644643	6.548972612	6.826136749
H	-1.234126301	6.452066392	8.314698888
C	-0.061923816	11.376965937	9.224554728
H	-1.139010693	11.428513961	9.052580267
H	0.308808980	12.400901326	9.331621727
H	0.111403350	10.846165284	10.163017237
C	2.444319542	10.570984854	13.500692104
H	2.057019348	10.466538624	12.484941972
H	2.224965656	11.5855590200	13.846443383
H	1.914071139	9.867616607	14.149428295
C	4.494398908	10.557091412	14.989194589
H	4.017851634	9.872137735	15.696932646
H	4.253213515	11.576801139	15.303528318
H	5.578307658	10.433684991	15.058514461
C	-2.347654720	8.998891573	8.103527124
H	-2.266383658	8.773225630	9.170417404
H	-3.282212954	8.566167478	7.734692144
H	-2.408817999	10.081999303	7.979341750
H	2.207306306	9.806809456	10.472753086

Table S10. Cartesian coordinates of **1*i*PrPO_FIA** at the TPSS-D3(BJ)/def2-TZVPP level of theory.

Ge	6.903021842	11.301323435	6.800289863
P	7.056887761	10.034593429	9.708624743
P	6.419542947	13.225159620	4.285327849
F	6.147413364	12.662541978	7.654533643
O	6.000211967	12.053188151	5.192904074
O	7.685736028	10.857814075	8.568872161
C	5.879525965	8.548128515	7.644169834
C	5.962627343	9.574602062	6.636055665
C	5.251574381	7.330222202	7.255166270
C	5.420348050	9.297054814	5.380770730
H	5.471977266	10.069859268	4.625508419
C	8.402122836	9.593704999	10.860789406
H	7.952154142	9.002849519	11.667336155
C	8.692016246	11.646169547	6.084492895
C	10.400931426	13.006079064	5.034466163
C	6.327005206	8.564865895	9.010838813
C	8.135544850	13.646938220	4.540837483
C	4.716515553	7.084620520	5.970709122
C	9.017874790	12.746379434	5.228139579
C	10.911535480	14.114946663	4.323912362
C	4.798475274	8.079216481	5.025322568
H	4.403459194	7.953329998	4.021684730
C	5.360456928	14.691081764	4.522488072
H	5.662515807	15.399932030	3.739956940
C	5.077333916	6.210318238	8.101320620
C	8.651421139	14.747974456	3.855927617
H	7.964324760	15.426427404	3.357807318
C	11.436292320	12.186323569	5.534648193
C	6.233768842	12.619336092	2.565469861
H	5.215436790	12.207024903	2.556805755
C	6.151112557	7.452890419	9.833398802
H	6.511132382	7.497514987	10.857463778
C	9.729366283	10.842906459	6.551078678
H	9.481581204	10.006406077	7.195037277
C	4.129591738	5.691974237	5.919171106
H	4.613268967	5.089183012	5.143897251
H	3.063308058	5.722775583	5.673671999
C	4.376298762	5.105456394	7.343286383
H	3.439414852	4.826271928	7.835987890
H	4.993482801	4.201920390	7.308606982
C	12.423577093	14.073992259	4.353047724
H	12.823291498	14.954401950	4.867235709
H	12.842529553	14.084710272	3.342015986
C	11.096715973	11.071047071	6.267795999
H	11.847039341	10.391060544	6.660055979
C	5.755507882	10.947837273	10.620310211
H	6.167260867	11.957889285	10.741058643
C	5.532548039	6.263116681	9.401137104
H	5.426963228	5.427234161	10.085059835
C	7.236376274	11.477290843	2.323612353
H	8.260800098	11.860821677	2.313858518
H	7.167584378	10.703735793	3.092429521
H	7.035662478	11.015458926	1.352498636
C	10.033249150	15.016171214	3.757600025
H	10.374766151	15.896168356	3.222209452
C	9.465131291	8.749477113	10.138303016
H	9.039265576	7.847070496	9.692451972
H	9.942255150	9.336638124	9.349377373

H	10.237519274	8.450647825	10.852805393
C	12.774263577	12.757738886	5.117612451
H	13.415835014	12.948295227	5.983392540
H	13.314533208	12.055139088	4.474479886
C	3.885876637	14.301951977	4.309295955
H	3.697648535	13.921699094	3.301227675
H	3.583021758	13.538952359	5.031221917
H	3.256391242	15.183671661	4.458596829
C	5.596536809	15.331368775	5.900530760
H	5.339098590	14.635718729	6.701107849
H	6.639496008	15.631238059	6.030956578
H	4.968363467	16.222552815	5.990445902
C	5.479651617	10.326560808	12.000970544
H	5.112717210	9.299606378	11.903866151
H	6.359685173	10.324578335	12.648400967
H	4.697695488	10.906413289	12.499950986
C	6.346476248	13.709079317	1.490914865
H	5.621206862	14.514544509	1.634847973
H	7.351552072	14.140331882	1.473372110
H	6.161543447	13.265223294	0.508167959
C	9.010384469	10.881754500	11.448250471
H	9.413084555	11.510795662	10.649963167
H	8.280856737	11.467357972	12.013906746
H	9.828110487	10.617982931	12.124855473
C	4.459262155	11.023313969	9.793802727
H	4.623237107	11.481160975	8.818093133
H	4.034030998	10.025122256	9.655595161
H	3.729787215	11.632671560	10.335632728

Table S11. Cartesian coordinates of **SbF₅** at the TPSS-D3(BJ)/def2-TZVPP level of theory.

Sb	-0.31810000	2.24030000	0.66130000
F	-1.25800000	3.86080000	0.66130000
F	-0.31610000	2.24030000	2.54350000
F	1.55540000	2.24030000	0.66130000
F	-1.25810000	0.61980000	0.66130000
F	-0.31610000	2.24030000	-1.22090000

Table S12. Cartesian coordinates of **SbF₆** at the TPSS-D3(BJ)/def2-TZVPP level of theory.

Sb	-0.31850000	2.24030000	0.66130000
F	-1.84110000	3.40860000	0.66130000
F	-0.31850000	2.24030000	2.58030000
F	1.20410000	1.07200000	0.66130000
F	-1.48680000	0.71770000	0.66130000
F	-0.31850000	2.24030000	-1.25770000
F	0.84980000	3.76290000	0.66130000

Table S13. Cartesian coordinates of **B(PhF₅)₃** at the TPSS-D3(BJ)/def2-TZVPP level of theory.

F	-4.40370000	20.18610000	15.67490000
F	-4.15970000	15.60150000	16.66450000
F	-1.90620000	17.24280000	12.88480000
F	-5.58530000	19.52750000	12.79590000
F	-0.27620000	19.29850000	14.65930000
F	-5.05480000	18.11180000	17.25570000
C	-3.94360000	18.96430000	15.33550000
C	-4.28850000	17.91150000	16.17370000
F	-2.58800000	15.18320000	14.47350000
F	-2.12020000	20.94070000	10.58650000

F	2.18880000	19.49140000	13.60360000
C	-3.81160000	21.11280000	12.96520000
F	-7.40580000	21.43260000	12.26360000
C	-0.16540000	19.73970000	13.38980000
C	-3.12590000	18.80940000	14.20540000
F	-2.20750000	22.87320000	13.08370000
C	-6.12610000	21.77260000	12.47530000
C	-1.31240000	20.11130000	12.67130000
C	-3.02050000	16.41960000	14.76060000
C	-3.82790000	16.62880000	15.87820000
B	-2.74820000	20.01130000	13.27970000
C	-5.16640000	20.80900000	12.75930000
C	-2.67720000	17.50250000	13.96060000
C	-1.08200000	20.58220000	11.36910000
F	0.35510000	21.10660000	9.55010000
F	-6.65710000	24.05460000	12.15420000
F	2.52090000	20.39040000	11.04860000
F	-4.05310000	24.75920000	12.56820000
C	-3.47890000	22.47340000	12.87640000
C	1.11990000	19.83620000	12.87130000
C	1.29370000	20.29980000	11.56750000
C	0.18520000	20.67010000	10.80650000
C	-4.41350000	23.46870000	12.61920000
C	-5.74600000	23.11280000	12.41180000

Table S14. Cartesian coordinates of **B(PhF₅)₃-H** at the TPSS-D3(BJ)/def2-TZVPP level of theory.

F	-4.10930000	20.05000000	16.33350000
F	-4.41920000	15.34890000	16.18780000
F	-2.14540000	17.60990000	12.73950000
F	-5.19620000	19.48090000	12.72530000
F	0.18150000	20.04320000	14.90730000
F	-4.96670000	17.74010000	17.41560000
C	-3.79200000	18.90140000	15.68340000
C	-4.25470000	17.72350000	16.26320000
F	-2.99470000	15.32240000	13.84570000
F	-2.36690000	20.43250000	10.89830000
F	2.43900000	19.93660000	13.44630000
C	-3.71950000	21.28970000	13.24520000
F	-7.07260000	21.10740000	11.71860000
C	0.05600000	20.13730000	13.55910000
C	-3.05490000	18.95270000	14.49760000
F	-2.42340000	23.25890000	13.59890000
C	-5.91860000	21.63080000	12.19720000
C	-1.20810000	20.27990000	12.98300000
C	-3.25540000	16.50110000	14.46000000
C	-3.98100000	16.50780000	15.64540000
B	-2.53110000	20.40150000	13.94210000
C	-4.92730000	20.81280000	12.73700000
C	-2.81800000	17.70760000	13.91610000
C	-1.20130000	20.33850000	11.58960000
F	-0.10140000	20.34550000	9.46420000
F	-6.66340000	23.81670000	11.61600000
F	2.32670000	20.09320000	10.71050000
F	-4.31500000	24.87050000	12.56500000
C	-3.56640000	22.67540000	13.15580000
C	1.24040000	20.07270000	12.82930000
C	1.19040000	20.15040000	11.44170000
C	-0.04390000	20.28370000	10.81610000
C	-4.52340000	23.53310000	12.62100000

C	-5.71600000	23.00460000	12.13820000
H	-2.18340000	21.02630000	14.91610000

Table S15. Cartesian coordinates of **Me₃SiF** at the TPSS-D3(BJ)/def2-TZVPP level of theory.

Si	-0.87460000	1.46140000	0.00000000
C	-0.21810000	2.28520000	1.54690000
H	-0.55490000	3.32710000	1.60670000
H	-0.56540000	1.77130000	2.45010000
H	0.87740000	2.28870000	1.56240000
C	-2.74490000	1.39400000	-0.00010000
H	-3.17230000	2.40400000	-0.00010000
H	-3.12450000	0.87250000	-0.88570000
H	-3.12460000	0.87250000	0.88540000
C	-0.21790000	2.28500000	-1.54690000
H	0.87760000	2.28850000	-1.56220000
H	-0.56510000	1.77110000	-2.45000000
H	-0.55480000	3.32690000	-1.60680000
F	-0.33480000	-0.07330000	0.00010000

Table S16. Cartesian coordinates of **Me₃SiH** at the TPSS-D3(BJ)/def2-TZVPP level of theory.

Si	-0.86370000	1.43030000	0.00000000
C	-0.22280000	2.29620000	1.54590000
H	-0.56900000	3.33570000	1.58400000
H	-0.57060000	1.79640000	2.45660000
H	0.87230000	2.30940000	1.57080000
C	-2.74760000	1.40460000	-0.00010000
H	-3.15290000	2.42330000	-0.00010000
H	-3.13980000	0.89090000	-0.88470000
H	-3.13990000	0.89090000	0.88450000
C	-0.22260000	2.29600000	-1.54580000
H	0.87250000	2.30930000	-1.57060000
H	-0.57020000	1.79610000	-2.45660000
H	-0.56880000	3.33560000	-1.58410000
H	-0.36700000	0.02420000	0.00010000

Table S17. Cartesian coordinates of **Me₃Si** at the TPSS-D3(BJ)/def2-TZVPP level of theory.

Si	-1.05180000	1.96440000	0.00000000
C	-0.20390000	2.31580000	1.58820000
H	-0.42250000	3.36320000	1.85630000
H	-0.57850000	1.69000000	2.40350000
H	0.88290000	2.22400000	1.50500000
C	-2.79870000	1.40460000	-0.00010000
H	-3.43550000	2.30520000	0.00130000
H	-3.04930000	0.83390000	-0.89900000
H	-3.04870000	0.83170000	0.89760000
C	-0.20370000	2.31570000	-1.58810000
H	0.88330000	2.22670000	-1.50420000
H	-0.57630000	1.68770000	-2.40260000
H	-0.42500000	3.36200000	-1.85800000

Bibliography

- [S1] B. Peddi, S. Khan, R. G. Gonnade, C. B. Yildiz, M. Majumdar, *Chem. Sci.* 2023, **14**, 13755.
- [S2] Hübschle, C. B.; Sheldrick, G. M.; Dittrich, B. ShelXle: A Qt Graphical User Interface for SHELXL. *J. Appl. Cryst.* 2011, **44**, 1281–1284.
- [S3] Dolomanov, O. V.; Bourhis, L. J.; Gildea, R. J.; Howard, J. a. K.; Puschmann, H. OLEX2: A Complete Structure Solution, Refinement and Analysis Program. *J. Appl. Cryst.* 2009, **42**, 339–341.
- [S4] Neese, F., Software Update: The ORCA program system, Version 5.0. *WIREs Comput. Mol. Sci.* 2022, **12(5)**, e1606.
- [S5] Weigend, F. Accurate coulomb-fitting basis sets for H to Rn. *Phys. Chem. Chem. Phys.* 2006, **8(9)**, 1057-1065.
- [S6] Gaussian 16, Revision B.01, 2016, Frisch, M.J.; Trucks, G.W.; Schlegel, H.B.; Scuseria, G.E.; Robb, M.A.; Cheeseman, J.R.; Scalmani, G.; Barone, V.; Petersson, G.A.; Nakatsuji, H.; Li, X.; Caricato, M.; Marenich, A.V.; Bloino, J.; Janesko, B.G.; Gomperts, R.; Mennucci, B.; Hratchian, H.P.; Ortiz, J.V.; Izmaylov, A.F.; Sonnenberg, J.L.; Williams-Young, D.; Ding, F.; Lipparini, F.; Egidi, F.; Goings, J.; Peng, B.; Petrone, A.; Henderson, T.; Ranasinghe, D.; Zakrzewski, V.G.; Gao, J.; Rega, N.; Zheng, G.; Liang, W.; Hada, M.; Ehara, M.; Toyota, K.; Fukuda, R.; Hasegawa, J.; Ishida, M.; Nakajima, T.; Honda, Y.; Kitao, O.; Nakai, H.; Vreven, T.; Throssell, K.; Montgomery Jr., J.A.; Peralta, J.E.; Ogliaro, F.; Bearpark, M.J.; Heyd, J.J.; Brothers, E.N.; Kudin, K.N.; Staroverov, V.N.; Keith, T.A.; Kobayashi, R.; Normand, J.; Raghavachari, K.; Rendell, A.P.; Burant, J.C.; Iyengar, S.S.; Tomasi, J.; Cossi, M.; Millam, J.M.; Klene, M.; Adamo, C.; Cammi, R.; Ochterski, J.W.; Martin, R.L.; Morokuma, K.; Farkas, O.; Foresman, J.B.; Fox, D.J. Gaussian; Inc., Wallingford CT
- [S7] NBO Version 3.1, Glendening, E.D.; Reed, A.E.; Carpenter, J.E.; Weinhold, F.
- [S8] Wiberg, K.B. Application of the pople-santry-segal CNDO method to the cyclopropylcarbinyl and cyclobutyl cation and to bicyclobutane. *Tetrahedron* 1968, **24**, 1083-1096.
- [S9] Nielsen, A.B.; Holder, A.J. (2009) Gauss View 5.0, User's Reference. GAUSSIAN Inc., Pittsburgh.
- [S10] a) Muller, L. O.; Himmel, D.; Stauffer, J.; Steinfeld, G.; Slattery, J.; Santiso-Quinones, G.; Brecht, V.; Krossing, I., Simple access to the non-oxidizing Lewis superacid PhF \rightarrow Al(OR^F)₃ (R^F = C(CF₃)₃). *Angew. Chem. Int. Edit.* 2008, **47 (40)**, 7659-7663; b) Bohrer, H.; Trapp, N.; Himmel, D.; Schleep, M.; Krossing, I., From unsuccessful H₂-activation with FLPs containing B(Ohfip)₃ to a systematic evaluation of the Lewis acidity of 33 Lewis acids based on fluoride, chloride, hydride and methyl ion affinities. *Dalton Trans.* 2015, **44 (16)**, 7489-7499.